

A review of the geology and geodynamic evolution of the Palaeoproterozoic Earaheedy Basin, Western Australia

Franco Pirajno ^{a,b,*}, Roger M. Hocking ^a, Steven M. Reddy ^c, Amanda J. Jones ^d

^a Geological Survey of Western Australia, East Perth, Australia

^b School of Earth and Geographical Sciences, The University of Western Australia, Crawley, Australia

^c Dept. Applied Geology, Curtin University of Technology, Perth, Australia

^d 27, Chadwick Street, Hilton WA 6163, Australia

ARTICLE INFO

Article history:

Received 12 March 2008

Accepted 17 March 2009

Available online 27 March 2009

Keywords:

Earaheedy Basin

Capricorn Orogen

passive margin

granular iron-formation

ABSTRACT

The Palaeoproterozoic Earaheedy Basin is one of a series of basins that extend for about 700 km east–west and are part of the Capricorn Orogen, situated between the Archaean Pilbara and Yilgarn Cratons. The Earaheedy Basin contains sedimentary rocks that were deposited on the northern passive continental margin of the Yilgarn Craton, probably as a result of continental breakup at 1.8 Ga. The sedimentary rocks of the Earaheedy Group are divided into two Subgroups, Tooloo and Miningarra, each representing different depositional environments and aggregating about 3000 m in thickness. The Tooloo Subgroup consists of basal siliciclastic rocks with minor platform carbonates, overlain by a 600-m-thick succession of Fe-rich rocks (granular iron-formation and hematitic shales). The Miningarra Subgroup is predominantly siliciclastic, but includes stromatolite-bearing carbonate sequences and was deposited during a more active depositional regime. Far-field tectonic events at 1.76 and 1.65 Ga resulted in the deformation of the sedimentary package with progressive intensity from north to south, forming the Stanley Fold Belt and giving an overall asymmetric structure to the Basin. These events were followed by a large meteorite impact (Shoemaker Impact Structure), probably in the Neoproterozoic. The Earaheedy Basin is well endowed with Fe resources, represented by the granular iron-formation (Frere Formation, Tooloo Subgroup), particularly in the Stanley Fold Belt, where there was secondary enrichment.

© 2009 Elsevier B.V. All rights reserved.

Contents

1. Introduction	40
2. Previous work	42
3. Tectonic setting and regional geology	42
3.1. Pre- and post-Earaheedy igneous activity	44
3.1.1. Imbin Inlier	44
3.1.2. Glenayle and Prenti dolerites	45
3.1.3. Lamprophyres	45
4. The Earaheedy Basin	47
4.1. Geochronology	47
4.1.1. Ar–Ar dating	48
4.1.2. Detrital zircon ages and provenance studies	48
4.2. Lithostratigraphy	51
4.2.1. Yelma Formation	51
4.2.2. Frere Formation	52
4.2.3. Depositional environment of the Tooloo Subgroup and the origin of the iron formations	61
4.2.4. Chiall Formation	63
4.2.5. Wongawol Formation	68
4.2.6. Mulgarra Sandstone	69
4.2.7. Depositional environment of the Miningarra Subgroup	69

* Corresponding author. Geological Survey of Western Australia, East Perth, Australia.

E-mail addresses: franco.pirajno@dmp.wa.gov.au, franco.pirajno@uwa.edu.au (F. Pirajno).

5. Stanley Fold Belt	69
5.1. Folds, faults and linear (E–W, N–S and NW–SE) structures	70
5.2. Quartz veins	70
6. Shoemaker meteorite impact structure	70
6.1. Hydrothermal alteration	71
7. Depositional setting and geodynamic evolution of the Earaheedy Basin	71
8. Discussion and conclusions	74
Acknowledgements	75
Appendix A. Supplementary data	75
References	75

1. Introduction

The Earaheedy Basin, together with the Yerrida, Bryah and Padbury basins, form a series of Palaeoproterozoic basinal structures that extend for about 700 km east–west along the southeastern margin of the Capricorn Orogen and the northern margin of the Yilgarn Craton and covers a total area of approximately 70 000 km² (Cawood and Tyler, 2004; Pirajno et al., 2004) (Fig. 1). The development of these

basins began at about 2.2 Ga and continued for at least 400 Myrs, to about 1.8 Ga and possibly as young as 1.65 Ga, recording periods of sedimentation and igneous activity. The present-day geometry of these basins is the combined result of tectonic movements that occurred during the ca. 2.0–1.96 Ga Glenburgh Orogeny (Occhipinti et al., 2004), the ca. 1.83–1.78 Ga Capricorn Orogeny (Cawood and Tyler, 2004 and references cited therein) and to a lesser extent the 1.79–1.76 Ga Yapungku Orogeny (Bagas, 2004) and the 1.68–1.62 Ga

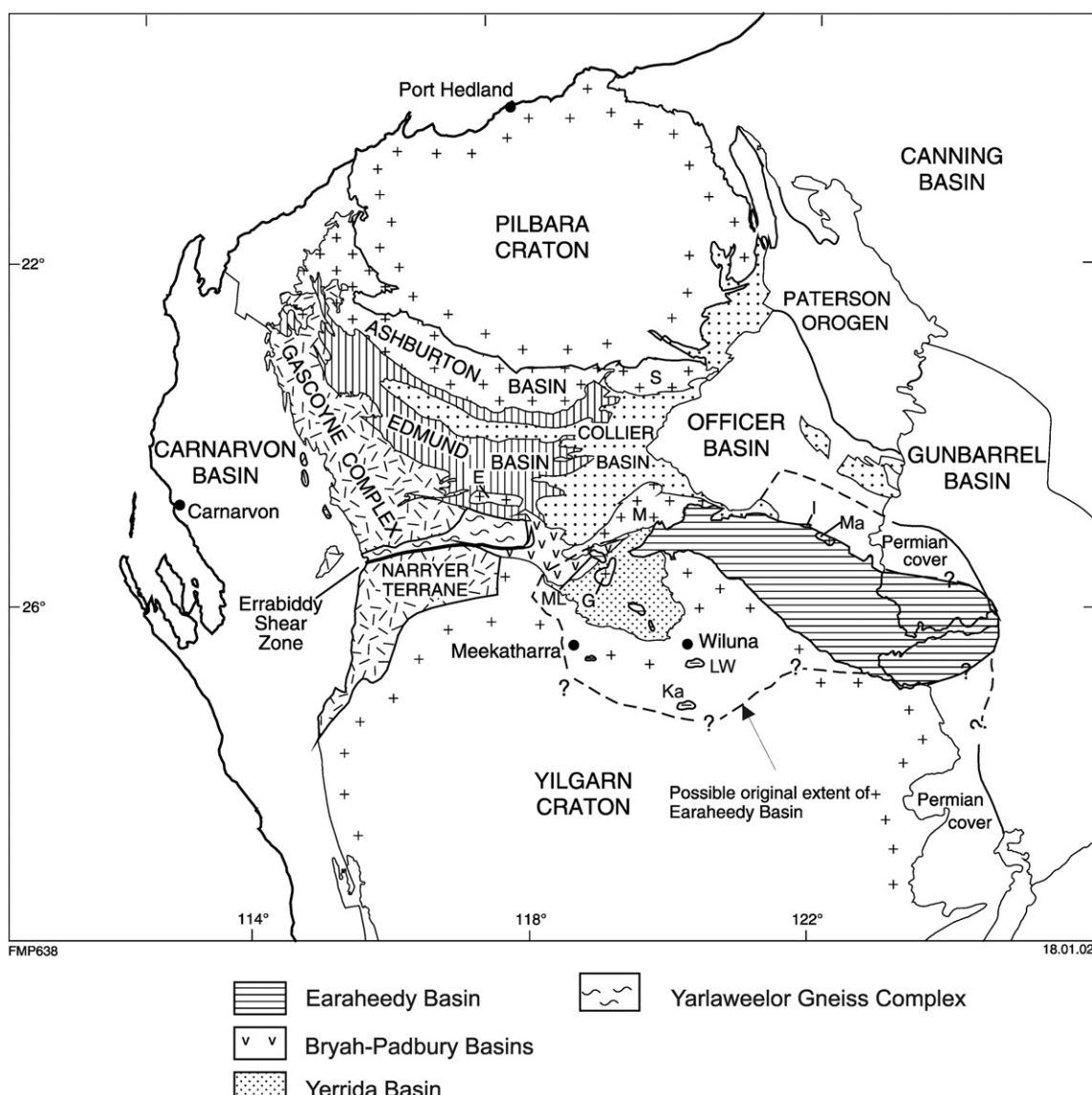


Fig. 1. Tectonic units of the Capricorn Orogen and position of the Earaheedy Basin; E Egerton Inlier, M Marymia Inlier, S Sylvania Inlier, Ma Malmac Inlier, I Imbin Inlier; ML Mt Leake outlier, Ka Kaluweerie Hills outlier, LW Laurence Wells-Mt Wilkinson outliers. Modified from Pirajno et al. (2004).

Table 1

Summary of major tectono-thermal events in the Capricorn Orogen that are relevant to the geodynamic evolution of the Earaheedy Basin.

Approx. age (Ga)	West: Bryah, Yerrida, Padbury	East: west-central: Earaheedy	Other related events
>2.6	Northern Yilgarn Craton; Goodin and Marymia Inliers	Northern Yilgarn Craton; Malmac Inlier	
<2.2–2.1	Deposition of lower Yerrida Group (Windplain Subgroup, evaporite and siliciclastics), in intracratonic sag basin		
2.0	Sea-floor spreading in ocean separating Glenburgh terrane from northwest margin of Yilgarn Craton; birth of Narracoota ocean floor.		West- or northwest facing subduction on Glenburgh terrane (Southern Gascoyne Cx)
2.0–1.99 Glenburgh Orogeny	<ul style="list-style-type: none"> • Convergence of Yilgarn Craton and Glenburgh terrane (southern Gascoyne complex); • Emplacement of oceanic crust (Narracoota Formation) and rifting of Marymia Inlier from northern margin of Yilgarn; eruption of basaltic hyaloclastites • Closing of oceanic arm between NW Yilgarn and Glenburgh terrane and accretion of juvenile crust to NW Yilgarn margin and Yerrida sag structure. <p>Deposition of Bryah Group (Narracoota, Ravelstone Fms).</p>	Emplacement (?tectonic?intrusive) of rhyodacite (Imbin Inlier); possible correlative of Dalgaranga Supersuite (Southern Gascoyne terrane).	Emplacement of 2.0–1.98 Ga granites of Dalgaranga Supersuite Emplacement of 1.97 Ga Nardoo granite (Glenburgh terrane);
1.96			
~1.83 Capricorn Orogeny	<ul style="list-style-type: none"> Deposition of Padbury Gp, in small foreland basin on top of Bryah Group; • Convergence and oblique collision of Pilbara and Yilgarn cratons; compression with uplift and deformation around Goodin and Marymia inliers; Bryah and Padbury Basins become a fold-and-thrust belt; associated orogenic gold lodes. • Yerrida Basin evolves from a sag to a foreland basin, with deposition of immature sediments (Thaduna–Doolgunna Fms) from orogenic highlands; • Rejuvenation and deepening of Yerrida Basin ahead of compression front, leads to reactivation of ancient fractures with eruption of continental tholeiites (Killara Fm); sedimentation of immature sediments continues; • Continental volcanism ceases, deposition of lake sediments (Maraloof Fm) in Yerrida Basin 		1.82 Ga Moorarie Supersuite; granite intrusions in Narreyer terrane (Yarlaweelor Cx); emplacement of 1.81–1.79 Ga granites of Moorarie Supersuite in Glenburgh terrane (Sheppard et al. and Occipinti et al., this volume)
Post-Capricorn Orogeny			Continental breakup and sea floor spreading to the ?east and/or northeast; mid-ocean ridge volcanism supplies dissolved Fe and Mn to the Earaheedy passive margin
1.79–1.74 Yapungku Orogeny	Convergence of North Australian and West Australian cratons; south-directed compression	<ul style="list-style-type: none"> Initiation of passive margin along northeast and east margins of Yilgarn Craton; deposition of Tooloo Subgp (Earaheedy Basin) • Yelma shelf carbonates and sandstone; sediments provenance from orogenic uplifts in west and Yilgarn in the south); • Deposition of granular iron formation on shelf, black shales in deeper waters (continental rise). Fe and Mn oxide mineralisation <p>Mild uplift and erosion of Tooloo Subgroup</p>	Cessation of sea floor spreading north and east of Yilgarn Craton
1.68–1.62 Mangaroon Orogeny			
1.64	Deposition of Edmund Group (Edmund Basin)		
1.46	Intrusion of dolerite sills into Edmund Group		
<1.46–1.22	Deformation of Edmund Group		
1.20–>1.07	Deposition of Collier Group (Collier Basin)		
1.13–0.8			
1.07	Intrusion of mafic sills and dykes into Collier and Edmund Groups		
<1.07–>0.85	Edmundian Orogeny and deformation of Edmund and Collier Basins		
0.83			Warakurna LIP
		<ul style="list-style-type: none"> Initial deposition in NW Officer Basin, of basal sand overlain by evaporitic mixed sequence (Bulday Group) 	

Mangaroon Orogeny (Sheppard et al., 2005). A synopsis of the geological events that formed and shaped the Palaeoproterozoic basins in the eastern Capricorn Orogen is presented in Table 1.

The Earaheedy Basin (Bunting, 1986; Pirajno et al., 2004) contains the Earaheedy Group and lies at the easternmost end of the Capricorn Orogen (Myers et al., 1996; Tyler et al., 1998; Cawood and Tyler, 2004). The Basin represents a coastal to outer shelfal, dominantly siliciclastic, sedimentary accumulation, with a locally preserved basal fluvial sandstone and conglomerate, interpreted by Jones et al. (2000) and Pirajno et al. (2004) to have accumulated at a passive continental margin along the northeastern edge of the Yilgarn Craton. This passive margin may ultimately represent a continental breakup at 1.8 Ga, perhaps linked to the impingement of a mantle plume, as will be elaborated in Section 7.

Basement to the exposed Earaheedy Basin is the Archaean Yilgarn Craton, and to the west the Yerrida Basin. To the north the Earaheedy Basin is overlain by the sedimentary successions of the Bangemall Supergroup (Scorpion and Salvation Groups). A small outlier of 1.9 Ga rhyodacitic rock (Inbim Inlier) on the northern margin is unconformably overlain by rocks of the Earaheedy Group (Yelma Formation, see below). Locally the Earaheedy Group is intruded by dykes and sills of the Glenayle Dolerite and Prenti Dolerite (Morris and Pirajno, 2005), which are part of the 1076 Ma Warakurna Large Igneous Province (WLIP; Wingate et al., 2004), and by scattered lamprophyre dykes and pipes of unknown age. Apart from the WLIP there are no other igneous rocks that are associated with the sedimentary succession of the Earaheedy Basin, except for minor and thin volcanoclastic horizons in the Frere Formation.

The Earaheedy Basin has an exposed area of 35 308 km², in south-central Western Australia. Numerous possible outliers are present about 50–60 km south of the westernmost exposures (Fig. 1). These outliers, such as the Kaluweerie Hills (Allchurch and Bunting, 1975), Mount Laurence Wells and Mount Wilkinson south of Wiluna (Langford et al., 2000) have sedimentary rocks that include stromatolitic carbonates, which could be part of either the Yerrida Basin or Earaheedy Basin successions. To the west is the easterly trending Mount Leake outlier (Mount Leake Formation), which straddles the Goodin Fault that marks the tectonic boundary between the Yerrida and Bryah Basins, clearly demonstrating that the Mount Leake Formation was deposited well after the tectonic juxtaposition of the Bryah and Yerrida Basins. The Mount Leake Formation consists of a basal jasperoidal chert and green chert breccia about 2 m thick, followed upward by a ferruginous sandstone layer and by beds of cross-bedded, locally glauconitic, quartz arenite. Pirajno and Occhipinti (1998) interpreted the jasperoidal and chert breccia material as a palaeoregolith, developed on an unconformity surface of the Bryah Group. On the basis of stromatolite taxa that are present in the Mount Leake rocks, Pirajno and Adamides (2000) proposed a correlation with the Yelma Formation. The presence of these outliers suggests that the original extent of the Basin could have been much larger (Fig. 1).

The Geological Survey of Western Australia (GSWA) began a systematic re-mapping program of the Earaheedy Basin in 1997. The outcome of this program was the publication of the second edition 1:250 000 Nabberu, and thirteen 1:100 000 series geological maps (Merrie, Cunyu, Fairbairn, Methwin, Nabberu, Granite Peak, Mudan, Glenayle, Earaheedy, Wongawol, Collurabie, Lee Steere and Von Trueur). The layout of these map sheets with the simplified geology of the Earaheedy Basin is shown in Fig. 2. The name of these map sheets are used to identify localities discussed in the text. For more accurate details (e.g. coordinates) on localities, the interested reader is encouraged to contact the first author.

In this paper the results of the field geological mapping, integrated with geochemical data, petrographic and sedimentological work and the available geochronology on rocks of the Earaheedy Basin are presented and discussed, with a view to introducing a model that in the present state of knowledge best explains the geodynamic evolution of the Basin.

2. Previous work

In the last quarter of the 19th century a few explorers ventured into the interior of Western Australia, and those that visited areas within the Earaheedy Basin, include Ernest Giles (Giles, 1889), David Carnegie, Lawrence Wells and John Forrest, who named several localities, such as Frere Range, Sweeney Creek and Pierre Spring. The first geological accounts and maps of the area were published by Talbot (1910, 1914, 1919, 1920, 1926).

Modern geology began with the works of Horwitz (1975a,b, 1976), Hall and Goode (1975, 1978) and Hall et al. (1977). The Earaheedy Basin made international news with the publication of two papers on Gunflint-type microbial assemblages from the Frere Formation (Walter et al., 1976; Tobin, 1990).

In the late 1970s, the Geological Survey of Western Australia commenced regional geological mapping of the map sheets that encompass the Earaheedy area, which resulted in the publication of 1:250 000 scale geological maps and accompanying Explanatory Notes (Bunting, 1980a,b; Bunting et al., 1982; Brakel and Leech, 1980; (Leech and Brakel, 1980). These works culminated with the publication of GSWA Bulletin 131 (Bunting, 1986), which comprehensively describes the lithostratigraphic units, derivation of stratigraphic names and type localities of the Earaheedy Basin. These definitions are not repeated in this paper. The latest GSWA mapping of the Basin, carried out between 1997 and 2004, resulted in some modifications of the stratigraphy as discussed in Pirajno et al. (2004) and detailed in later sections.

Mining companies conducted exploration work in the Earaheedy Basin aimed primarily at the assessment of the iron potential of the iron-formation beds of the Frere Formation and at the Mississippi-Valley type (MVT) mineralization hosted in the carbonate rocks of the Yelma Formation. Other exploration activities included the search for diamonds in lamprophyre dykes, gold in the metamorphosed and deformed rocks in the Stanley Fold Belt and uranium in calcrete. Mineral systems of the Earaheedy Basin are not considered in this paper; these are discussed in some detail in Pirajno et al. (in press).

3. Tectonic setting and regional geology

Post-Archaean tectonic events resulted in the reworking and possible fragmentation of the Yilgarn Craton's northern margin and the formation of depositional systems, while to the northwest, collision and accretionary processes were taking place. North of the Craton's present-day boundary are the Goodin, Marymia and Malmac inliers, all of which represent Archaean granite-greenstone terranes and the northern extension of the Yilgarn Craton (Fig. 1). These inliers are located within the 700-km long belt of Palaeoproterozoic volcano-sedimentary and sedimentary basins, which are considered part of the Capricorn Orogen (Fig. 1). These basins (Bryah-Padbury, Yerrida and Earaheedy), record periods of rifting, sedimentation and volcanism, along the northern passive margin of the Yilgarn Craton. The Yerrida Basin, is the oldest (ca. 2.17 Ga), and began its history as an intracontinental sag, within which low-energy siliciclastics and evaporites accumulated.

To the west, the Bryah-Padbury basins formed during accretion and collision processes, related to the ca. 2.0–1.9 Ga Glenburgh and ca. 1.83–1.78 Ga Capricorn orogenies. An uplift and rifting event affected the Yerrida Basin at 1.84 Ga, resulting in coarse and immature clastic sedimentation together with the eruption of flood basalts (Mooloogool Group). This event also caused the uplift of the Goodin Inlier with its cover of basal siliciclastic and evaporites of the Yerrida Basin, resulting in the formation of olistostrome units (Pirajno et al., 2004; Pirajno 2007). This uplift was followed by stress relaxation and extensional tectonics with asthenospheric upwelling and outpouring of the above-mentioned flood basalts.

To the east a passive margin developed, probably later than this uplift but the precise timing is poorly constrained. Sedimentation in this passive margin consisted of shallow-water clastic and chemical

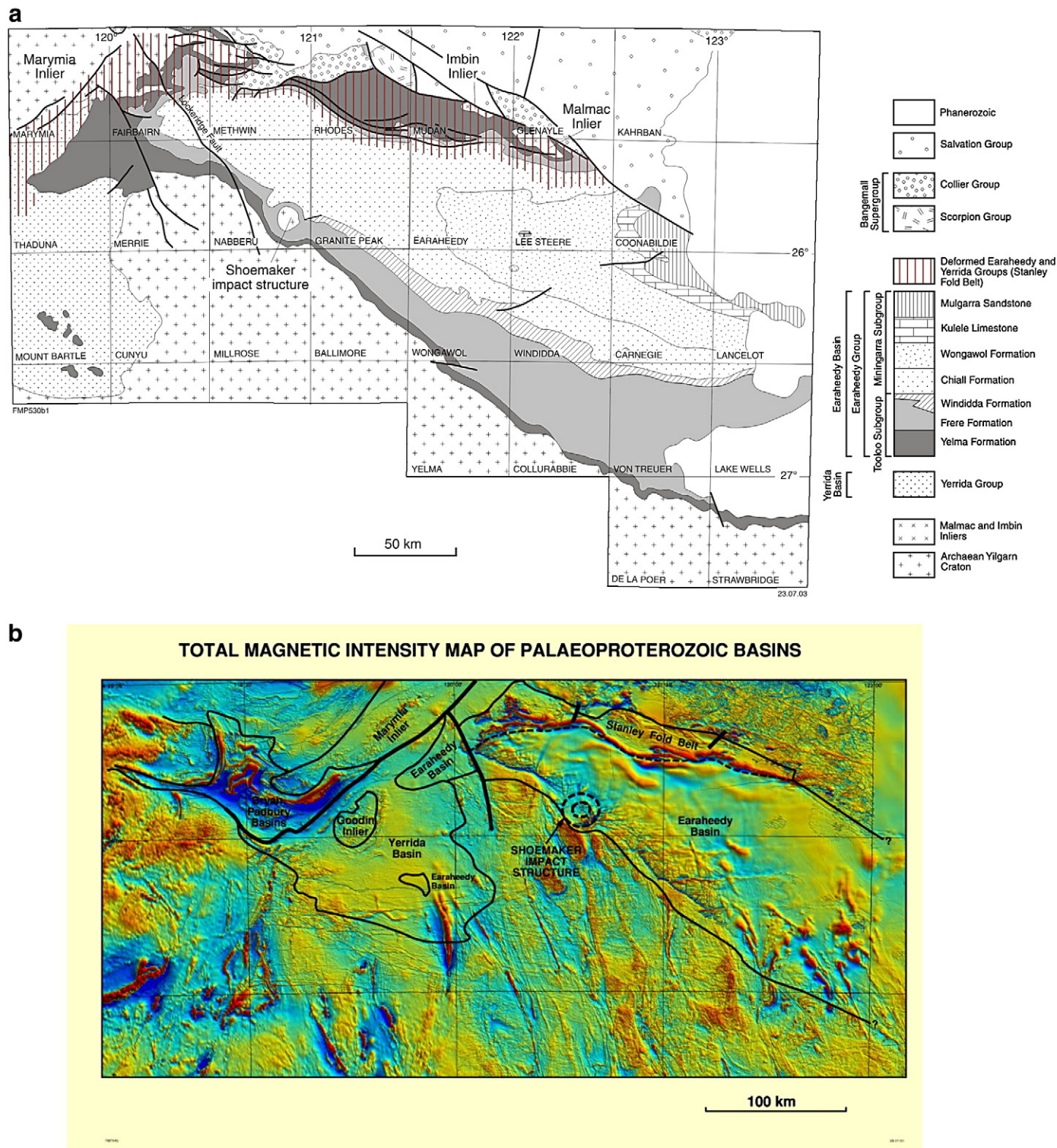


Fig. 2. a) Simplified geology of the Earaheedy Basin and covering 1:100000 scale map sheets; b) Aeromagnetic image of the northern margin of the Yilgarn Craton and eastern Capricorn Orogen basin systems (outlined); note scale difference with (a).

sediments (granular iron formation; GIF), which form the basal succession (Tooloo Subgroup) of the Earaheedy Group. Deposition of the upper part of the Group, the Miningarra Subgroup, was in a uniformly northeast-facing coastal to shelfal basin, with relatively low-energy conditions suggestive of a passive margin. No regional unconformity has been recognized between the two subgroups, but a disconformity may be present. A conglomerate at the base of the Miningarra Subgroup on Wongawol (Fig. 2), composed entirely of

cobble- to boulder-size clasts of the underlying Windidda Member of the Frere Formation set in a ironstone matrix, may record an unconformity. Such an unconformity may be a far-field effect of the ca 1.74 Ga Yapungku Orogeny (Bagas, 2004).

The northern margin of the Earaheedy Basin and the western parts of the Yerrida Basin were deformed, to form the Stanley Fold Belt (Fig. 2), before deposition of the Scorpion Group began at ca. 1.63 Ga. The most probable cause of this was the 1.68–1.62 Ga Mangaroon

Orogeny (Sheppard et al., 2005). Detrital zircons dated at 1.8 Ga have been recovered from the upper stratigraphic levels of the Miningarra Subgroup (Halilovic et al., 2004), lessening the probability that the ca 1.74 Ga Yapungku Orogeny was responsible for the Stanley Fold Belt.

The basal units of both the Yerrida and Earaheedy basins, although separated by ca. 300 million years, are characterised by extensive aprons of clastic sediments, mostly mature sandstone. These sediments were generated by erosion of peneplaned surfaces. Peneplanation and the generation of large volumes of siliciclastic sediments have been related to domal uplift of continental crust (Pirajno et al., 2004). Basins were starved of clastic sediments after stripping of the craton, resulting in shallow-marine to coastal carbonate and evaporite deposition, which in the Earaheedy Basin coincided with increases in dissolved iron and silica, initiating deposition of chert and iron formations. The subgroup divisions of the Earaheedy Basin indicate a change in the depositional settings, imposed by a higher energy tectonic regime, most likely due to orogenic uplifts, as previously mentioned. The Earaheedy Basin is also characterised by an asymmetry in preserved cross-section, with little deformed southern platform margins and northern margins of intensely deformed rocks (Stanley Fold Belt), typical of foreland basin architecture. There is, however, little indication of foreland basin architecture during deposition. Neither subgroup shows the characteristic, sand-rich, coarsening-upwards pattern ('molasse') with supply from the north, or of a foreland bulge near the southern limb of the Earaheedy Basin. The

basin's asymmetry is therefore attributed to orogenic activity after the basin became inactive, primarily during the Mangaroon Orogeny.

3.1. Pre- and post-Earaheedy igneous activity

The Earaheedy Basin is exclusively filled with sedimentary rocks with no temporally associated igneous activity. However, the Earaheedy sedimentary succession is spatially associated with igneous intrusive rocks of Palaeo- and Mesoproterozoic age, which both intrude or juxtapose the Earaheedy Group. These igneous rocks include, the 1.99 Ga rhyodacitic rocks of the Imbin Inlier, the Glenvale and Prenti Dolerite of the 1.07 Ga Warakurna large igneous province and a suite of ultramafic lamprophyres, some of which are diamondiferous, of uncertain age.

3.1.1. Imbin Inlier

Quartz–feldspar porphyry outcrops are present on the northern margin of the Earaheedy Basin, within the Stanley Fold Belt (Fig. 2). The outcrop area of this quartz–feldspar porphyry extends for approximately 7 km in a west-northwest trend, but aeromagnetic data indicate that its full extent may be in the order of 22 km. This quartz–feldspar porphyry, which was dated by SHRIMP U–Pb method yielding an age of 1990 ± 6 Ma (Table 2); Nelson, 2001a,b), is interpreted as a basement fragment to the Earaheedy Group. The Imbin quartz–feldspar porphyry consists of K-feldspar, quartz and plagioclase albite phenocrysts (about 20% by vol.), from 2 to 4 mm long, in a

Table 2
Summary of geochronological data for the Earaheedy Basin.

Formation	Locality	Coordinates	Rock/Mineral (detrital zircon age from youngest)	Age (Ma)	Method	Reference	
Earaheedy Basin							
Mulgarra Sandstone	LEE STEER	Not available	Sandstone/detrital zircon	1808 ± 36	U–Pb SHRIMP	Halilovic et al. (2004)	
Chiall Formation	WONGAWOL	Not available	Sandstone/detrital zircon	1876 ± 19	U–Pb SHRIMP	Halilovic et al. (2004)	
Wandiwarra Member	VON TUREUR	Not available	Sandstone/detrital zircon	2050–2500	U–Pb SHRIMP	Halilovic et al. (2004)	
Wandiwarra Member	KINGSTON 1:250 000, WONGAWOL	121° 57' E, 26° 14' S	Sandstone/glaucnrite	1685 ± 35	K–Ar	Horwitz (1975a,b)	
Yelma Formation	NE DUKETON 1:250 000, DE LA POER		Sandstone/glaucnrite	1590–1710	Rb–Sr	Preiss et al. (1975)	
	MUDAN	Not available	Sandstone/detrital zircon	1670–1710	K–Ar	Preiss et al. (1975)	
	NABBERU	120° 56' 33"E, 25° 53' 11"S	Sandstone/detrital zircon	2700–2600	U–Pb SHRIMP	Halilovic et al. (2004)	
				2027 ± 23	U–Pb SHRIMP	Nelson (1997)	
			Carbonate (<i>Yandilla meekatharrensis</i>)	2008 ± 68	Pb–Pb	Russell et al. (1994)	
	Stanley Fold belt	RHODES	Muscovite	1653.6 ± 14.4	Ar–Ar	This work	
		MERRIE	Not available	1946 ± 71	Pb–Pb	Russell et al. (1994)	
Mineralisation							
Yelma Formation	Sweetwaters Well Member	NABBERU 1:250 000, MERRIE	Dolomite/galena	~1700	Pb–Pb	Richards and Gee (1985)	
		NABBERU	Not available	Galena	1770–1740	Pb–Pb	Teen (1996)
		MEREWETHER					
		NABBERU 1:250 000, MERRIE	120.66356E/ 25.67088N	Dolomite/galena	~1650	Pb–Pb	This work
		NABBERU 1:250 000	119.94547E/ 26.53371S	Galena	~1700	Pb–Pb	Johnston and Hall, 1980
		MEREWETHER		Carbonate	~1650	Pb–Pb	Le Blanc Smith et al., 1995
Shoemaker Impact Structure	NABBERU	Not available	Quartz–albite whole rock	~1630	Rb–Sr	Bunting et al. (1980a,b)	
	NABBERU	120.92714E/ 25.83184S	Quartz–albite whole rock	2648	U–Pb SHRIMP	Nelson	
Basement	Lee Steere	122.14028E/ 25.49902S	Granite	1724	U–Pb SHRIMP	Nelson (2001a,b)	
Malmac Inlier	MUDAN	121.75981E/ 25.36113E	Rhyodacite/zircon	1990	U–Pb SHRIMP	Nelson (2001a,b)	
Possible? Outlier Earaheedy Basin	BRYAH	118.70438E/ 25.91409S	Quartz arenite/detrital zircon	1832 ± 37	U–Pb SHRIMP	Nelson (1997)	
Mt. Leake Formation	BRYAH	118.66766E/ 25.79373S	Sandstone/detrital zircon	1785 ± 11	U–Pb SHRIMP	Nelson (1997)	
	SW PEAK HILL 1:250 000	Not available	Sandstone/glaucnrite	1573	K–Ar	Butt et al. (1977)	

groundmass predominantly composed of a fine-grained K-feldspar-quartz mosaic with patches and flakes of green Fe-rich biotite (3–4% by vol). This biotite is of later generation as it fills microfractures and locally surrounds phenocrysts. Leucoxene is an accessory phase. Locally, plagioclase phenocrysts exhibit resorption textures.

3.1.2. Glenayle and Prenti dolerites

In the Glenayle and Carnegie areas a series of mafic sills (Glenayle Dolerite and Prenti Dolerite; Fig. 3) are associated with numerous northeasterly and west-northwesterly trending dykes. The mafic sills and dykes intruded a succession of siliciclastic sedimentary rocks of the Collier Basin (Salvation Group), north of the Earaheedy Basin, as well as parts of the northern and eastern Earaheedy Basin. This sill and dyke complex extends for about 150 km east-southeast and about 60 km in a northerly direction and is buried by Permian glaciogenic sedimentary rocks to the east. Individual sills are up to 100 m thick. Some sills consist of several thin (ca 1–2 m) sheets one above the other, each separated by a thin veneer of sedimentary rocks, indicating intrusion along bedding planes. Gabbroic textures are common in thicker sills. The total thickness of the Glenayle Dolerite sill complex is not known, but geophysical data suggest that it may extend to depths of 3–4 km (Morris et al., 2003). The mineralogy of the Glenayle Dolerite is dominated by plagioclase and clinopyroxene with or without orthopyroxene. The main feature of the Glenayle Dolerite is the presence of well developed interstitial granophyre, which tends to increase towards the top of the intrusion, where it can reach 20–30% by volume, locally forming pods and lenses. Accessory minerals include ilmenite, magnetite and titanomagnetite, quartz and apatite. In places, ilmenite and titanomagnetite occur as poikilitic blebs up to 5 mm across. Where altered, the alteration phases include biotite, hornblende, chlorite, sericite and prehnite. Accessory amounts of sulphides (pyrite and lesser chalcopyrite) are also present. Geochemical analyses of the Glenayle Dolerite can be found in Morris and Pirajno (2005).

The Prenti Dolerite is a petrological variant of the Glenayle Dolerite, and consists of aphanitic to very fine-grained dolerite sills and dykes of (Pirajno and Hocking, 2002). The Prenti Dolerite typically contains 50–55% by volume of plagioclase (An_{56-70}) and granular augite (partially replaced by chlorite and biotite), with an intergranular–glomeroporphyritic texture, defined by bunches of fresh plagioclase crystals. In some samples, disseminated Fe-Ti oxides make up to 10% of the rock. The Glenayle and Prenti Dolerite are part of the 1076 Ma Warakurna Large Igneous Province (Wingate et al., 2004), which covers about $1.5 \times 10^6 \text{ km}^2$, extending from the sill complexes of the Mesoproterozoic Edmund basin (Bangemall Supergroup; Martin and Thorne, 2004), through to the Glenayle–Prenti sill complexes in the Collier and Earaheedy basins in central Western Australia (Martin and Thorne, 2004; Pirajno et al., 2004), to the Giles mafic-ultramafic layered intrusions in the Musgrave complex in southern central Australia; a total west to east distance in excess of 2400 km. The formation of WLIP is postulated to be the result of a mantle plume that impinged onto the base of the lithosphere at about 1100 Ma (Morris and Pirajno, 2005).

3.1.3. Lamprophyres

Western Mining Corporation (WMC, now BHP Billiton) discovered ultramafic lamprophyre intrusions in the Bulljah Pool area of the Basin and south of the Lee Steere Range, in the eastern and northeastern parts, respectively, of the Earaheedy Basin. These rocks are unusual in that they contain small diamonds, a privilege normally reserved for kimberlites and lamproites. The lamprophyre intrusions in the Earaheedy Basin, together with marginally diamondiferous kimberlites and lamprophyres that intruded the Archean Marymia Inlier belong to the Nabberu Kimberlite Province (Shee et al., 1999).

Little published or unpublished information is available for the Jewill lamprophyre intrusions in Lee Steere (Fig. 2). The Jewill lamprophyre intrudes rocks of the Wongawol Formation and forms an east-northeast-trending linear body along a distance of 1.3 km, within

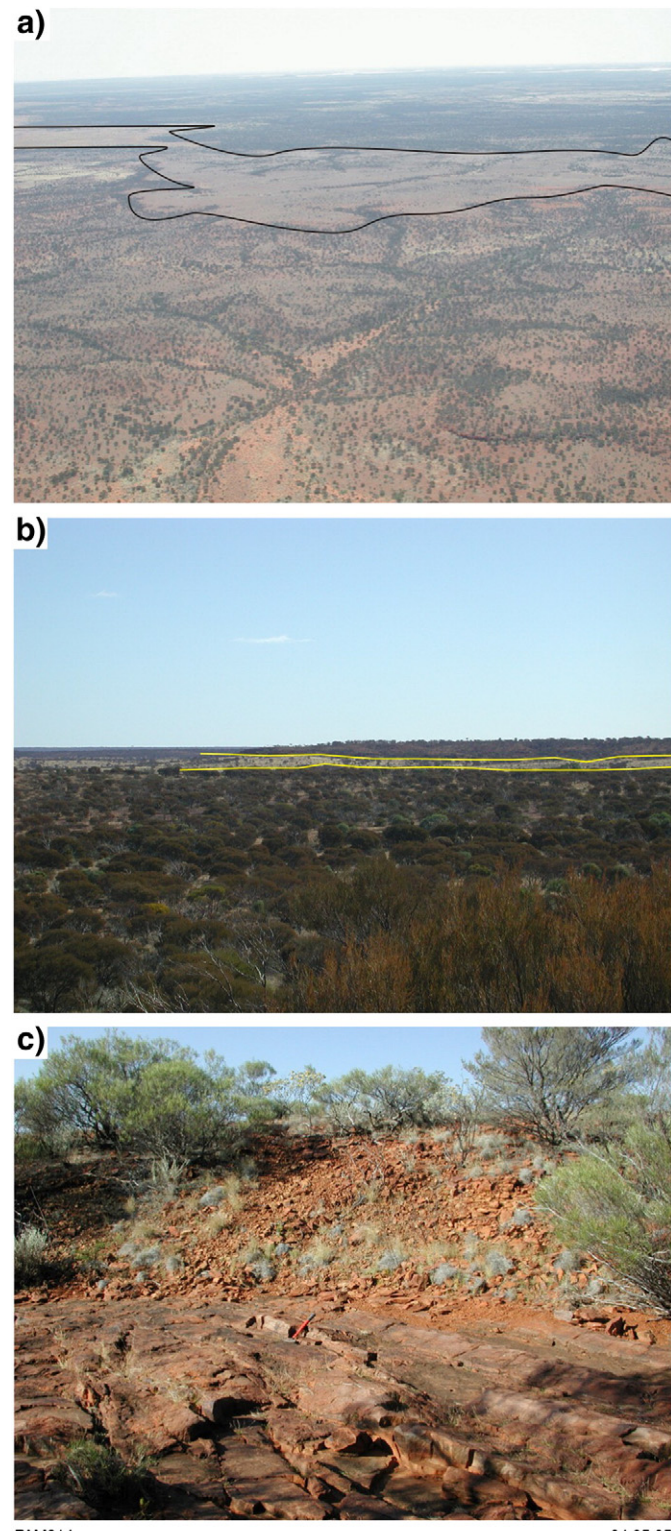


Fig. 3. Field photographs of Prenti Dolerite on Von Treuer; a) aerial view of a Prenti Dolerite sill (outlined); b) view of the same sill from the ground; c) outcrop of Prenti Dolerite in contact with sandstone of the Chiail Formation. After Morris and Pirajno (2005).

which four intrusive bodies (J1 to J4) were identified by drilling and another four inferred from drainage sampling (Carnegie Minerals N. L. Annual Reports 1994; 1995).

The Bulljah Pool ultramafic lamprophyres were studied by Hamilton (1992) and Hamilton and Rock (1990). The age of these

rocks remains unresolved. Hamilton (1992) cited a Rb-Sr mica age of 849 ± 9 Ma and an unpublished U-Pb zircon age of 305 ± 4 Ma. The Bulljah Pool lamprophyres intruded gently dipping units of the Kulele Limestone and Mulgarra Sandstone (described below). The four known intrusions were named BJ1, BJ2, BJ4 and BJ5 (a BJ3 feature was later recognised not to be a lamprophyre). BJ1 is sill-like, northwest trending and was traced for about 1 km. BJ2 is possibly a pipe or a lens-like intrusive body with an easterly strike and traced for about 400 m. The sedimentary country rocks (sandstone) display felsic alteration. BJ4 is small weathered outcrop. BJ5 is the most extensively explored Bulljah Pool ultramafic lamprophyre, whose surface expression appears to be a pipe about 50 m in diameter. Drilling beneath the pipe-like body, however, revealed that BJ5 consists of small dykes contained

in a pipe-like breccia with a steep northeasterly dip (Hamilton, 1992). Samples obtained from drill cuttings show that the Bulljah Pool lamprophyres mainly consist of abundant phlogopite, perovskite, iron spinel, almandine, diopside, olivine, titanomagnetite, chromite, apatite and trace amounts of picroilmenite, barite, zircon, pyrite, pyrrhotite, K-feldspar and rutile. Calcite and quartz veining are present. Alteration and/or weathering products include gibbsite, chlorite, hematite, kaolinite and smectite (Hamilton and Rock, 1990). The abundant phlogopite is a reddish-brown type, showing zoning and locally chloritised. Olivine is pseudomorphed by serpentine, chlorite and lesser carbonate. Chlorite also forms pools that may pseudomorph nepheline or melilitite (Hamilton and Rock, 1990). Mineral phases recovered from concentrates obtained from loam samples, in addition

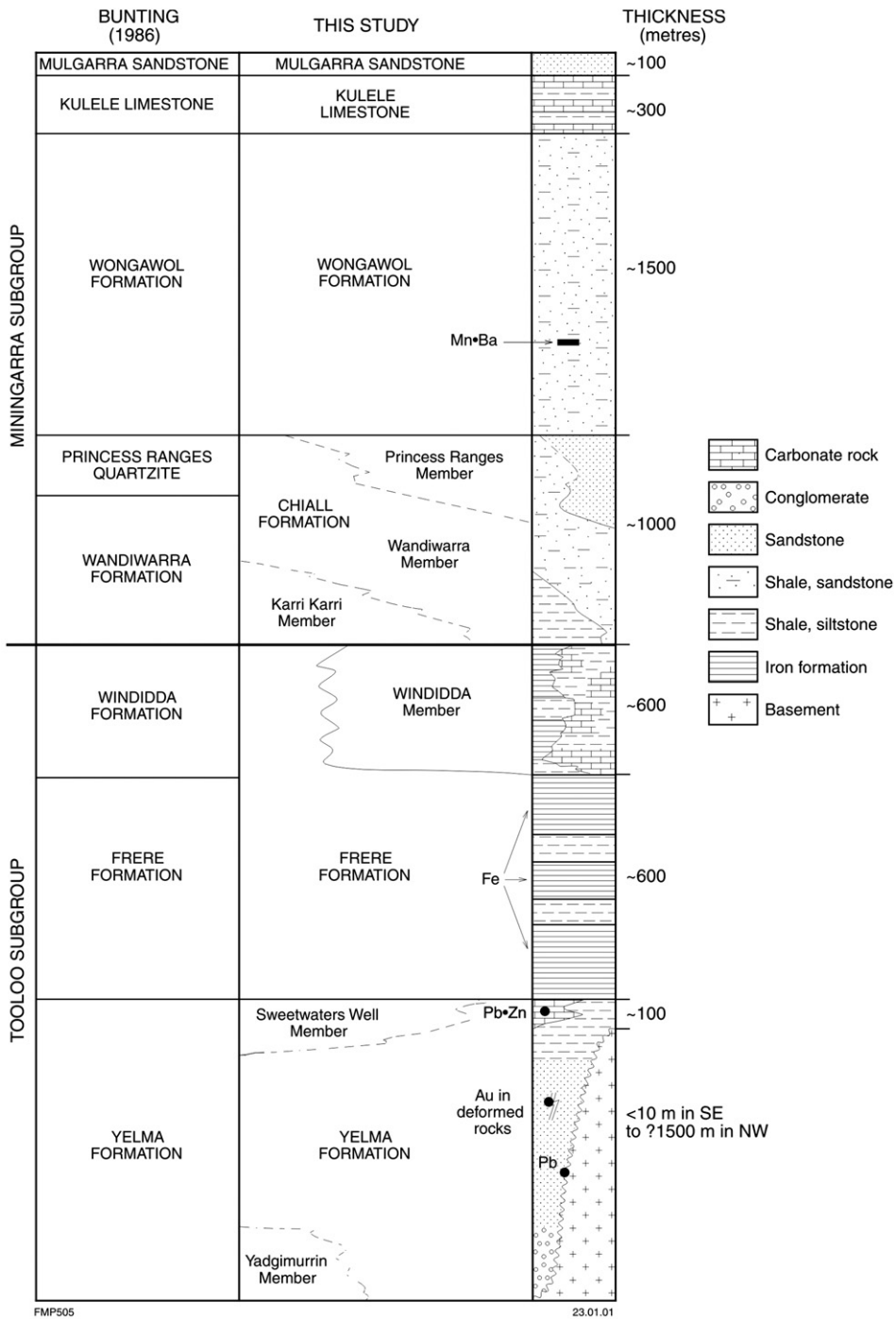


Fig. 4. Stratigraphic column of the Earaheedy Group.

to small diamonds, include chrome pyropes, spinels, ilmenites macro-crysts, chrome diopsides, garnets.

Mineral chemistry studies carried out by Hamilton and Rock (1990) show that the phlogopites are Ba-bearing titanian tetra-ferri-phlogopites. This type of phlogopite is common in the groundmass of kimberlites and lamproites, as well as ultramafic lamprophyres (Rock, 1990). Indeed, these micas fall within the field of ultramafic lamprophyres as defined by Rock (1990).

4. The Earaheedy Basin

The Earaheedy Group, as preserved, is a 5-km-thick succession of shallow marine clastic and chemical sedimentary rocks that is divided into two subgroups (Fig. 4; Hall et al., 1977). The Tooloo Subgroup consists of the Yelma Formation (base) and the Frere Formation (top). The overlying Miningarra Subgroup consists of the Chiall Formation (base), Wongawol Formation, Kulele Limestone, and Mulgarra Sandstone (top; Fig. 4). A schematic north-to-south section across the Earaheedy Basin is shown in Fig. 5. The regional structure is an asymmetric east-plunging syncline, with a vertical to locally overturned northern limb, due to compressive movements from the northeast, which created a zone of intense deformation along the exposed northern margin of the Earaheedy Basin. This zone of deformation, the previously mentioned Stanley Fold Belt, is characterised by reverse faults and shear zones that consistently dip steeply to the north, the development of slaty cleavage and phyllitic rocks and the appearance of metamorphic minerals (e.g. muscovite, sericite, chlorite). The intensity of deformation gradually decreases southward, but abruptly decreases to the north. Isolated small outcrops immediately north of the fold belt dip at low angles and are otherwise undeformed. In the sections ahead we discuss the available geochronology and describe in some detail the lithostratigraphy of the Earaheedy Group.

4.1. Geochronology

The geochronological data for the Earaheedy Basin are summarised in Table 2. A maximum stratigraphic age of 1.84 Ga is provided by the Mooloogool Group of the Yerrida Basin (Rasmussen and Fletcher,

2002), which the base of the Earaheedy Group unconformably overlies. A minimum stratigraphic age is provided by the overlying Scorpion Group (Bangemall Supergroup, maximum age of 1645 Ma; Martin and Thorne, 2001). In lieu of other data, Pirajno et al. (2000, 2004) and Jones et al. (2000) attributed deformation of the Earaheedy Group in the fold belt to the second phase of the Yapungku Orogeny (1790 to 1760 Ma; Bagas and Smithies, 1998; Bagas et al., 2000), which records the initial collision of the North Australian and West Australian Cratons (Myers et al., 1996). This is now considered a less probable cause than the Mangaroon Orogeny (1680–1620 Ma; Sheppard et al., 2005), which is known largely from the northwestern Capricorn Orogen. Supporting this correlation is an unweighted mean Ar–Ar age of 1648 ± 12 Ma from a muscovite in a schist rock in the Stanley Fold Belt and a detrital U–Pb Shrimp age of 1800 Ma from the upper Mulgarra Sandstone (see details below).

Minimum isotopic ages on glauconite grains in sandstone are provided for the Earaheedy Group by K–Ar and Rb–Sr ages of 1670–1710 Ma and 1556–1674 Ma, respectively (Preiss et al., 1975) from the Yelma Formation, and a K–Ar age of 1685 Ma (Horwitz, 1975a,b) from the base of the Chiall Formation. These ages may be related to post-depositional resetting during a deformational event, or by a thermal event possibly related to igneous activity, or a combination of these events. Pb–Pb mineralization ages of 1.65 Ga and 1.77–1.74 Ga are recorded, from outliers of Yelma Formation overlying the Yerrida Basin and the Sweetwaters Well Member (Fig. 2; Richards and Gee, 1985; Teen, 1996) respectively. These may reflect fluids mobilised during the late stages of the Yapungku Orogeny.

Grey (1994) suggested a depositional age of 1900–1800 Ma based on the stromatolite taxa of the Earaheedy Group and their similarity to taxa in the Duck Creek Dolomite of the upper Wyloo Group (Grey and Thorne, 1985). Pb–Pb whole-rock dating of carbonate in the Yelma Formation returned ages of 2010 Ma and 1950 Ma (Russell et al., 1994).

The current age constraints indicate a maximum age for the upper part of the Earaheedy Group of ca 1800 Ma, which could reflect deposition during the Capricorn Orogeny (1830–1780 Ma; Cawood and Tyler, 2004), or the Mangaroon Orogeny (1680–1620 Ma; Sheppard et al., 2007). The lower part of the Earaheedy Group is even less well constrained. It is unclear from current age constraints

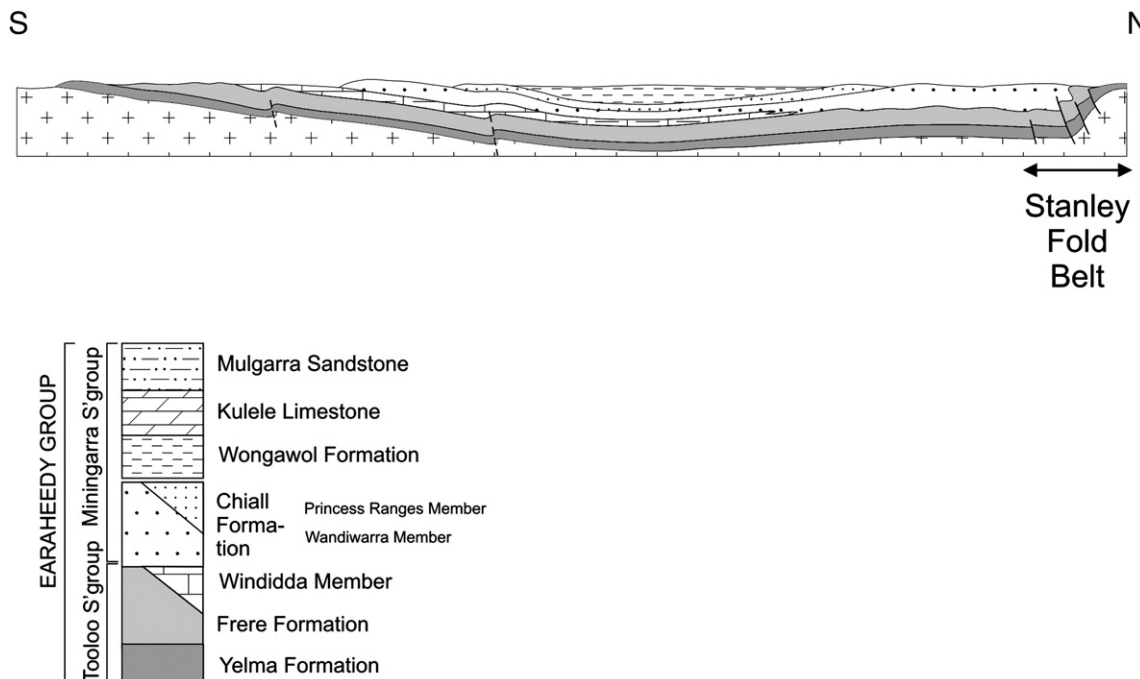


Fig. 5. Schematic north–south cross-section of the Earaheedy Basin and stratigraphy; note that the Mulgarra Sandstone and Kulele Limestone are not shown in this section.

whether there was a significant time break between the Mooloogool Group and the lower part of the Earaheedy Group. There is little evidence in the Earaheedy Group to suggest major active tectonism within the exposed depocentre for the Earaheedy Basin, although there is evidence to support continued sporadic tectonism, such as earthquakes, as suggested by the common presence of ball-and-pillow structures that may be seismites in rocks of the Chiall and Wongawol Formations.

4.1.1. Ar–Ar dating

A sample of quartz–muscovite schist, collected from drill cuttings (ca. 50 m depth) located approximately 5 km southeast of Well 7 on the Canning Stock Route was collected for $^{40}\text{Ar}/^{39}\text{Ar}$ analysis. The sample is possibly derived from deformed and metamorphosed siltstone interbeds in granular iron formation rocks of the Frere Formation and contains aligned muscovite and chlorite in a polygonal aggregate of recrystallised quartz grains. The rock was deformed during the formation of the Stanley Fold Belt.

Argon data were collected from two single grains of white mica (Grain 1 = 400×200 μm ; Grain 2 = 500×300 μm) hand picked from the crushed whole rock sample. These grains were chosen for analysis because they showed no signs of being broken fragments of larger grains and showed no visible signs of alteration. Analytical procedures and instrument details have been described elsewhere (Reddy et al., 2004). Argon data were collected by infra-red laser step-heating of single grains at the Western Australian Argon Isotope Facility, Curtin University of Technology. Data were corrected for measured background, mass spectrometer discrimination and nuclear interference reactions. Correction factors are as follows: $(^{36}\text{Ar}/^{37}\text{Ar})\text{Ca} = 0.000255$, $(^{39}\text{Ar}/^{37}\text{Ar})\text{Ca} = 0.00065$, and $(^{40}\text{Ar}/^{39}\text{Ar})\text{K} = 0.0015$. Corrections for $(^{38}\text{Ar}/^{39}\text{Ar})\text{K}$ and $(^{38}\text{Cl}/^{39}\text{Ar})\text{K}$ were not undertaken because of the Proterozoic age and low Cl characteristics of the samples and the short amount of time between irradiation and the time of analyses. $^{40}\text{Ar}/^{39}\text{Ar}$ ages were calculated using the decay constant quoted by Steiger and Jager (1977). J values and 1σ errors are noted in Appendix A. Errors shown in step-heating profiles (Appendix A) represent analytical errors and do not include J value uncertainties.

4.1.1.1. $^{40}\text{Ar}/^{39}\text{Ar}$ results. Muscovite age spectra are reported with 1σ errors in Appendix A and plotted with respect to cumulative $^{39}\text{Ar}\%$. Each step-heating profile represents the analysis of a single mica grain and both white mica grains yield similar ages. All mica analyses have negligible ^{36}Ar , indicating that there is no significant atmospheric ^{40}Ar component in the samples and also precluding the use of inverse isochron ($^{39}\text{Ar}/^{40}\text{Ar}$ vs $^{36}\text{Ar}/^{40}\text{Ar}$) plots to recognise any excess ^{40}Ar component. White mica data from individual Grain 1 yield relatively flat apparent age profiles with a range from 1628 to 1662 Ma and an unweighted mean age of 1648.2 ± 11.7 Ma. Individual step ages show some age variability but this variation is not systematic. Three of the steps define a plateau age of 1658.2 ± 1.4 Ma (MSWD = 1.5) that account for 57.6% of ^{39}Ar release from the sample. Grain 2 shows a similar range of ages (1632–1673 Ma) that yield an unweighted mean age of 1653.6 ± 14.4 Ma. In this case the spectra do not define a statistically valid plateau. In both grains there is no systematic relationship between age and either Cl or Ca content. The data from the two white mica grains therefore yield similar ages of ca. 1650 Ma.

4.1.2. Detrital zircon ages and provenance studies

Halilovic et al. (2004) conducted a study of sediment provenance based on the U–Pb SHRIMP age of detrital zircons. The results of this work are summarised below. Zircon (ZrSiO_4) is widely used for detrital dating studies because it is common in many rock types, and is chemically and physically resistant, which enables it to survive cycles of burial, metamorphism and erosion. The application of U–Pb dating of detrital zircons in sedimentary successions provides important constraints for the palaeogeography and tectonic settings of sedi-

mentary basins (e.g. Cawood and Nemchin, 2000; Nelson, 2001a,b). Age spectra provide insights into the nature and age of the source region. In addition, they constrain the timing of sedimentation with the youngest detrital zircons, giving a maximum age for the deposition of the sediments, whereas the oldest U-bearing minerals grown in situ provide both a lower limit of deposition, as well as valuable information on the timing of later tectonothermal events (McNaughton et al., 1999; Halilovic et al., 2004).

U/Pb data were obtained from 285 detrital zircons from six samples. Three from the basal Yelma Formation, one from the Wandiwarra Member and one from the Princess Range Member of the Chiall Formation, one sample from the stratigraphically youngest unit the Mulgarra Sandstone. Additional to this dataset are 27 zircons from a fine-grained arenite (Yelma Formation) analysed by Nelson (1997). Archaean and Proterozoic zircon populations are present in all samples except for one sample (JHE-42) of Yelma Formation from the northern margin of the basin, which contains only Archaean zircons. Results are shown on the frequency distribution diagram of Fig. 6.

Sample JHE-31b is a coarse-grained quartz arenite from the base of the Yelma Formation, about 0.5 m above the unconformity surface with granitic rocks of the Yilgarn Craton. Of the 74 zircon grains analysed, 18 show a range in age from approximately 3280 to 2000 Ma (Fig. 6). Zircons with Archaean ages fall into three groups with the youngest analyses of these groups showing a concordia age of 2531 ± 66 Ma. Zircons with a Palaeoproterozoic age fall into four groups, in which the youngest gave an age of 1983 ± 51 Ma (91% concordance).

Forty four zircons were extracted from sample JHE-143 (Yelma Formation, also from just above the basement unconformity), of which 37 show greater than 90% concordance. This sample's Archaean population has a range of ages from 2.95 to 2.60 Ga with a peak at 2.65 Ga (Fig. 6). The Palaeoproterozoic zircon populations show two distinct groups at 2.2 and 2.0 Ga, with the youngest discordant analysis yielding an age of 1990 ± 21 Ma.

Sample JHE-42 is from a fine-to-medium-grained arenite collected from the northern margin of the basin. Here the Yelma Formation is deformed in the Stanley Fold Belt. This sample yielded 15 zircons of which 12 were analysed. Ten analyses with more than 95% concordance gave a unimodal age distribution of between 2.7 and 2.6 Ga (Fig. 6).

Sample JHE-149, a sandstone from the Wandiwarra Member of the Chiall Formation, taken from the southern margin of the Basin. Of the 69 analysed zircons, 48 show a 90% concordance. The Archaean population contains two groups that are clustered around 3.0 and 2.8–2.6 Ga (Fig. 6). The oldest grain indicates an age of 3242 ± 15 Ma. The Palaeoproterozoic population of two groups exhibits age peaks at 2.25 and 2.06 Ga.

Sample JHE-40 is from a quartz arenite of the Princess Ranges Member of the Chiall Formation on Wongawol (Fig. 2). Palaeocurrent data from this site suggest a general northeasterly direction of sediment transport. Of the 40 grains analysed, 25 have concordancy of 90% or above. The oldest grain yielded an age of 3465 ± 13 Ma, but the majority having a range of between 2.9 and 2.6 Ga. The Palaeoproterozoic zircon population yielded ages ranging from 2.3 to 1.8 Ga, with the youngest single grain (97% concordance) having an age of 1876 ± 19 Ma.

Finally, a glauconitic quartz sandstone of the Mulgarra Sandstone, sample JHE-160, was taken from the base of the unit. From this sample 46 detrital zircons were analysed of which 25 show 90% or above concordancy. The Archaean population consists of a single analysis dated at 3190 ± 10 Ma and a series of analyses with a broad peak at 2.7–2.6 Ga (Fig. 6). The Palaeoproterozoic population consists of two groups, one with a peak at around 2.3 Ga, the other with a continuum of ages in the range 2.2 to 1.8 Ga. The youngest grain, 90% concordant, gave an age of 1796 ± 58 Ma. Four discordant analyses range from 1.79

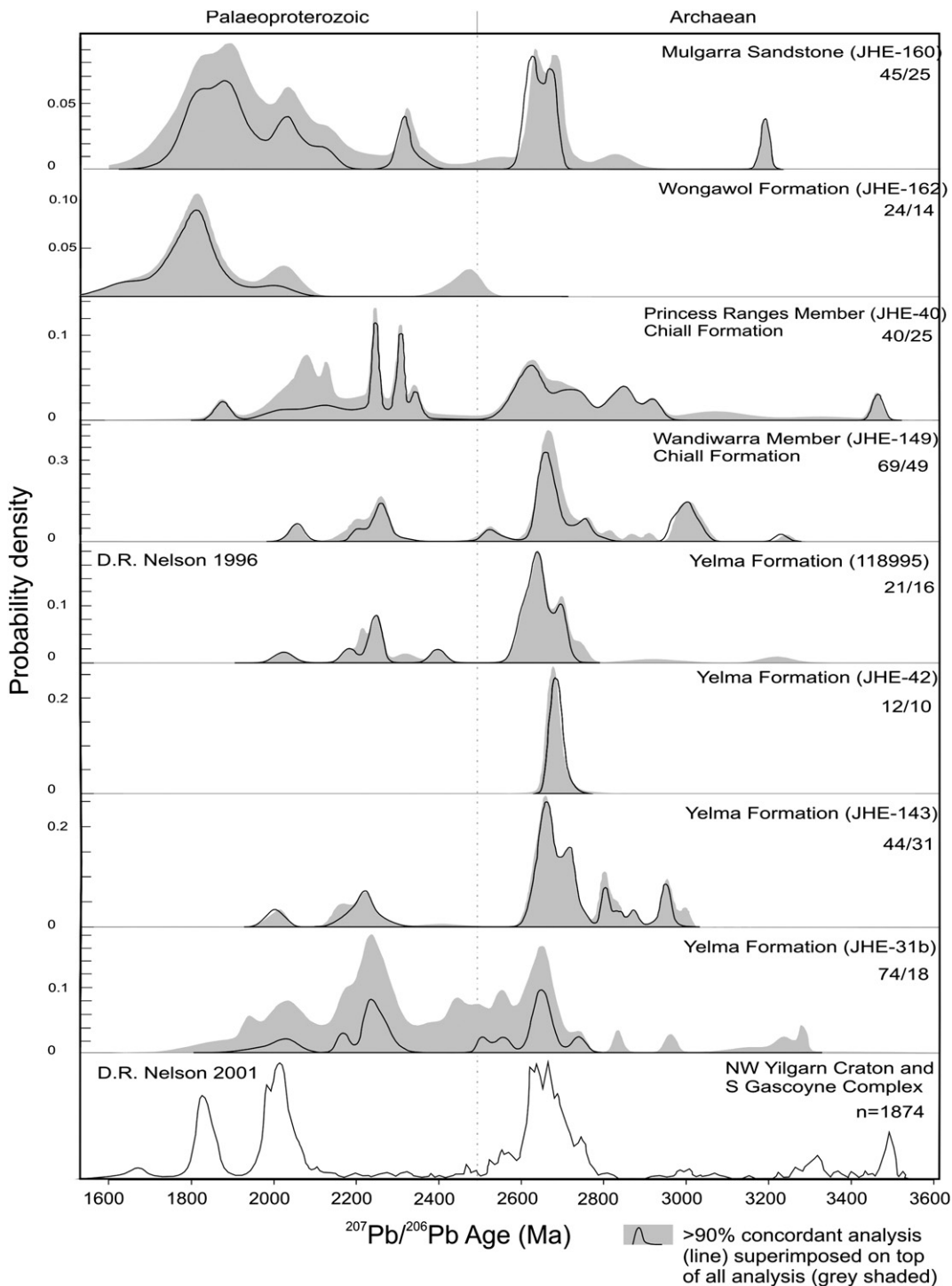


Fig. 6. Frequency distribution diagram of SHRIMP zircon ages of six samples from the Yelma Formation; also includes a summary plot from Nelson (2001a,b). The dashed line is the Archean–Proterozoic boundary taken at 2500 Ma. Numbers (e.g. 12/10) refer to total number of zircon analyses (shaded area) against the number of analyses more than 90% concordant (line on graph). After Halilovic et al. (2004).

and 1.73 Ga, but with large errors. The youngest most concordant age is 1808 ± 36 Ma.

Cathodoluminescence imaging showed that both Archean and Proterozoic grains have oscillatory zoning suggesting an igneous origin. The Archean zircons are well rounded or are broken fragments of larger grains. A number of Palaeoproterozoic zircons show evidence of recrystallisation.

The analyses of the 285 zircons, augmented by the earlier analyses of 27 zircon grains (Nelson, 1997) show multiple age peaks in Fig. 6 that clearly indicate detrital input from source regions of different

ages. The Palaeoproterozoic detritus is dominated by peaks in the age range of 2.3–2.2, 2.0 and 1.8 Ga, whereas those of Archean age are dominantly in the range 2.7–2.6 Ga, with the oldest in the 3.5 Ga bracket. A likely source of detritus with ages of 2.0 and 1.8 Ga is the southern part of the Gascoyne Complex (Sheppard et al., 2004). More specifically, this detritus could have derived from the granitic rocks of the 2005–1970 Ma Dalgaringa Supersuite of the Glenburgh Terrane (Sheppard et al., 1999; Occhipinti and Sheppard, 2001), whereas the 1.8 Ga zircon grains could have derived from the granites of the 1830–1780 Ma Moorarie Supersuite (Occhipinti et al., 1998). A possible

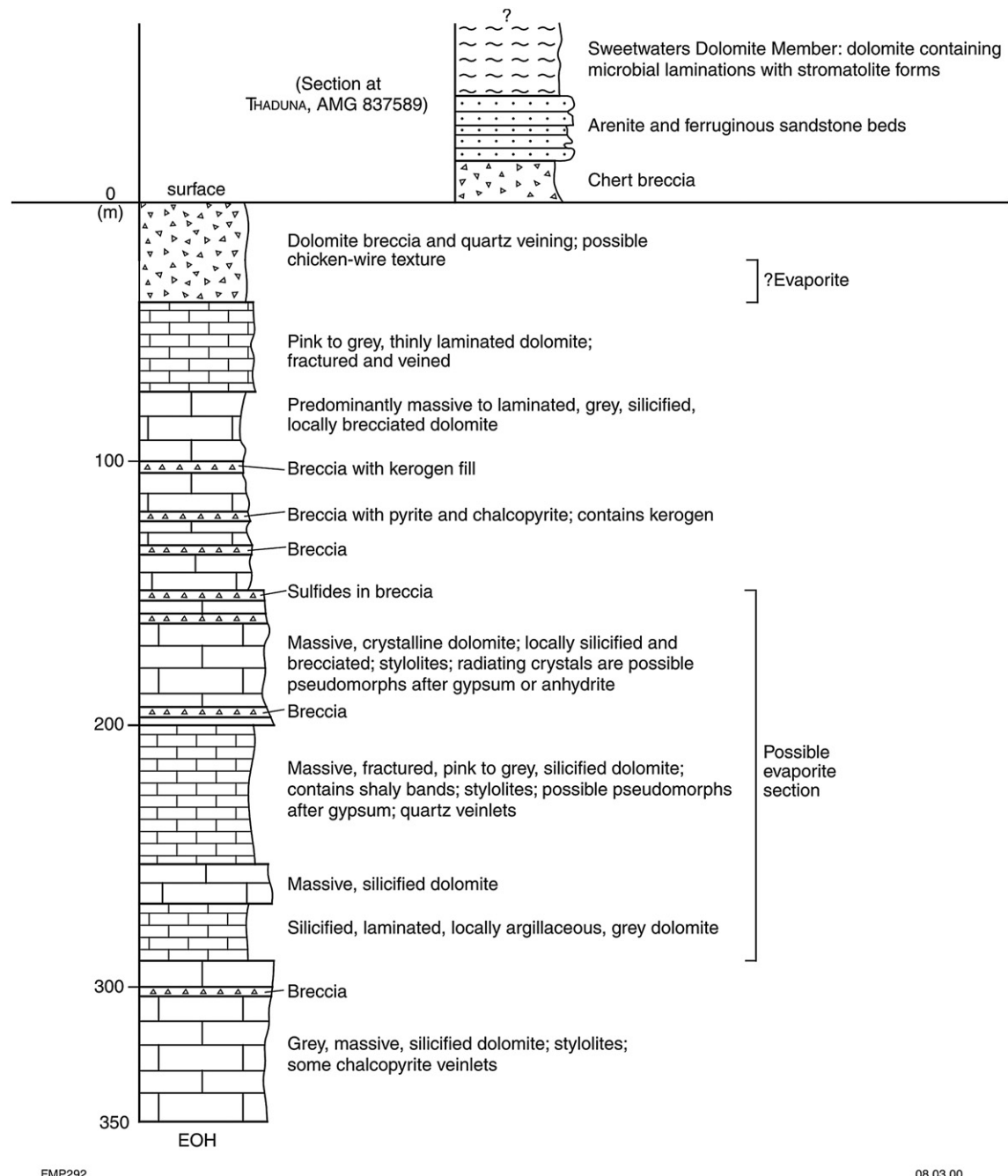


Fig. 7. Stratigraphy of the Yelma Formation on THADUNA, derived from drillhole CTW002 and outcrops near Lake Gregory. After Pirajno and Adamides (1998).

source region for the 2.3–2.2 Ga zircons is the Glenburgh terrane (Gascoyne Complex), on the basis of rims on zircons in basement gneiss of this terrane, which yielded ages of about 2.2–2.4 Ga (Kinyi et al., 2004). The youngest, single zircon grain, dated at 1.8 Ga, is from the Mulgarra Sandstone, and provides a maximum age for the upper Miningarra Subgroup. Another maximum age, for the base of the Eraheedy Group, is given by a U-Pb monazite age of 1843 ± 14 Ma (Rasmussen and Fletcher, 2002) from the Maraloou Formation, which is the youngest lithostratigraphic unit in the Yerrida Basin and is unconformable beneath the western Eraheedy Basin. Both ages are much younger than Pb-Pb carbonate ages for the Yelma Formation (see Table 2; and Russell et al., 1994) of 2.01 and 1.95 Ga, and the $\delta^{13}\text{C}_{\text{carb}}$ positive excursion in the same rocks suggesting an age of 1.9 Ga (Lindsay and Brasier, 2002). If the latter are correct, they could

be taken as supporting the concept of a significant hiatus between the Tooloo and Miningarra Subgroups.

In conclusion, detrital zircon populations, Ar-Ar dating of mica, and a monazite age from immediately beneath the basin, indicate that the deposition in the Eraheedy Basin began at most at about 1.84 Ga, concluded after 1.8 Ga but before 1.65 Ga. Palaeocurrent directions gathered during mapping show that the sediments of its depositional system had a significant source to the west and southwest, which may be related to uplift in the southern Gascoyne Province during the Capricorn Orogeny. The basin succession was deformed, and the Stanley Fold Belt developed, during the 1.68–1.62 Ga Mangaroon Orogeny (Sheppard et al., 2005), and possibly the Yapungku Orogeny at 1.79–1.76 Ga (Bagas, 2004), although the latter is very close in age to the maximum depositional age of the Mulgarra Sandstone.

Alternatively, the Yapungku Orogeny may mark, and be the cause of, an unconformity between the Tooloo and Miningarra Subgroups.

4.2. Lithostratigraphy

The Tooloo Subgroup contains the Yelma and Frere Formations (Figs. 2 and 4). The Miningarra Subgroup comprises, from older to younger, the Chiall Formation, Wongawol Formation, Kulele Limestone and Mulgarra Sandstone (Figs. 2 and 4), aggregating approximately 3000 m in thickness. These lithological units are discussed below.

4.2.1. Yelma Formation

The Yelma Formation is the basal unit of the Earaheedy Group and contains sandstone, shale, carbonate and minor siltstone and conglomerate and records a regional marine transgression. The formation is quite variable laterally and vertically in both thickness and composition. Sandstone beds in the southeast are trough cross-bedded, with local asymmetric ripples and mudcracks. Scattered stellate pseudomorphs may be after evaporitic minerals. A 100 m-thick stromatolitic carbonate facies in the southwest of the basin is differentiated as the Sweetwaters Well Member. At and near the surface, this stromatolitic dolomite is generally altered to chert. A sandy dolomite unit near the base of the Sweetwaters Well Member contains thin intercalations of volcaniclastic shard-rich silty beds that were presumably derived from contemporaneous, but distal, explosive volcanic eruptions. A localised conglomeratic unit, the Yadgimurrin Member, lies at the base of the Yelma Formation in the western part of the Earaheedy Basin (Merrie; Fig. 2).

The upper contact with the Frere Formation is marked by the first major occurrence of chert or granular iron-formation (Bunting, 1986), although in places stromatolitic forms persist between granular iron beds for up to 5–6 m above the contact. The thickness of the formation ranges from 3 m in the southeast, through 150 m in the type area (Hall et al., 1977), to at least 500 m in a drillhole in the northwestern part of the basin. Bunting (1986) estimated a thickness of 1500 m in the Stanley Fold Belt, but we interpret this as due to structural repetition.

In the westernmost parts of the Earaheedy Basin, the Yelma Formation is a unit of clastic and dolomitic sedimentary rocks at the base of the Earaheedy Group. This unit occupies much of the northeastern portion of Thaduna (Fig. 2) and consists mainly of quartz arenite, stromatolitic dolomite and chert breccia. In this area, the base of the Yelma Formation, includes quartz lithic sandstone and quartz conglomerate, which lie unconformably on quartz arenite of the Finlayson Member of the Juderina Formation (Yerrida Basin), and is exposed on the southern edge of Lake Gregory (Thaduna, Fig. 2). The main constituents of the lithic sandstone, near the base of the formation are quartzose and sericitised lithic grains, and subordinate polycrystalline quartz, chlorite and turbid feldspar.

Two boreholes drilled 3 km south of Little Well in Thaduna (Fig. 2), together with field observations, provide a representative 400 m-thick stratigraphic section of the Yelma Formation. This section, schematically represented in Fig. 7, consists of grey to pink, massive, silicified dolomite beds in the lower part. Argillaceous interbeds are locally present between 350 m and about 200 m below surface. This interval is overlain by a 120 m-thick unit of dolomite with solution breccia interbeds, containing some interstitial kerogen material and sulphides. This is in turn, overlain by about 100 m of pink to grey thinly laminated dolomite, dolomite breccia, ferruginous sandstone and arenite, followed by 20 m of dolomite with microbial laminae. The latter is a distinct rock, which may be part of the Sweetwaters Well Member.

Outcrops on the northwest side of Lake Gregory, consist of dolomite breccia, that is commonly chertified, cream-coloured and fine- to medium-grained, bedded and laminated dolomite with minor lenses of ferruginous sandstone and siltstone, associated with

stromatolitic dolomite. In the area around Edingunna Spring (Marymia; Fig. 2), outcrops of these units include silicified chert breccia, underlain by coarse breccia. This material is underlain by pebble beds, about 2 m thick, comprising subrounded to rounded pebbles up to 5 cm in diameter, dominantly of quartz and chert, and a coarse-grained, poorly sorted quartz (and feldspar?) arenite. The latter is probably the base of the Yelma Formation and may correlate with the Yadgimurrin Member (see below).

Most dolomitic rocks consist of a packed aggregate of small (averaging 0.1 mm) dolomite rhombs, with interstitial iron oxides. The dolomite also locally contains disseminated quartz grains and submicroscopic stylolites. Siltstone interbeds contain quartz, kaolinite, illite and sericite.

Sandstone in the Yelma Formation is typically well sorted and composed of well rounded quartz grains and minor detrital tourmaline and zircon. They are grain-supported and with a diagenetic microcrystalline quartz or chalcedonic quartz cement. Quartz sandstone is present in the eastern parts of the central uplift of the Shoemaker impact structure (Section 6). This rock is cross-bedded and consists of a packed aggregate of rounded quartz grains, showing diagenetic quartz overgrowths and minor detrital tourmaline and interstitial recrystallized quartz.

The Yelma Formation was deposited in a fluvial to coastal setting, with carbonates of the Sweetwaters Well Member developing in a saline coastal-lagoonal environment. Limited palaeocurrent data for the Yelma Formation on Wongawol suggest that sediment transport was towards the north-northwest. The Yelma Formation is interpreted to record a marine transgression over the Yilgarn Craton. Sedimentary structures suggest a shallow water to partly emergent, fluvial to coastal marine depositional environment, which was locally evaporitic at the base of the Yelma Formation. The upper part of the Yelma Formation suggests quiet water conditions and may reflect deposition in a lagoonal environment developed behind a carbonate bank, possibly represented by the Sweetwaters Well Member. As mentioned in Section 4.1.2, the detrital zircon populations are dominantly 2.6–2.7 Ga in age, with a smaller 2.2 Ga population, and minor 2.0 Ga zircons and suggest the Yilgarn Craton and southern Gascoyne Complex were important sediment sources during basin development.

4.2.1.1. Sweetwaters Well Member. The Sweetwaters Well Member is about 100 m thick and consists mainly of stromatolitic dolomite with sandy dolomite and dolomitic feldspathic sandstone beds at top and bottom of the dolomitic succession. The dolomitic feldspathic sandstone unit at the top of the dolomite grades eastward to a micaceous sandstone and is overlain by granular iron formation rocks of the Frere Formation. The lower contact is marked by about 15 m of transitional interbedded sandstone and dolomite passing upward to a sandy and feldspathic dolomite unit that contains quartz, microcline, albite, chert and micritic dolomite embedded in a coarse-grained dolomite cement. The Sweetwaters Well Member dolomite is light grey to grey in colour, massive to algal laminated, commonly with stromatolite forms. In northwest Nabberu (Fig. 2), the Sweetwaters Well Member was intersected in a number of drillholes sunk through the Frere Formation (Pirajno, 2004, 2002). Samples of stromatolitic dolomite collected from drill core show two phases or domains of dolomite, one is an aggregate of coarse-grained dolomite crystals, the other is microcrystalline (micritic) and is associated with microbial laminae. The coarser-grained dolomite has intergranular microcrystalline quartz and sericite. In some cases micritic dolomite forms peloids that are cemented by chalcedonic quartz. Locally, the carbonate material is replaced by cryptocrystalline quartz (chert) and chalcedonic quartz.

Along the southern shore of Lake Nabberu (Nabberu; Fig. 2), scattered outcrops of Sweetwaters Well Member are generally chertified, except for an area along a small tributary, where there

are good exposures of subhorizontal stromatolitic dolomite. Here, the dolomite exhibits fine microbial laminae and includes the stromatolites *Murzuna nabberuensis*, *Omachtenia teagiana* and *Asperia digitata* (Fig. 8; Grey, 1984, 1994). Drillcore sections indicate that stromatolites are generally present in metre-scale upward-shallowing cycles. They include *A. digitata* (Grey, 1984, 1994), which is believed to have grown in restricted, quiet water environment, possibly supratidal ponds; *Pilbaria deverella* (Grey, 1984) indicative of moderately high-energy, lagoonal conditions; and *Ephyaltes edingunnensis* (Grey, 1994), which formed in deeper quiet water, and *M. nabberuensis* (Grey, 1984) which colonised moderate energy patch reefs. Details of stromatolite taxa of the Earaheedy Basin can be found in Grey (1984, 1994). Grey (1994) suggested that these stromatolite forms are indicative of an upward shallowing, lagoon to supratidal, environment (Fig. 9a,b). It should be pointed out that the use of stromatolite taxa to identify depositional settings and relative ages is still contentious (see Altermann, 2004 for a brief review). However, in this work the identification of stromatolites does provide useful and reasonable constraints for depositional models, which are also supported by sedimentological evidence.

A sedimentological study, aimed at constraining the depositional environment of the Frere Formation, was carried out by Price (2003). In his study, Price (2003) defined 8 facies in the Frere Formation (see below) and 2 in the Yelma Formation. The facies of the Yelma Formation are: 1) Stromatolitic dolostone and 2) Dolostone. The former is a white creamy dolostone, with gentle wavy laminations and with alternating, ~20 m thick, horizons of *A. digitata* and *P. deverella*. The second facies, is a creamy white dolostone, with weakly developed wavy laminations and rare ripple cross-laminations and has

crystalline mosaic fabric. This facies contains rare *P. deverella*, which as mentioned above may have formed in a shallow lagoonal system.

4.2.1.2. Yadgimurrin Member. This is a localised very coarse, poorly sorted conglomeratic unit with sandstone lenses, about 100 m thick (Bunting, 1986) at the base of the Yelma Formation (Fig. 4), about 10 km southeast of the Baumgarten Reward gold deposit in the Marymia Inlier (Bagas, 1998a,b). The Member contains clasts that range from approximately 50 mm to 1 m in size, are well rounded and include granite, quartzite, chert, and chert breccia enclosed in an arkosic matrix. Pods and veins of jasperoidal chert and quartz are associated with this conglomerate and may be the result of localised hydrothermal fluid flow along the tectonic contact between the Marymia Inlier and the Yelma Formation (Adamides et al., 2000). Bunting (1986) suggested that some of these clasts are derived from the underlying Mooloogool Group of the Yerrida Basin (Pirajno et al., 2004). The Yadgimurrin conglomerate was assigned to the Yelma Formation by Bunting (1986) on the basis of the nature of the clasts and a distinct easterly dip. The Yadgimurrin Member is interpreted as a local conglomeratic fan, associated with syndepositional fault movements (Adamides et al., 2000).

4.2.2. Frere Formation

The Frere Formation, formally defined and described by Hall et al. (1977), records the onset of major Fe oxide precipitation within the Earaheedy Basin and consists of up to four major granular iron-formation intervals, separated by at least three major shale and siltstone bands, and minor carbonate (Fig. 10). The Frere granular iron formation (GIF), an important iron resource, is similar to the Superior

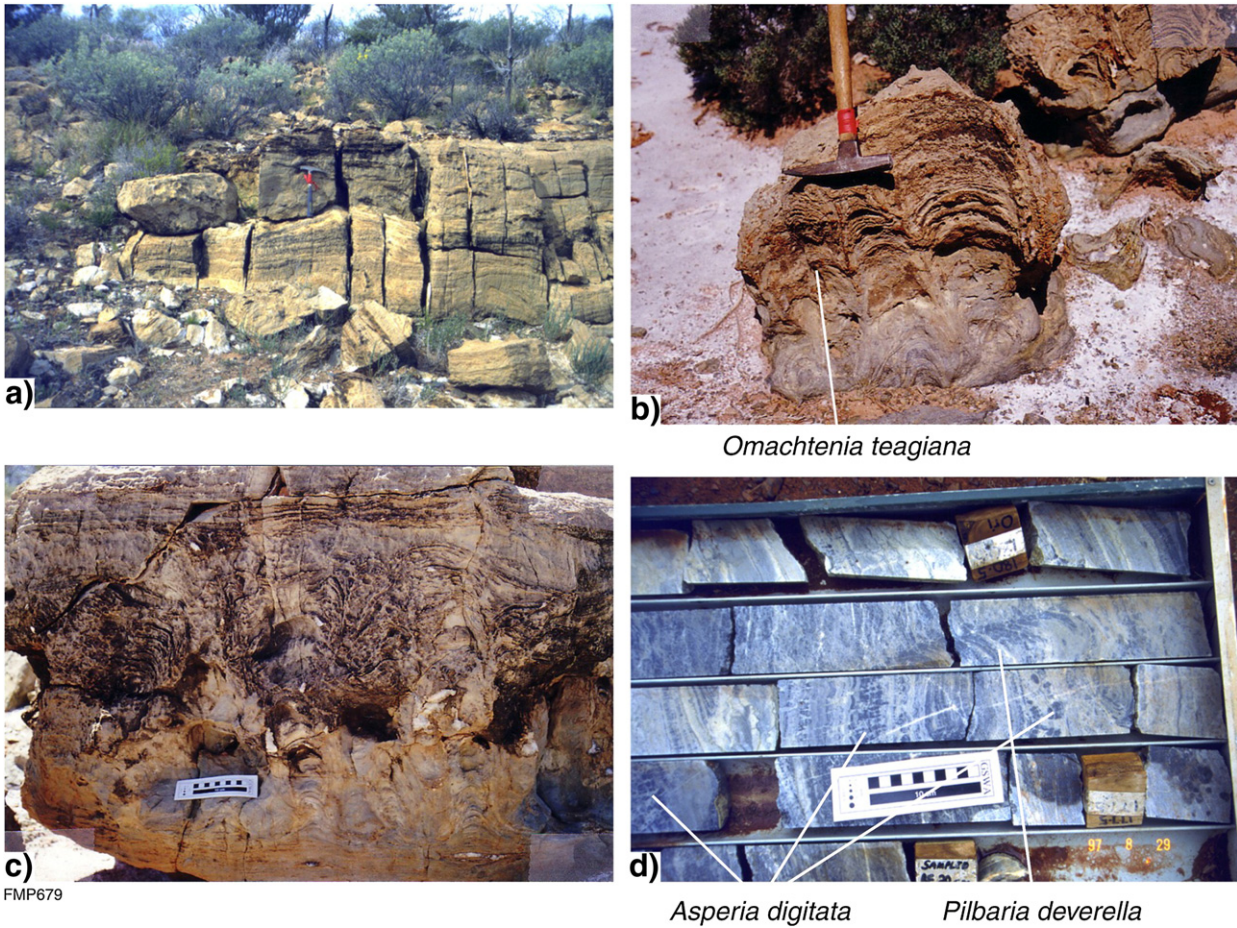


Fig. 8. Outcrops of Sweetwaters Well Member stromatolitic; a) microbial laminites; b) *Omachtenia teagiana* (Grey, 1984); c) unidentified stromatolite forms; d) drill core with *Asperia digitata* and *Pilbaria deverella* (Grey, 1984). After Pirajno et al. (2004).

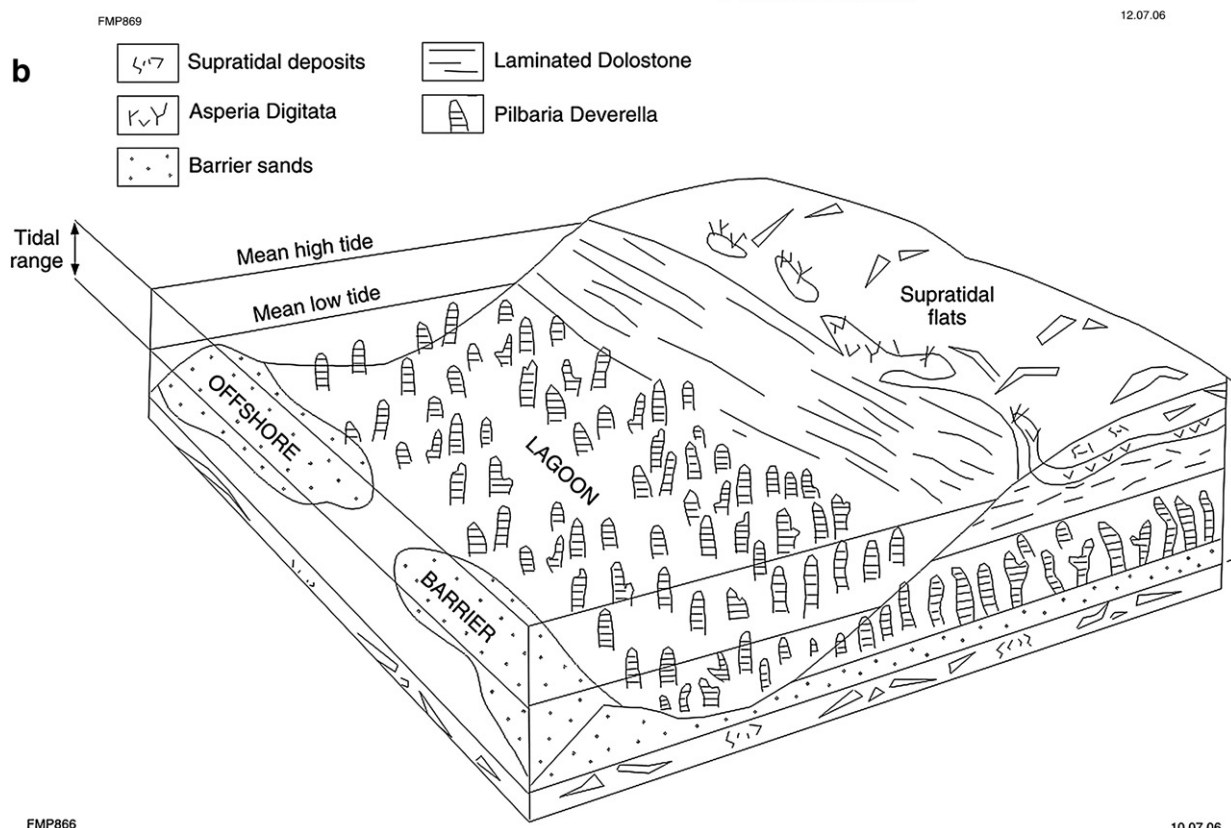
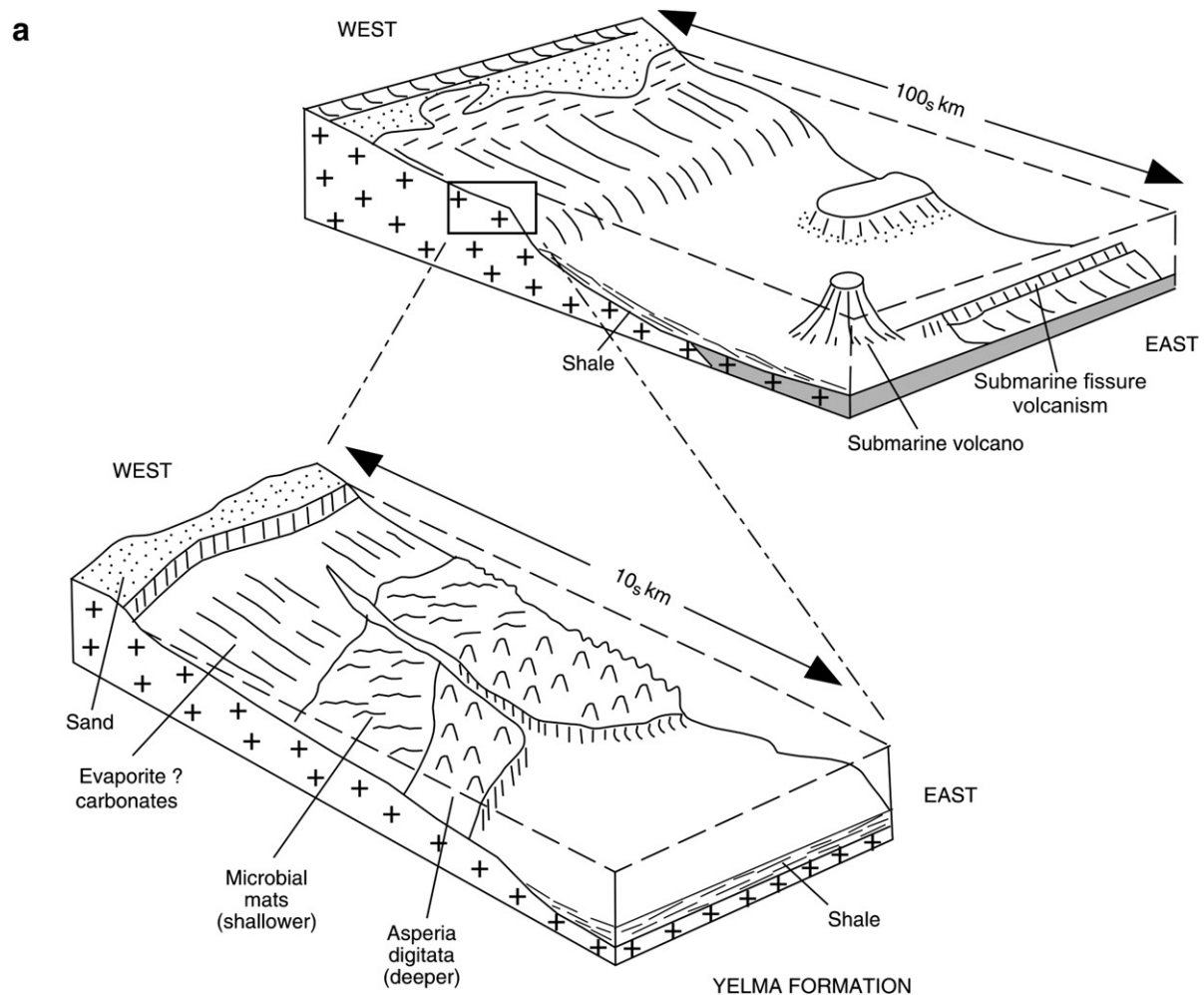
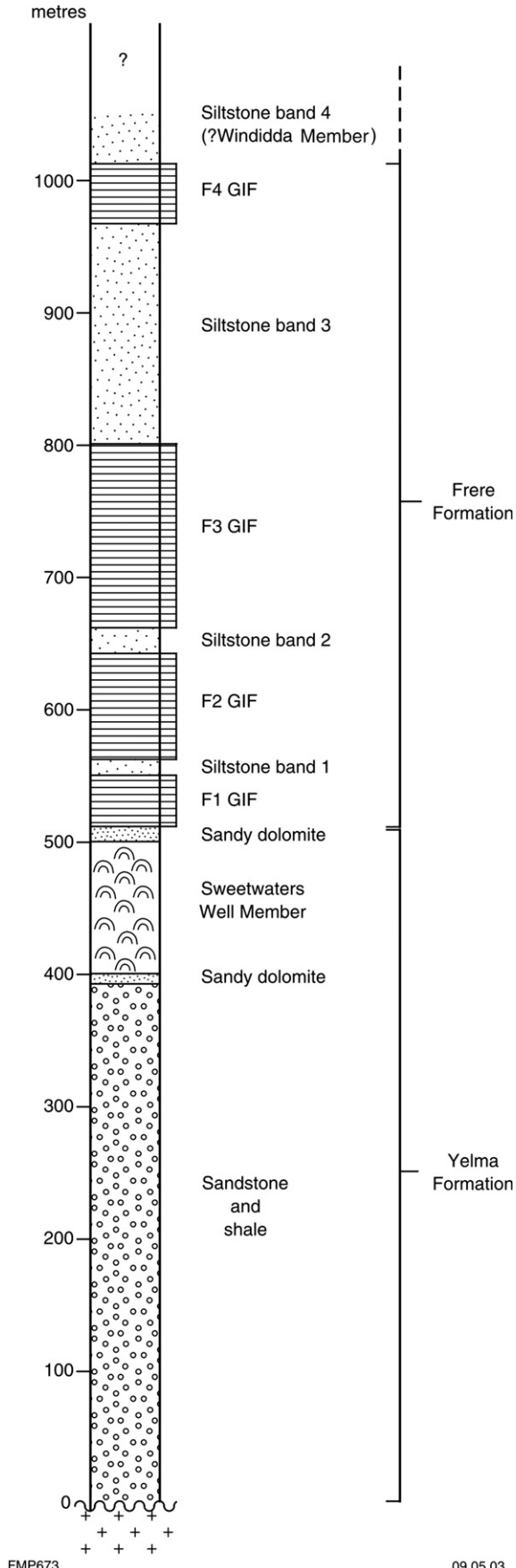


Fig. 9. Models of depositional environment for the Yelma Formation and associated stromatolite colonies (not to scale).



FMP673

09.05.03

iron formations and is one of few of these types of GIF recorded outside of North America (Goode et al., 1983; Trendall, 2002). The Frere Formation is exposed along the southern and northern margins of the Earaheedy Basin. On the southern margin the Formation is unmetamorphosed, undeformed or only mildly deformed, forming layers that are shallow-dipping to the north. On the northern margin of the Basin, the Frere Formation is deformed and folded into a south-verging synclinal structure with a steep to overturned limb (Stanley Fold Belt, see below). The total thickness of the Frere Formation was estimated by Bunting (1986) at about 1200–1300 m, but field evidence, suggests this thickness may be exaggerated due to structural repetition and we estimate the actual thickness of the Formation to be about 600 m.

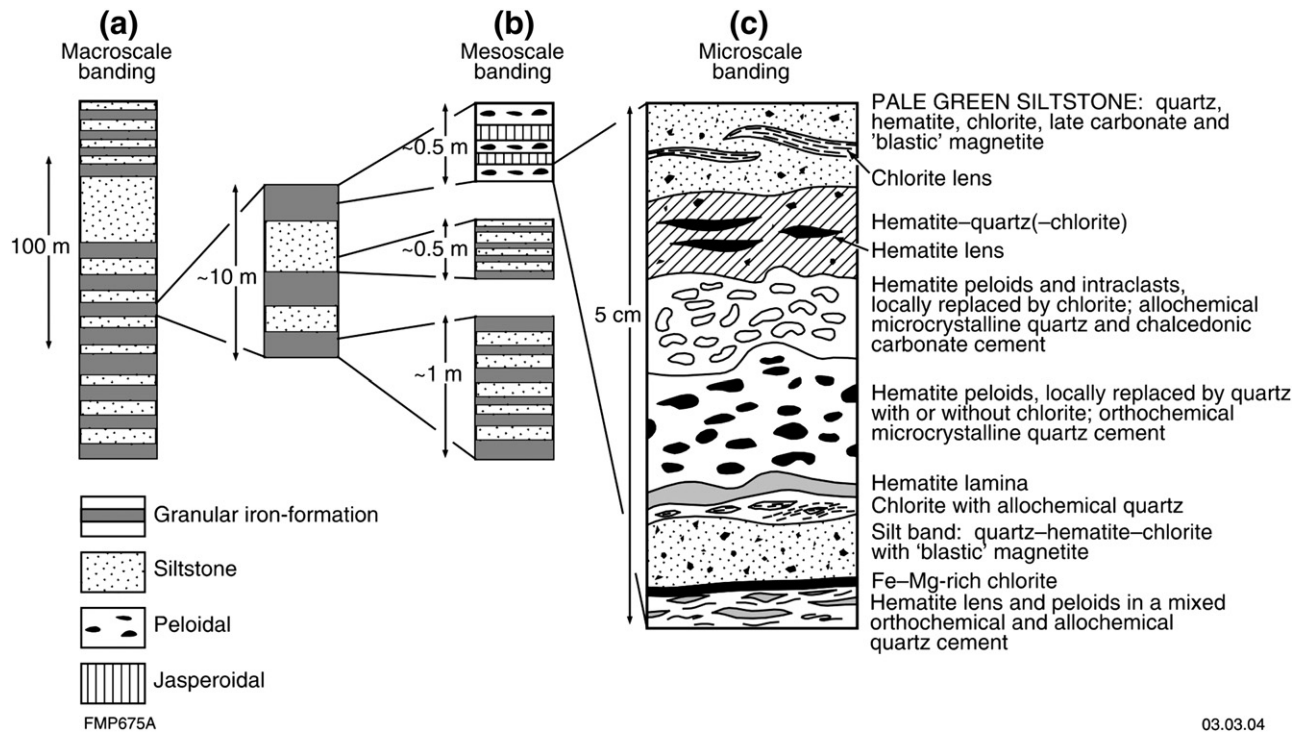
The Frere Formation consists of alternating beds of hematitic shale, green chloritic siltstone and granular iron-formation. Granular iron-formation horizons consist of granular iron-beds, typically between 0.5 cm and 20 cm thick, interbedded with jasper, chert, shale and siltstone. Drillcore and outcrop show that chert intraclasts are common and range in size from 1.5 cm to 35 cm. Contact between granular iron beds and siltstone units are commonly irregular and typically marked by soft-sediment structures, such as rip-up clasts, load and flame structures. The scale of the granular iron beds and siltstone banding ranges from millimetre to metre and up to 100s of metres (micro-, meso- and macroscale) and is similar to that recorded for banded iron-formations (Trendall, 2002; Fig. 11). The intercalated shale bands appear to increase in thickness at the expense of the granular iron-formation, towards the southeast. The upper contact with the Karri Karri Member of the Chiail Formation is transitional and defined as the last major chert, jasper or iron-formation (Hall et al., 1977).

Granular iron formation in the Frere Formation has a strong magnetic signature even through significant overburden, and is negatively magnetised in the south and positively magnetised in the north (Stanley Fold Belt). Overall the Frere Formation forms an almost continuous zone of high total magnetic intensity on aeromagnetic images, delineating the present-day geometry of the basin (Fig. 2b). Along the southern margin of the basin, northwest-trending structures are negatively magnetized, whereas east- and north-trending structures, as well as the circular structures that define the Shoemaker impact structure, are positively magnetized. In the Stanley Fold Belt strong positive magnetic signatures define deformation structures such as folds, reverse faults and shear zones.

The granular iron-shale/siltstone couplets of the Frere Formation are indicative of cyclic changes in primary sediment composition that probably relate to sea level changes and supply of iron and silica. Cross-bedding is locally visible in GIF beds, and in general sedimentary structures indicate traction-current deposition.

Granular iron formation in the Frere Formation is texturally and mineralogically similar to those in the Lake Superior region, North America. Walter et al. (1976) and Tobin (1990) described and compared microfossils within the iron-formation with those in the Gunflint Formation in the Superior Province. The Gunflint Iron Formation from that region contains microfossils (Gunflint-type microbial communities) that are similar to those found in the Frere Formation and in the Windidda Formation (Walter et al., 1976; Hall and Goode, 1978; Goode et al., 1983; Tobin, 1990). Gunflint-type microbiota are considered to be characteristic of marine subtidal environments (Tobin, 1990). These microfossils consists of contorted and/or randomly oriented filaments and include *Gunflintia minuta*, *Animikiae septata*, *Eoastrion simplex*, *Eoastrion bifurcatum*, *Huraniospora psilate*, *Kakabekia umbellata* and *Archaeorestis schreiberensis* (Walter et al., 1976; Tobin, 1990).

Fig. 10. Simplified stratigraphic column of the Tooloo Subgroup, compiled from drill core and field observations. The granular iron-formation has at least four bands (F1 GIF to F4 GIF) with three intercalated shale-siltstone bands; the topmost siltstone band could belong to the Windidda Member.



03.03.04

Fig. 11. Macro- (a), meso- (b), and microscale (c) banding of granular iron-formation of the Frere Formation; hematite peloids are cemented by quartz or quartz-carbonate. After Pirajno (2008).

In the Stanley Fold Belt, the Frere Formation is intensely deformed, with tight folds, sheared limbs, and reverse faults. On Rhodes and parts of Mudan (Fig. 2), the Frere Formation is intensely tectonised, forming mylonitic zones that resemble banded iron-formation (Pirajno et al., 2000; Pirajno and Hocking, 2001a,b). Similarly, in the northeast corner of Granite Peak (Fig. 2), exposures of the Frere Formation lie within the Stanley Fold Belt, where the GIF is tightly folded, tectonised and well-laminated, and is termed laminar iron-formation. It resembles banded iron-formation, but contains a pervasive fabric that is interpreted to be a tectonic overprint of the original bedding. Lamellae vary from reasonably continuous to discontinuous lenses and are generally between 10 and 50 mm thick. The limbs of folds in northeast Granite Peak are commonly brecciated and cut by quartz vein stockworks. On Nabberu, the Frere Formation is well-exposed in the Frere Range, along the northern side of Lake Nabberu, and in the Shoemaker impact structure, where it forms the inner collar (Pirajno, 2002).

Shale and siltstone intervals which separate GIF beds are similar to those of the Yelma Formation and the Karri Karri Member of the Chiall Formation. They commonly have a bedding fissility, accentuated by weathering. Siltstone is parallel-laminated, and trough and planar cross-laminated. Ripples are typically linguoidal or sinuous and interference patterns are common. Individual laminae are 1 mm to 10 mm in thickness. Massive greenish chert is locally present and exhibits remnant peloidal textures and quartz filled fractures, and lies parallel to a northwest trending, negatively magnetized structure. It is interpreted to be GIF that has been strongly silicified and fractured due to fluid flow along this structure.

An interesting aspect of the GIF rocks in the Earaheedy Basin is their common association with a small shrub. This shrub, *Micromyrtus ciliata*, is characterised by tiny, crowded bright leaves, pink buds and small white flowers. Where present, *M. ciliata* is the exclusive vegetation covering areas underlain by granular iron-formation rocks.

4.2.2.1. Textural features, petrography and mineralogy. The textural and petrological features of granular iron-formation were described in detail by Hall and Goode (1978) and Goode et al. (1983). A typical thin

section, sketched in Fig. 11, provides a good example of microscale banding. A granular iron horizon contains a 1-cm-thick band of closely packed hematite peloids and intraclasts, cemented by orthochemical cryptocrystalline silica (chert) and/or allochemical chalcedony. This band is overlain and underlain by 1–4 mm thick laminae of pale green silt composed of green iron-rich chlorite (Fig. 12b), anhedral hematite, abundant disseminated euhedral magnetite crystals and angular quartz, overprinted by carbonate, and lenses of chlorite-quartz.

Individual granular iron-formation beds consist of chert (cryptocrystalline silica), iron oxides (hematite and/or magnetite; Fig. 12c, d, e), microplaty hematite (Fig. 12f), and jasper (cryptocrystalline silica with finely disseminated hematite) peloids in a cherty, chalcedonic (allochemical) or jasperoidal (orthochemical) cement (Fig. 12a, b, c). Peloids commonly exhibit concentric laminae, especially where the peloids are partially replaced by microcrystalline quartz (Fig. 13a, b, c, d). Hematite is replaced by microplaty hematite and/or magnetite in GIF beds deformed in the Stanley Fold Belt. In fractures and zones of deformation the granular iron formation beds are pervasively silicified, with the peloids and the interbedded iron-chlorite-rich shale replaced by stilpnomelane. Maghemite and martite replace the hematite and magnetite in zones of supergene alteration. Shale and siltstone units are parallel-laminated, and contain quartz, iron-rich chlorite and disseminated euhedral magnetite. The sphericity of peloids is highly variable and generally depends on the degree of early diagenetic compaction and lithification. The average spherical dimensions of over one hundred peloids indicate the long axes of the ellipse average 0.52 mm, whereas the short axes average 0.26 mm, with a length to width ratio of 2.0. Peloids commonly contain syneresis cracks infilled with quartz or chalcedony.

Examination of drill core reveals that thin bands (few cm) of peloidal carbonate are locally intercalated with the granular iron-formation. Typically, carbonate peloids exhibit close packing, are plastically deformed and commonly replaced by stilpnomelane and/or euhedral magnetite (Fig. 13d, e, f).

Reflected-light petrographic studies of the granular iron beds reveal that the main iron minerals are hematite (microplaty, blades and irregularly-shaped blebs), magnetite, maghemite, martite and

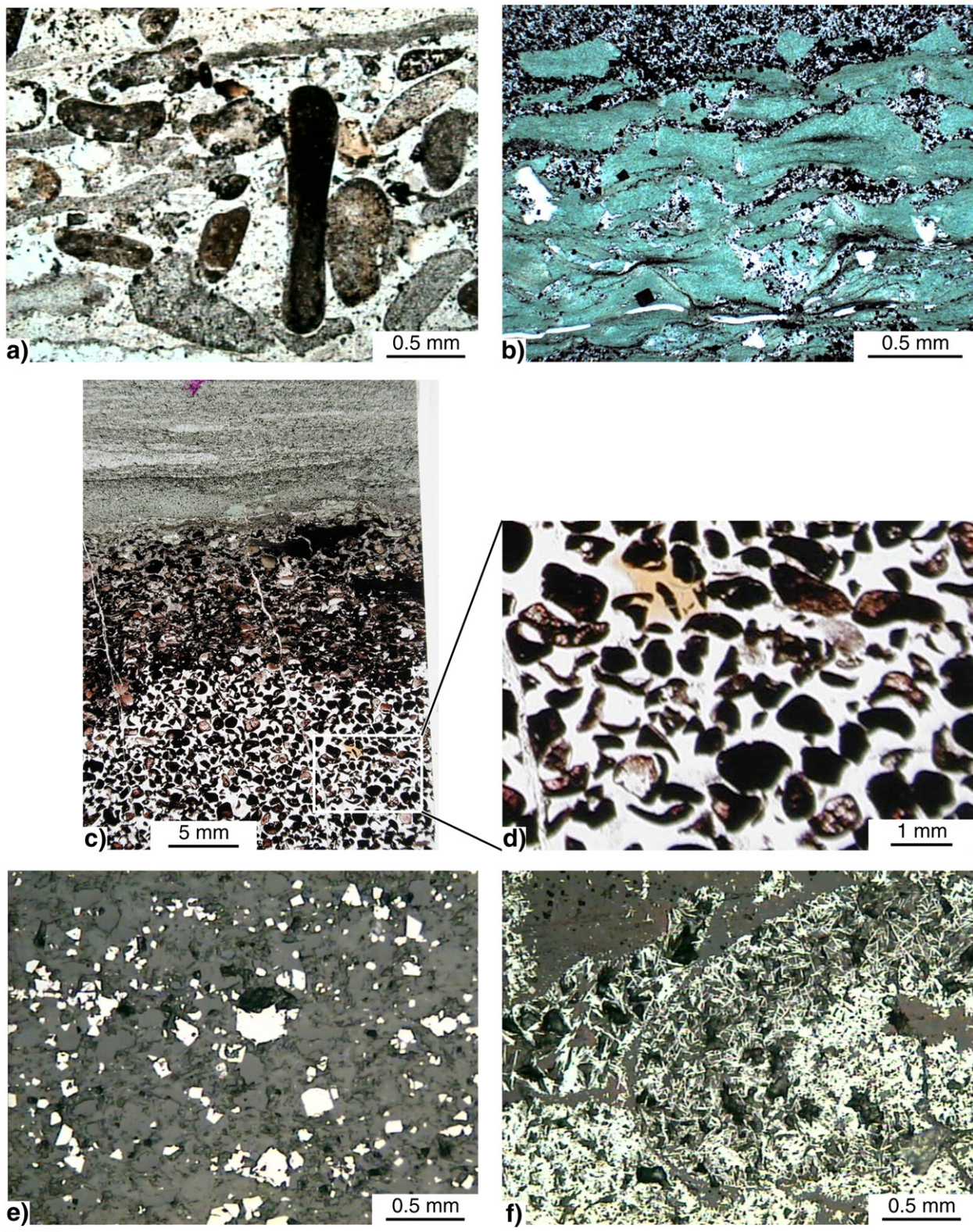
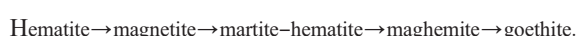


Fig. 12. Photomicrographs of granular iron-formation in the Frere Formation: a) intraclast and jasperoidal peloids in a siliceous matrix; b) chloritic shale intercalated with peloidal iron-formation. The pale green chlorite is a ferroan clinochlore (X-ray diffraction analysis) associated with quartz, kaolinite, and opaque; c) peloidal ironstone; d) detail of (c); e) disseminated euhedral magnetite crystals in chloritic siltstone band; f) detail of peloid composed of microplaty hematite minerals. a) to d) plane-polarized light; e) and f) reflected light. After Pirajno et al. (2004).

goethite (Fig. 12e, f). Maghemite and martite are products of the oxidation of magnetite, whereas goethite is related to recent weathering. Magnetite crystals are especially common along faults and in deformed Frere Formation.

A possible paragenesis of the iron minerals is:



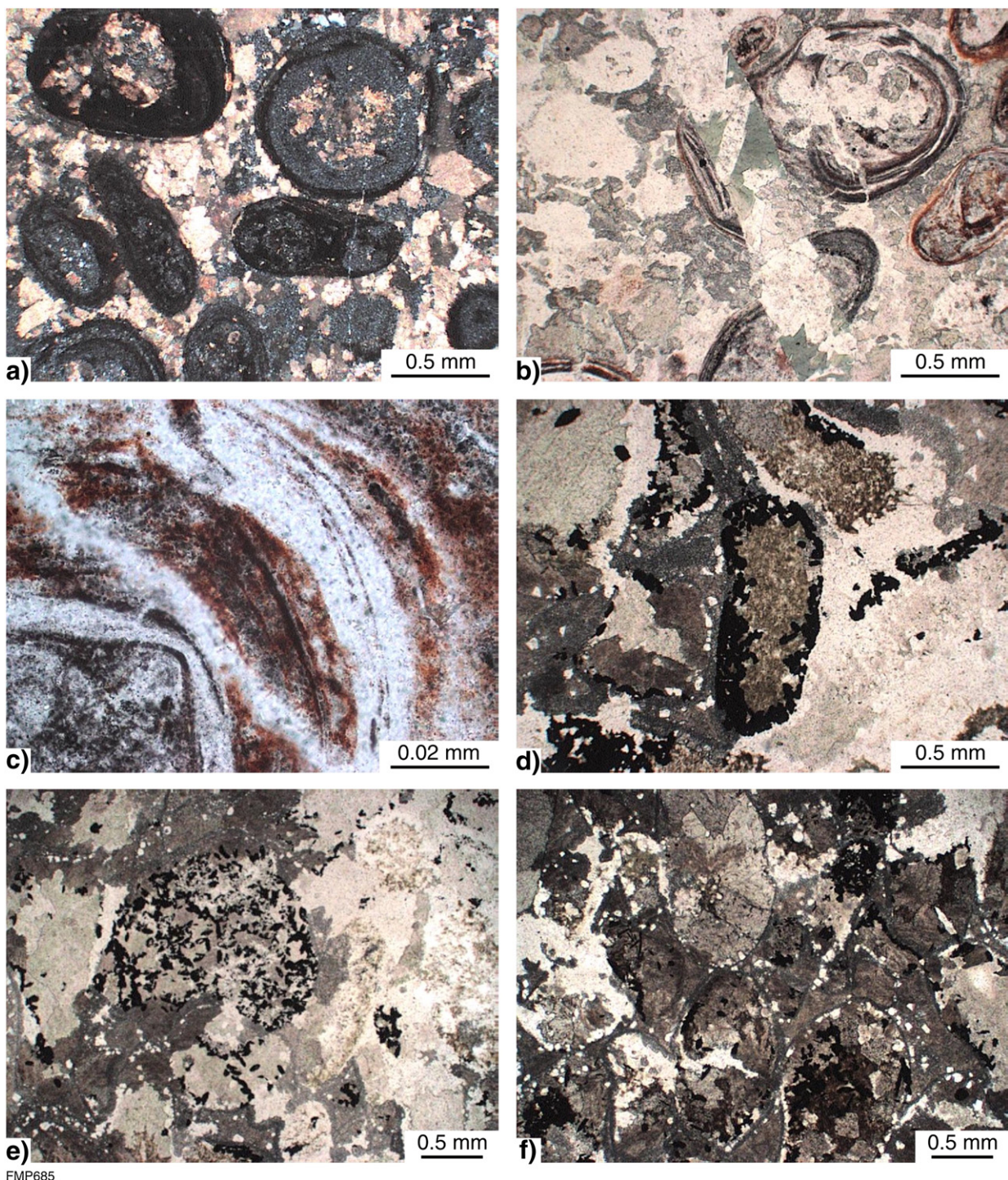
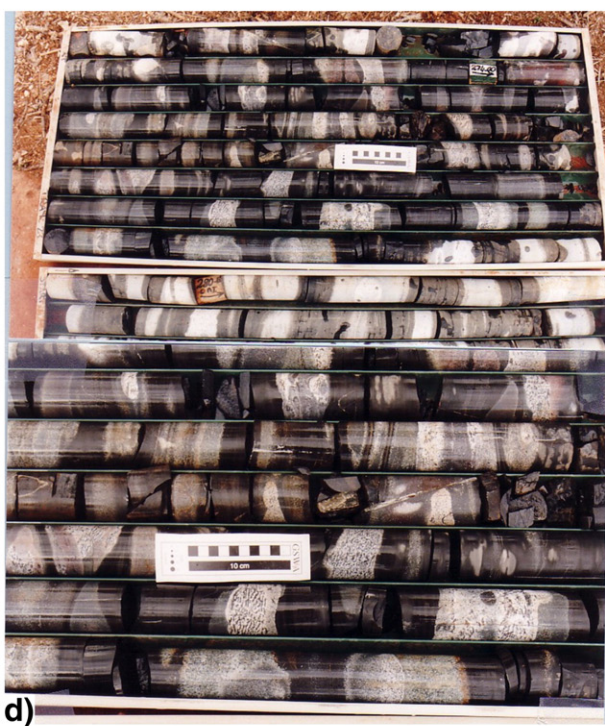
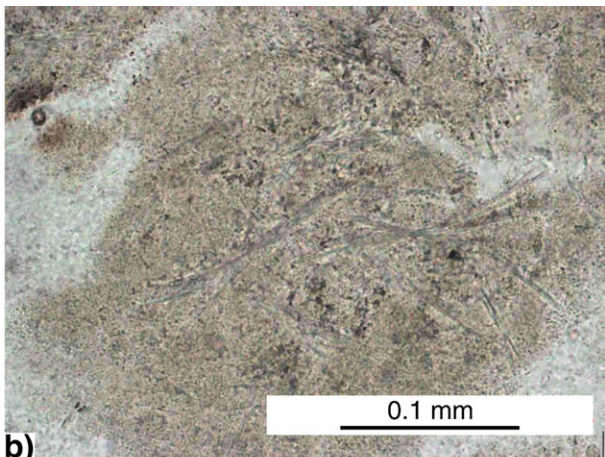
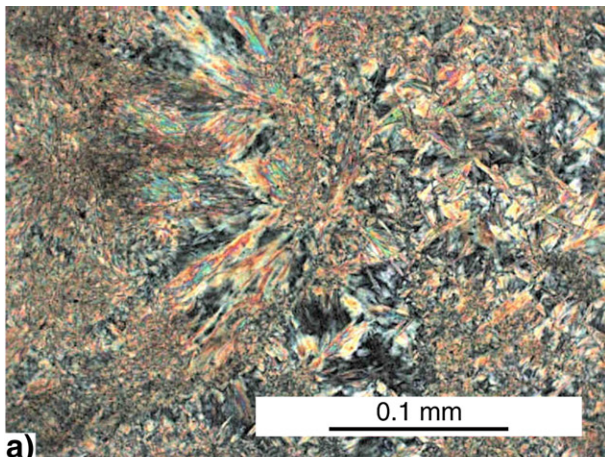


Fig. 13. Photomicrographs showing aspects of alteration of granular iron-formation in the Frere Formation: peloids partly replaced by cryptocrystalline quartz (chert) and cemented by allochemical dolomite; b) with cross-cutting quartz–chlorite–carbonate veinlet; dark concentric laminae in the peloids are composed of hematite; c) detail of replacement of peloid by cryptocrystalline quartz; d) peloidal carbonate intercalated with granular iron-formation; here the peloid in centre of photomicrograph is replaced by chlorite (core) and microplaty hematite along the margins, surrounding material is dolomite, chlorite, and microcrystalline quartz; e) and f) carbonate peloids partly replaced by hematite and cemented by chlorite,?orthochemical dolomite and locally stilpnomelane (not visible in this section). All in plane-polarized light, except for a) which is with crossed polars. After Pirajno et al. (2004).

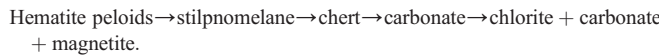
This sequence may have resulted from the deposition of primary hematite, followed by hydrothermal magnetite along fault zones, subsequent to oxidation to produce martite and maghemite, and late supergene redistribution of iron to precipitate the goethite.

4.2.2.2. Alteration of granular iron-formation. Alteration of the Frere Formation is common, especially along faults and in fractures around the

Shoemaker impact structure and close to the Lockeridge Fault (Fig. 2). This alteration is manifested by cryptocrystalline (chert), microcrystalline and chalcedonic quartz, and carbonate that replace the Fe oxide peloids and the orthochemical ferruginous or jasperoidal matrix. Stilpnomelane and minnesotaite are also present and may be locally abundant. In places, stilpnomelane forms pervasive replacements. Some of the more typical alteration features are illustrated in Figs. 14 and 15.



West-northwest of the Shoemaker structure, diamond drillholes intersected Frere Formation rocks that exhibit varying degrees of stratabound alteration. This alteration consists of more than one phase of silicification and replacement by stilpnomelane and carbonate (probably dolomite). The paragenesis of this alteration is difficult to gauge because the same alteration minerals appear in more than one event. However, in general, the following paragenetic sequence can be reconstructed, on the basis of petrographic studies:



In places, only one event can be seen, e.g. carbonatisation (Fig. 15a, b), or total replacement of the chloritic siltstone by stilpnomelane (Fig. 15a, b). In other instances two or more alteration events are observed, such as partial silicification overprinting peloids that had been earlier replaced by stilpnomelane (Fig. 15e), and by late magnetite (Fig. 15d, f). Similarly, all stages of carbonatisation are present, from localised development of carbonate rhombs (Fig. 15b, c) to more pervasive carbonate alteration. Late alteration phases include magnetite, which overprints dolomite (Fig. 15f) or magnetite + stilpnomelane + chlorite in late fractures that cut across all phases. Peloidal carbonate also exhibits alteration, which consists of microcrystalline silica, chlorite and stilpnomelane, with a late overprint by euhedral magnetite (Fig. 15e, f).

Carbonate porphyroblasts and dolomitisation are also associated with the sulphide mineralization in the Sweetwaters Well Member stromatolitic dolomite (Pirajno, 2002).

Stilpnomelane, a complex K, Ca, Na, Fe, Mg, Al hydrous silicate, is common in iron-formation world-wide and is generally found in Fe and Mn-rich low-grade regionally metamorphosed sedimentary rocks (Deer et al., 1965). Stilpnomelane-rich beds have been reported from the banded iron-formation of the Transvaal Supergroup in South Africa (LaBerge, 1966; Beukes and Klein, 1990) and the Hamersley province in Western Australia (LaBerge, 1966; Trendall, 2002). Here, the stilpnomelane beds have been interpreted as products of low-grade metamorphism of volcanic ash (LaBerge, 1966; Beukes and Klein, 1990). The stilpnomelane, silica and carbonate replacement of beds of granular iron-formation rocks in the Earaheedy Basin is interpreted to be related to K-Si-Ca-CO₂-rich basinal fluids (Pirajno et al., in press). Stilpnomelane preferentially replaces Fe-chlorite-rich siltstone interbeds and a possible reaction to explain the change from Fe-rich chlorite-dominated siltstone beds to stilpnomelane-dominated beds is (Deer et al., 1965):



4.2.2.3. Facies analysis. Price (2003) recognised 8 facies in the Frere Formation, determined on the basis of sedimentary structures, grain size, composition, matrix/cementing material. Details are given in Table 3.

4.2.2.4. Rare earth elements (REE) geochemistry. Price (2003) also conducted a comparative study of the abundance of REE in the granular iron formation with those of two other Precambrian iron formations, Gunflint in Canada and Griquatown in South Africa. The following is summarised from Price's work.

The Gunflint iron formation in Ontario is also a granular iron formation, composed of peloids and ooides in a predominantly quartz cement. Whole rock Sm-Nd isochron dating indicates that the Gunflint iron formation was deposited at around 1900 Ma (Jacobsen and Pimentel-Klose, 1988). The geochemical dataset used by Price (2003) was taken from Derry and Jacobsen (1990). The Griquatown

iron formation of the Transvaal basin in South Africa is a granular iron formation that overlies the Kuruman microbanded iron formation (Beukes and Klein, 1990). The Griquatown iron formation consists of chert-rich peloids and intraclasts in a chert cement (Beukes and Klein, 1990). Radiometric ages indicate that the Kuruman and Griquatown iron formations were deposited between 2357 ± 53 and 2239 ± 90 Ma (Walraven et al., 1990). The geochemical dataset of the Griquatown iron formation was taken from Beukes and Klein (1990). REE patterns for the Gunflint and Griquatown iron formation are shown in Fig. 16.

The distribution of samples of peloidal granular iron formation collected during field mapping is shown in Fig. 17a. In addition to REE, these samples were also analysed for major and trace elements by Genalysis Laboratory Services (Perth) using ICP-MS and results are presented in Table 1 in Appendix A. Eleven samples were selected for the study of REE abundances, all containing in excess of 15 wt.% Fe₂O₃. The data were normalised to NASC (North American Shale Composite; Gromet et al., 1984) and the relevant diagram shown in Fig. 17b. The REE patterns show a slight HREE depletion relative to LREE, with the exception of 3 samples. Some samples show a marked negative Ce anomaly, and all samples exhibit a weak positive Eu anomaly. By comparison with the Gunflint and Griquatown iron formation, the Frere Formation contains higher REE concentrations. The positive Eu and negative Ce anomalies in the Gunflint and Griquatown possibly represent high temperature hydrothermal input in a seawater dominated system (Beukes and Klein, 1990; Bau and Moller, 1993; Klein and Ladeira, 2000). The similar REE patterns for the Gunflint and Griquatown iron formation suggest a similar depositional mechanism. The differences of the Frere Formation REE patterns may be due to one or more of the following: 1) contamination in the Frere rocks by clastics; this is supported by the high abundances of TiO₂ and Al₂O₃ (see Appendix A). 2) The Frere rocks were probably deposited in shallower water than the Gunflint or the Griquatown iron formations; this is shown by differences in HREE patterns and the Ce anomalies.

4.2.2.5. Windidda Member. Bunting (1986) considered the Windidda Formation as a separate unit that overlaid the Frere Formation, but subsequent to mapping showed that the former Windidda Formation is stratigraphically equivalent to the upper part of the Frere and for this reason it is now considered a Member of the Frere Formation. The Windidda Member is typically characterized by poorly defined low relief outcrops and consists of stromatolitic carbonate, shale and siltstone, minor jasperoidal beds and minor granular iron-formation. The shale and siltstone are very similar to shale and siltstone of the Frere Formation. Locally, peloidal jasper is interstitial to stromatolites and thin granular iron beds are interbedded with stromatolitic carbonate. The Karri Karri Member was first mapped as part of the Windidda Formation, but during later work was re-interpreted as part of the Chiall Formation (Fig. 4). The contact of the Windidda Member with the overlying Chiall Formation is defined as the top of the uppermost carbonate horizon (Hall et al., 1977). The lower contact with the Frere Formation is placed at the first occurrence of carbonate or the last occurrence of iron formation, chert or jasper. The thickness of the Windidda Member varies laterally. Bunting (1986) estimated the thickness in the type area to be about 800 m, but more reasonable estimates are in general between 60 m and 150 m, and perhaps up to 500 m. In places, the proportion of granular jasper is high, forming GIF beds. The cores of concentrically zoned larger granules locally consist of a yellow-green iron silicate mineral, possibly glauconite or chamosite, which is partially replaced by hematite, suggesting iron-oxides in this sample may be secondary.

Stromatolite forms in the Windidda Member range up to 30 cm in diameter and include *Carnegia wongawolensis*, *Nabberubia tooloensis*,

Fig. 14. Stilpnomelane alteration of granular iron-formation in the Frere Formation: a) photomicrograph showing sheafs of acicular stilpnomelane (crossed polars); b) photomicrograph showing green-pleochroic stilpnomelane crystals cutting through chalcedonic quartz (brown; plane polarized light); c) drillcore showing typical granular iron-formation beds (red bands with chert intraclasts), intercalated with dark-coloured shale; d) drillcore of silicified and stilpnomelane-altered granular iron-formation and shale interbeds; e) close-up of core showing massive stilpnomelane (dark material) and partially silicified and stilpnomelane-altered peloidal ironformation. After Pirajno et al. (2004).

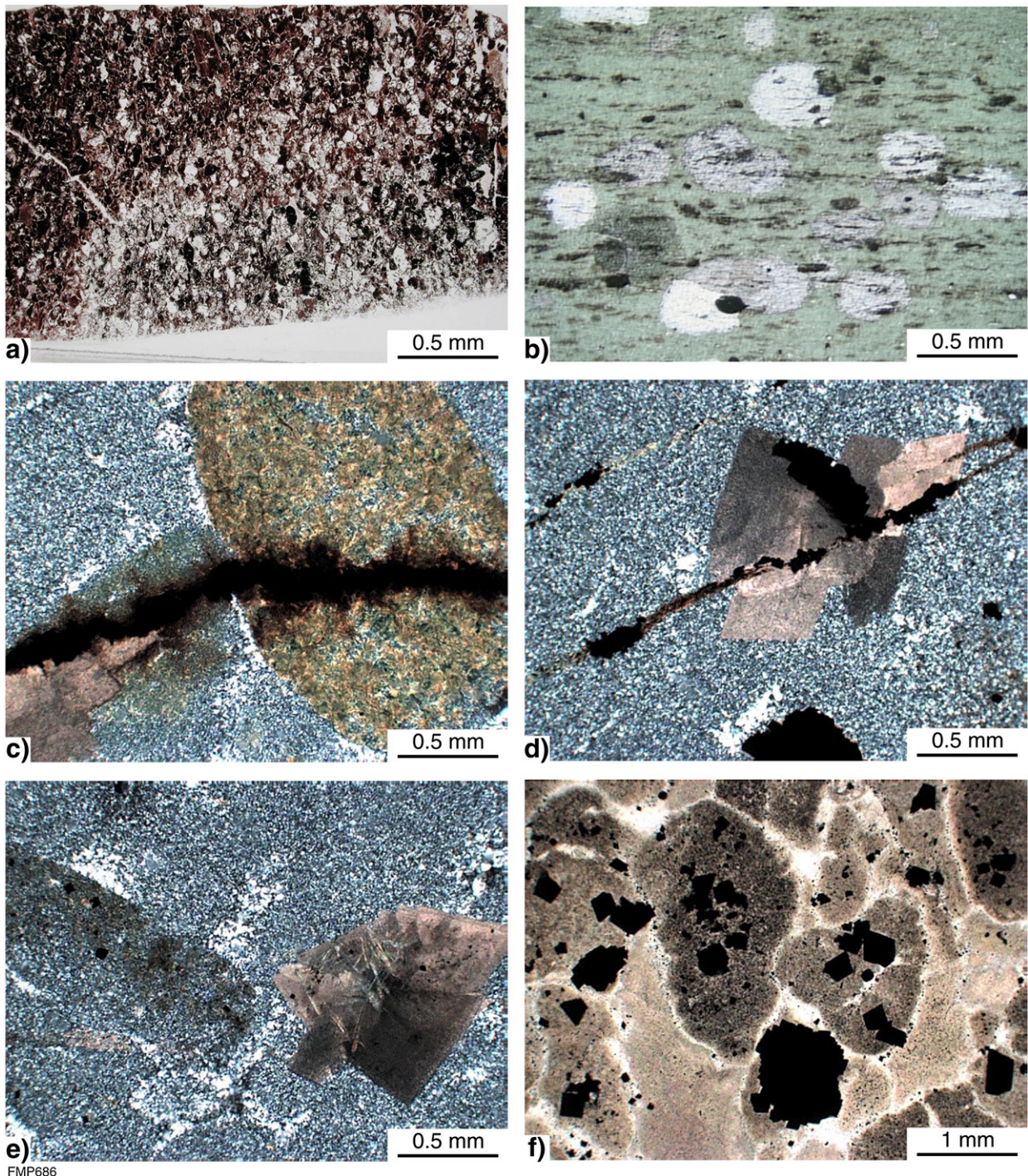


Fig. 15. Photomicrographs showing aspects of alteration of granular iron-formation in the Frere Formation: a) transitional boundary between hematite peloids (lower right) and carbonate replacement (left); b) chloritic shale intercalated with granular iron-formation, showing disseminated carbonate blebs (up to 2 mm across) overprinting the chlorite minerals; c) peloid entirely replaced by stilpnomelane and cut by a veinlet of iron oxides (?magnetite); the matrix is crypto- and microcrystalline quartz; d) pervasively silicified (crypto- and microcrystalline quartz) granular iron-formation overprinted by euhedral dolomite, which is in turn cut by a veinlet of iron oxides and stilpnomelane; e) granular iron-formation pervasively replaced by crypto- and microcrystalline quartz (light-coloured areas), overprinted by euhedral dolomite. Note ghost of peloid on left of image; f) complex alteration patterns are represented in this section; iron oxide peloids are replaced by stilpnomelane and perhaps minnesotaite, the matrix is entirely silicified (chalcedonic quartz is brown and microcrystalline quartz is white), and both are overprinted by euhedral magnetite. a), b), and f) plane-polarized light; c–e) crossed polars. After Pirajno et al. (2004).

Windidda granulosa and *Kulparia* (Grey, 1984). *C. wongawolensis*, is the dominant form recognized on Wongawol (Fig. 2) and forms colonies of branching forms. Locally, peloidal jasper is interstitial to stromatolites and is incorporated within stromatolite laminae. *W. granulosa* and the associated abundant ooids in the Windidda Member, are suggestive of sandy shoals and a more agitated environment. The palaeoecological

significance of the Sweetwaters Well stromatolites was treated in detail by Grey (1994).

Shale and siltstone dominated units contain laminated to massive carbonate beds of variable thickness that are generally <1 cm. Jasper beds, which are up to 10 cm in thickness, are interbedded with carbonate in carbonates dominated units. In addition, granular or peloidal jasper

locally forms a matrix to stromatolites. Intraclastic carbonate breccias are common in the Windidda Member, becoming more abundant towards the upper part of the formation. Locally, carbonate conglomerate is exposed at the top of the Windidda Member and is commonly transitional to a siliciclastic conglomerate at the base of the Chiail Formation. Clasts are generally well-rounded, up to 15 cm in length, occasionally imbricate and are dominantly carbonate or siltstone. Rare small stromatolites are contained in this horizon. Clasts are cemented by carbonate and contain a glauconite and quartz sandstone matrix.

The Windidda Member is interpreted to reflect a carbonate bank and lagoonal environment that developed synchronous with deposition of granular iron-formation. Minor jasper granules washed into the carbonate bank and lagoonal environment and intraclastic breccias probably reflect storm events.

4.2.3. Depositional environment of the Tooloo Subgroup and the origin of the iron formations

The Earaheedy Basin has a special importance in the tectonostratigraphic record of Palaeoproterozoic terranes because of the presence in the basin stratigraphy of the GIF units of the Frere Formation. The presence of the Frere Formation GIF could be related to a period of mantle plume(s) breakout, which resulted in global magmatism at ca 1.8 Ga, supercontinent breakup, trailing margins and deposition of iron-formations (cf. Barley et al., 2005). In addition, oxygenic photosynthesis associated with the GIF may have contributed to the rise of oxygen levels in the Earth's atmosphere. Granular iron-formation formed in shallow marine continental shelf to coastal conditions. Ferruginous peloids were deposited after some reworking by mechanical processes, with variable terrigenous contamination. The deposition of GIF in the Earaheedy Basin coincides with a decrease in the supply of sand-sized siliciclastic detritus into the basin. According to Beukes and Klein (1992), ferruginous

peloids form by accretion in wave- and current-agitated iron-rich waters and following reworking are deposited with variable amounts of terrigenous contamination. In modern clastic-starved marine shelves, amorphous Fe oxide and/or oxyhydroxide peloids (or ooids) appear to form as concretions a few centimetres below the sea floor, as a result of Fe and silica exhalative fluids that rise from the substrate (Heikoop et al., 1996; Donaldson et al., 1999). An alternative view is that the ooids grow from the precipitation of Fe-rich clays that become oxidised to goethite at the sediment-water interface (Donaldson et al., 1999). In either case the Fe oxide/oxyhydroxides alternate with silica to form the concentric laminae. The reason for the Fe oxide-silica alternations is not understood, but it may relate to pulses of fluid emission based on episodic temperature variations (high T, Fe precipitation; lower T silica precipitation). Dehydration and diagenesis would produce hematite and at higher temperatures magnetite and the formation of these ooidal or peloidal structures would occur in a geologically short time. Mechanical reworking by wave action and/or strong currents would account for the classic shape of the ooids (Heikoop et al., 1996).

Cross-bedding, locally recognized in GIF beds, indicates dominantly moderate-energy conditions. Local, peloidal carbonate beds that are intercalated with beds of iron-formation do not show evidence of current transport and may represent a particulate sediment that accumulated *in-situ* (Blatt et al., 1980, p. 469). However, the intercalated shale and siltstone horizons show structures best explained by traction-current deposition, from Granite Peak southwards (Fig. 2).

The GIF beds, shale, and siltstone all have different iron and silica content both within and between units. This points to a complex, varying interrelationship between clastic influx, dissolved silica and dissolved iron. The supply of dissolved silica appears to have been variable at all scales, and can be interpreted as a result of fluctuating concentrations. The supply of iron is also interpreted as the result of

Table 3
Frere Formation GIF Facies (after Price, 2003).

Name	Description	Depositional processes
Planar-laminated siltstone	Dark to light grey siltstone. Planar laminations. Light laminae are composed of quartz, dark laminae are clay rich. Angular quartz and mica are the dominant grains, with an average grain-size of 0.05 mm (<0.1 mm). Chlorite replacement is common.	Very low energy. Suspension settling (very flat planar laminae) or weak traction current activity (gentle wavy laminations)
Peloidal GIF	Red, white or grey GIF. Lack of internal laminations (no platy minerals), allochems elongated horizontally from load deformation. Allochems are 0.5 to 3 mm, can be peloids (ferruginous chert, rounded to angular), pisoids or ooids (round, concentric laminations). Peloids are the dominant allochem. Can be broken and angular and have cracks. Allochems set in a jasper or chert cement and/or matrix.	Agitated, oxic environment to form peloids High energy to rework the peloids, and redeposit.
Iron-rich siltstone	Green to black siltstone. Planar laminations. Dominated by iron-rich iron-oxides and chlorite with quartz and clay.	Very low energy. Suspension settling (planar laminae) or weak traction current activity (gentle wavy laminations)
Stromatolitic GIF	Red to grey colour. Laminations are wavy. In thin section, angular iron oxide grains define laminations of Windidda granulosa & cf. ?Kulparia. Pisoids and ooids are the dominant allochems, ~2 mm diameter. These are round, have concentric laminations and are locally concentrated. Relatively undamaged. The fabric is a mosaic of 0.01 to 1 mm carbonated crystals with irregular crystal boundaries (xenotopic).	Traction currents to produce wavy sediment laminations Abundant life suggests warm and oxygenated environment, above photic zone. Windidda granulosa indicates agitated environment (Grey, pers. comm.). Ooids formed in agitated shallow environment proximal to depositional environment
Quartzose GIF	Quartz rich 20–200 mm thick GIF units interbedded with 20–200 mm siltstone units. Weakly developed wavy laminations. Peloids 1.5 mm in diameter are carbonaceous or made up of 0.2 mm quartz grains. Chert matrix or recrystallised chalcedony cement	High energy to deposit the coarse grains.
Heterolithic claystone and siltstone	Black and white heterolithic siltstone/very fine sandstone and claystone. 5 mm-thick white and black layers. Wavy laminations. White: ~1.5 mm grains made up of chert and very fine quartz. Compressed, flat and round. Black: Claystone sized grains. Elongate, thin, white clay is present. There are 0.5 mm opaque iron oxides throughout facies, mainly in the chert.	Low to moderate energy. Weak traction currents to produce wavy laminations. Alternating energy conditions to produce grain-size variations. Heterolithic bedding suggestive of storm fluvial or tidal setting
HCS siltstone	Light grey siltstone. Laminations at low angles, and slightly wavy. Swaley cross-laminations and ripple cross-lamination are abundant. Scattered angular opaque grains and clay concentrate in thin layers. ~0.5 mm angular quartz grains dominant. Elongate brown-clay aligned with laminations, wavy and intergranular to quartz.	Combined directional flow to produce the ripple cross-laminations HCS suggestive of above storm wave-base and below fairweather wave-base.
Heterolithic cross-laminated siltstone	Light-grey siltstone and yellow fine-sandstone (heterolithic). Alternating coarser (0.15–0.2 mm) and finer layers (0.05 mm) shows the wavy, low-angle laminations. Ripple cross-laminations are common. Angular quartz grains are the dominant mineral, with some elongate brown clay.	Combined directional flow to produce ripple cross-laminations Alternating higher and lower energy to produce the grain-size variation. Heterolithic bedding suggestive of storm (below fairweather Wave base), fluvial or tidal setting

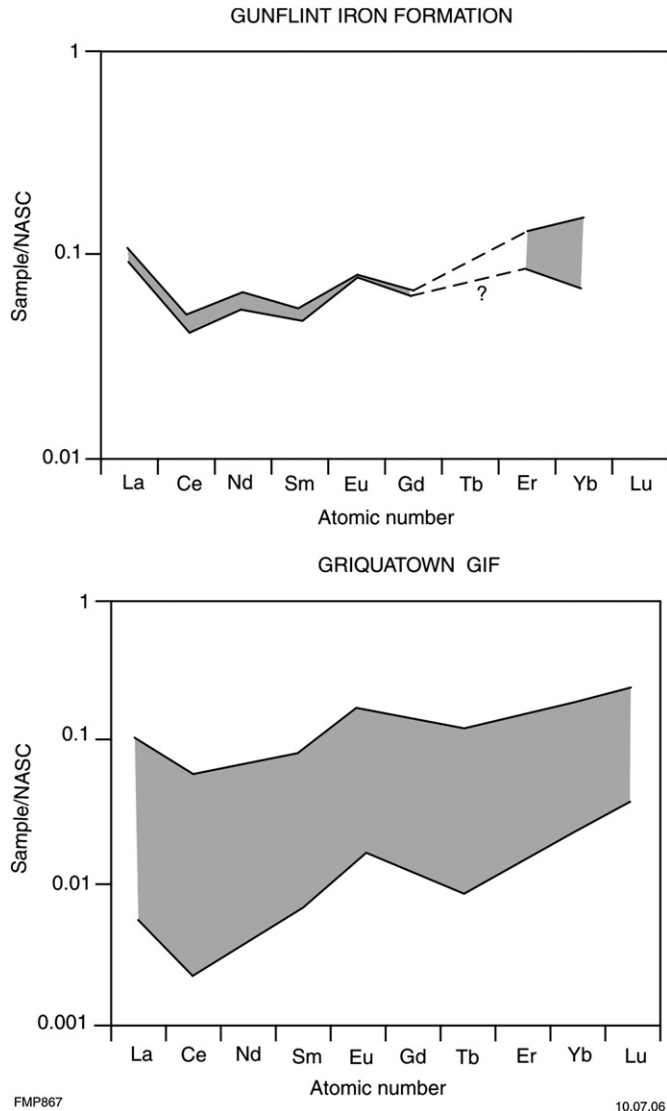


Fig. 16. Rare earth elements (REE) patterns for the Gunflint (Derry and Jacobsen 1990) and Griquatown (Beukes and Klein, 1990) granular iron formations, normalised to North American Shale Composite (Gromet et al., 1984). Note positive Eu anomalies and negative Ce anomalies. From Price (2003).

fluctuating concentrations but with a high proportion of iron remaining in suspension throughout deposition of the Frere Formation. The shale interbedded with granular iron-formation and in major shale horizons may indicate periods where the rates of silica and iron precipitation were low.

Both iron-rich and silica-rich fluids are interpreted to have a distal source. The supply of iron and silica is ultimately related to distal hydrothermal effluents such as a mid-ocean ridge and/or other subaqueous hot springs (e. g. Isley, 1995; Trendall, 2002). Upwelling currents would transport Fe^{2+} and Mn^{2+} away from the discharge vents and precipitation would occur just above the oxic-anoxic interface, where Fe^{2+} and Mn^{2+} are oxidised to Fe^{3+} and Mn^{4+} , respectively (Pirajno and Adamides, 2000). A depositional and tectonic model for the Yelma and Frere Formations (Tooloo Subgroup), based on the stratigraphic, sedimentological and genetic attributes of the granular iron-formation (Beukes and Klein, 1992; Isley, 1995; Trendall, 2002) is shown in Fig. 18.

Detailed studies on field and textural features of granular iron-formation in the Earaheedy Group (Hall and Goode, 1978; Goode et al., 1983; Bunting, 1986) clearly show similarities with the iron-forma-

tions of the Superior Province of North America (e.g. Kimberley, 1989). Peloidal and oncolytic textures, orthochemical and allochemical cements, iron-rich chlorite, the presence of mineral phases, such as minnesotaite and stilpnomelane, are common in both. These characteristic features have been interpreted as the result of chemical deposition, followed by mechanical reworking of the sediment, whilst still plastic (gel state) (Beukes and Klein, 1990, 1992). The model for the origin of the iron-formation proposed by Beukes and Klein (1990, 1992) and Isley (1995) accounts for the large volumes of iron, but it does not explain the association of iron and silica in grains of possible biogenic origin. Some of the grains classified as peloids (Fig. 12d), may have been originally oncolites (Fig. 13a-f; and Brown et al., 1995). If this is correct, then it is possible that biogenic activity may have played a major role in the development of the granular iron-formation, through a mechanism of bacterial iron oxidation (Nealson, 1982; Brown et al., 1995). Other models of BIF deposition (Konhauser et al., 2002; Kappler et al., 2005) propose a mechanism for the

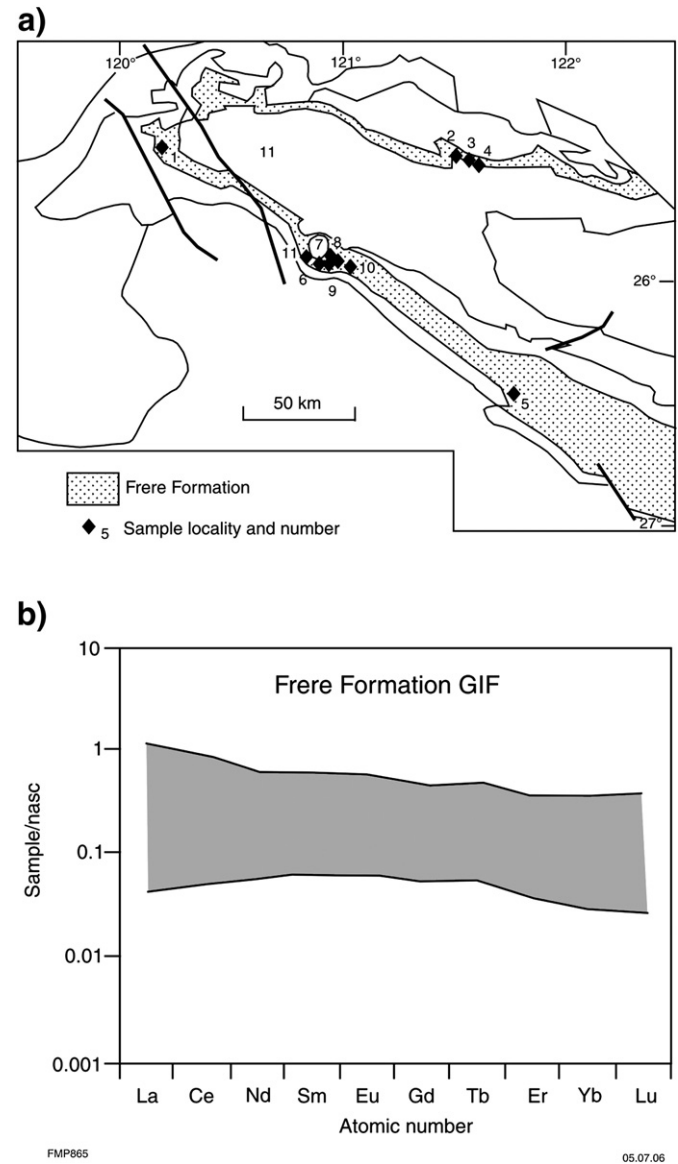
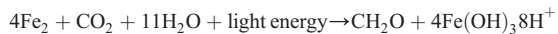


Fig. 17. a) Distribution of the Frere Formation in the Earaheedy Basin and locations of samples analysed for rare earth elements; b) REE patterns of the Frere granular iron-formation, normalised to North American Shale Composite (Gromet et al., 1984). Note weak positive Eu anomalies, Ce exhibits both positive and negative anomalies. After Price (2003) and Pirajno, unpublished data.

oxidation of hydrothermal Fe(II) to Fe(III) by anoxygenic photosynthetic bacteria. A possible bacteria-mediated reaction is:



The depositional setting of the Tooloo Subgroup is illustrated in Fig. 19.

4.2.4. Chiall Formation

The Chiall Formation combines, as members, the former Wandiwarra Formation and Princess Ranges Quartzite, as well as the Karri Karri Member (see Fig. 4). SHRIMP U-Pb dating of detrital zircons from the Chiall Formation reveal a maximum depositional age of ca 1.8 Ga (Halilovic et al., 2004). The Chiall Formation consists of shale, siltstone and mudstone intercalated with thick sandstone beds and intraclastic breccia. The formation represents a change from combined chemical and fine-grained clastic sedimentation, to coarser-grained clastic deposition. The base of the formation in the south is a breccia of poorly sorted, angular carbonate clasts in a ferruginized and glauconitic sandstone matrix, which led Bunting (1986) to interpret the boundary as a disconformity. Alternatively, the brecciated features of this horizon could have formed through a process of liquefaction and therefore may be a seismite or a tsunamiite, as defined by Einsele (2000) and described by Pratt (2002). To the north, the lower part of the Chiall Formation consists of a thick succession of shale, siltstone and mudstone, which has been assigned to the Karri Karri Member. Sandstone overlying the Karri Karri Member was probably deposited below fair-weather wave base, based on graded bedding, mass flow deposits and the lack of cross-bedding attributable to widespread current or wave action.

The thickness of the Chiall Formation was considered by Bunting (1986) to be up to 1500 m. Again, we suggest that there has been more structural repetition than was estimated by Bunting (1986), and that the maximum thickness of the formation may only be 1000 m. The contact between the Chiall Formation and the underlying Frere Formation is transitional and taken as the top of the last major chert bed or iron-formation. Where the Chiall Formation overlies the Windidada Formation, the contact is taken as the top of the last carbonate bed. The Chiall Formation (Hocking and Jones, 1999; Hocking et al., 2000a,b) consists predominantly of very fine-grained sandstone, siltstone, shale and mudstone punctuated by fine- to medium-grained sandstone beds and minor conglomerate. The Wandiwarra and Princess Ranges Members which, as mentioned above, were previously considered formations (Hall et al., 1977; Bunting, 1986) were relegated to member status within a single formation after the recognition that they are part of a single depositional package.

The base of the Chiall Formation is transitional and laterally variable. In the central part of Wongawol, the base of the Chiall Formation consists of very fine to fine-grained sandstone, siltstone, shale, and mudstone. Further east, conglomerate is interbedded with this facies at the base of the Chiall Formation, with the proportion of conglomerate increasing eastward.

Conglomerate at the base of the Chiall Formation is texturally variable, consisting of poorly-sorted boulder conglomerate and pebble conglomerate. Clasts are locally imbricate and clast type is variable and commonly reflects the underlying lithologies, suggesting a strong local source control. Fine-grained sandstone, siltstone, and carbonate are the dominant clast types with the proportion varying both vertically and along strike. Poorly sorted boulder conglomerate is generally laterally restricted and is weakly bedded. Clasts vary from subrounded to angular, but are typically angular. On Wongawol a poorly sorted, boulder conglomerate is up to 4 m thick and consists of angular clasts of dominantly carbonate and minor sandstone, in a coarse-grained sandstone matrix containing glauconite peloids and cemented by a ferruginous clay. Pebble conglomerate beds, which are interbedded with siltstone, mudstone and glauconitic very fine-

and fine-grained sandstone at the base of the Chiall Formation, are typically less than 50 cm thick.

Bunting (1986) suggested that conglomerate at the base of the Chiall Formation may represent a disconformity between the Tooloo and Miningarra Subgroups. However, there is little evidence to support a significant break in sedimentation between the two subgroups. The contact between conglomerate of the Chiall Formation and the Windidada Formation is transitional, except for localized exposures of cobble conglomerate, and reflects a change from carbonate-cemented conglomerate to conglomerate with a sandstone matrix. It is also important to recognize that basal conglomerate in the Chiall Formation is relatively restricted both laterally and vertically, and mostly overlies carbonate of the Windidada Formation.

Interbedded siltstone, mudstone, shale and fine- to very fine-grained sandstone, which is locally calcareous typifies the lower part of the Chiall Formation below the Princess Ranges Member and is similar to the lower part of the Wongawol Formation. Sandstone contains green iron silicate minerals, especially near the base of the Chiall Formation. These green iron silicate grains are mostly glauconite, but other iron-bearing species such as berthierine and chamosite are probably also present. In addition, jasper peloids are also common at the base of the Chiall Formation in fine and very fine-grained sandstone. Green iron silicate grains are commonly peloidal and oolitic. Locally, the green iron silicate grains are flattened and deformed in particular beds, indicating they must have been soft and plastic during compaction. The proportion of green iron silicate minerals in these beds is generally high.

Sedimentary structures at the base of the Chiall Formation include parallel lamination, load casts, and minor cross-lamination. These are overlain by symmetrical and asymmetrical ripples, wrinkle marks, and contorted bedding, which are overall more common sedimentary structures in the lower Chiall Formation.

Fine- to medium-grained sandstone-dominated units in the Chiall Formation form prominent topographic ridges in the central areas of the Basin. Textural and compositional maturity increases stratigraphically in fine- to medium-grained sandstone. Sandstone beds predominantly comprise subrounded to rounded quartz, minor chert, feldspar and glauconite, and accessory zircon and tourmaline. Glauconite is generally concentrated at the base of fine- to medium-grained sandstone-dominated units, suggesting it was reworked from underlying shale, siltstone and very fine-grained sandstone facies where glauconite abundances are high. In units mapped as fine- to medium-grained glauconitic sandstone, the proportion of glauconite is generally much higher than in other fine to medium-grained sandstone units in the Chiall Formation.

4.2.4.1. Karri Karri Member.

The lower Karri Karri Member consists dominantly of shale and siltstone, with thin interbedded sandstone

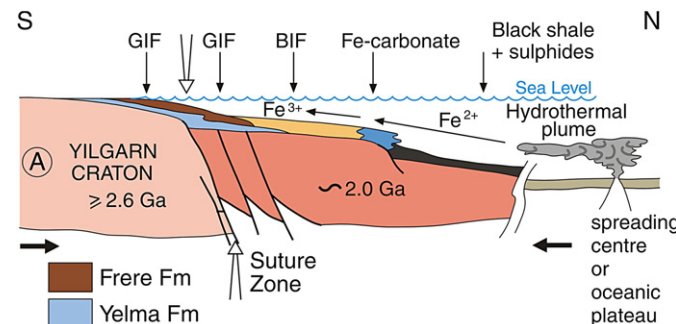


Fig. 18. Depositional and tectonic model for the Tooloo Subgroup of the Earaheedy Basin: at about 1800 Ma iron oxides were deposited on a continental shelf, with granular iron-formation at shallower depths and banded iron-formation deposited further down the continental slope. Lateral equivalents deposited in deeper settings consist of carbonate and sulphide facies. Iron was possibly sourced from hydrothermal effluents in an oceanic basin either from a spreading centre or from an oceanic plateau. After Pirajno et al. (2004) and Morris et al. (2003).

beds in the upper part of the member. The member is interpreted as having a maximum thickness of 600 m in the north of the Basin (e.g. on Methwin, Fig. 2). The lower contact is defined as the top of the last major chert or iron-formation. The upper contact with the Wandiwarra Member is transitional with thin interbedded sandstone beds becoming more common in the upper part of the Karri Karri Member. The contact is taken at the first occurrence of a thick sandstone. In the Stanley Fold Belt, exposures of the member are generally folded, cleaved and cut by small quartz veins.

Lithologically, shale and siltstone resemble similar lithologies to the underlying Frere and Yelma Formations, but generally contain a high proportion of coarse-grained siltstone. Without other stratigraphic control, the shales may be indistinguishable. They are typically delicately parallel laminated with individual lamellae between 1 and 10 mm. Individual sandstone beds in the upper part of the member are typically 5 to 20 cm thick, and fine- to medium-grained.

The delicate, continuous lamination in the Karri Karri Member is indicative of quiet-water deposition probably below fair-weather wavebase, subsequent to a transgression at the top of the Frere Formation. Sandstone beds are interpreted as mass-flow deposits rather than turbidite deposits because of the intraclastic mudstone clasts and traction structures. The iron-rich nature of the rocks indicates that iron remained in suspension even after deposition of the last GIF and the silica and iron supply to the basin had ceased.

4.2.4.2. Wandiwarra Member. The Wandiwarra Member consists dominantly of siltstone and shale, with scattered intercalations of sandstone. Siltstone and shale intervals are generally well exposed on breakaways. Sandstone intervals form resistant cappings on hills. Shale intervals are generally parallel laminated with minor cross lamination. Laminations are typically 0.5 to 5 cm thick. Interbedded sandstone beds range from 5 cm to, less commonly, about 1 m thick. Sandstone dominated intervals consist of sandstone beds with subordinate interbedded siltstone, generally as thin beds. Sandstone beds generally consist dominantly of rounded to subrounded quartz, with minor chert, feldspar, mica, glauconite and tourmaline, and become

more mature in the upper part of the member. Bed thickness varies from about 5 cm up to 1.5 m but is typically 10 to 20 cm in thickness. Bedsets generally range from 20 cm to 1 m in thickness. Sedimentary structures include cross-bedding, asymmetric ripples and hummocky cross-stratification in the lower part of the member. Current lineations, cross bedding, and ripples indicate a dominant palaeocurrent flow direction towards the north.

Sandstone intervals are fine- to medium-grained, poorly to moderately sorted sandstone, and dominantly consist of rounded to subrounded quartz grains and minor chert fragments. It is locally conglomeratic, and interbedded with siltstone, mudstone and shale. Mudchip intraclasts are common, especially at the base of individual beds. Sedimentary structures in the sandstone include tabular and trough cross-bedding, flute clasts and current lineation. Quartz grains are occasionally coated by hematite granules (Fig. 20a); in other instances Fe oxides tend to replace both quartz and interstitial matrix and can be an important component at some stratigraphic levels (Fig. 20b). Glauconite peloids vary from spherical to elliptical, with an average size of 0.22 mm. Locally, glauconite is oxidised to brown-coloured Fe oxides. It varies from colourless to light-green or brown when weathered, or blue-green when fresh and is locally replaced by a mosaic of quartz grains, which are not in crystallographic continuity with the surrounding authigenic silica. Locally, glauconite is oxidised to brown-coloured iron oxides.

Sedimentary structures in the sandstone include tabular and trough cross-bedding, flute clasts and current lineation. Sandstone pillows within siltstone are found at several localities, generally as a discontinuous horizon, suggesting sporadic earthquakes as a trigger mechanism. Spectacular megaripples in sandstone beds can be seen on outcrops of the outer collar of the Shoemaker impact structure (Fig. 21; Section 6). The sedimentary structures, in both the shale and sandstone intervals, suggest that the Wandiwarra Member was mostly deposited below wavebase in the wake of a basal transgression, and that shallowing occurred up the stratigraphic sequence.

Brecciated beds of limestone and glauconitic sandstone in a ferruginized sandy matrix are exposed at the base of the Wandiwarra Member 3 km southwest of Kennedy Bore on Wongawol (Fig. 22). The

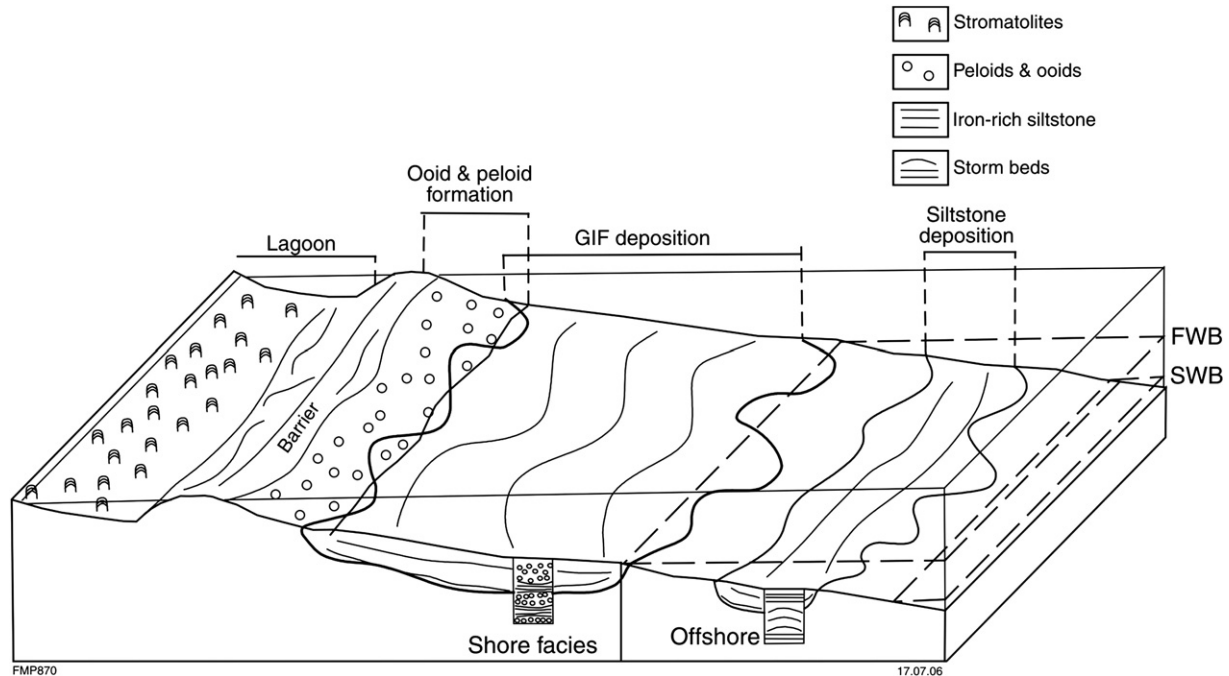


Fig. 19. Depositional system of granular iron-formation, ooids and peloids are shore facies and form as a result of wave action, siltstone and shale deposition occurs as offshore facies (not to scale). After Price (2003).

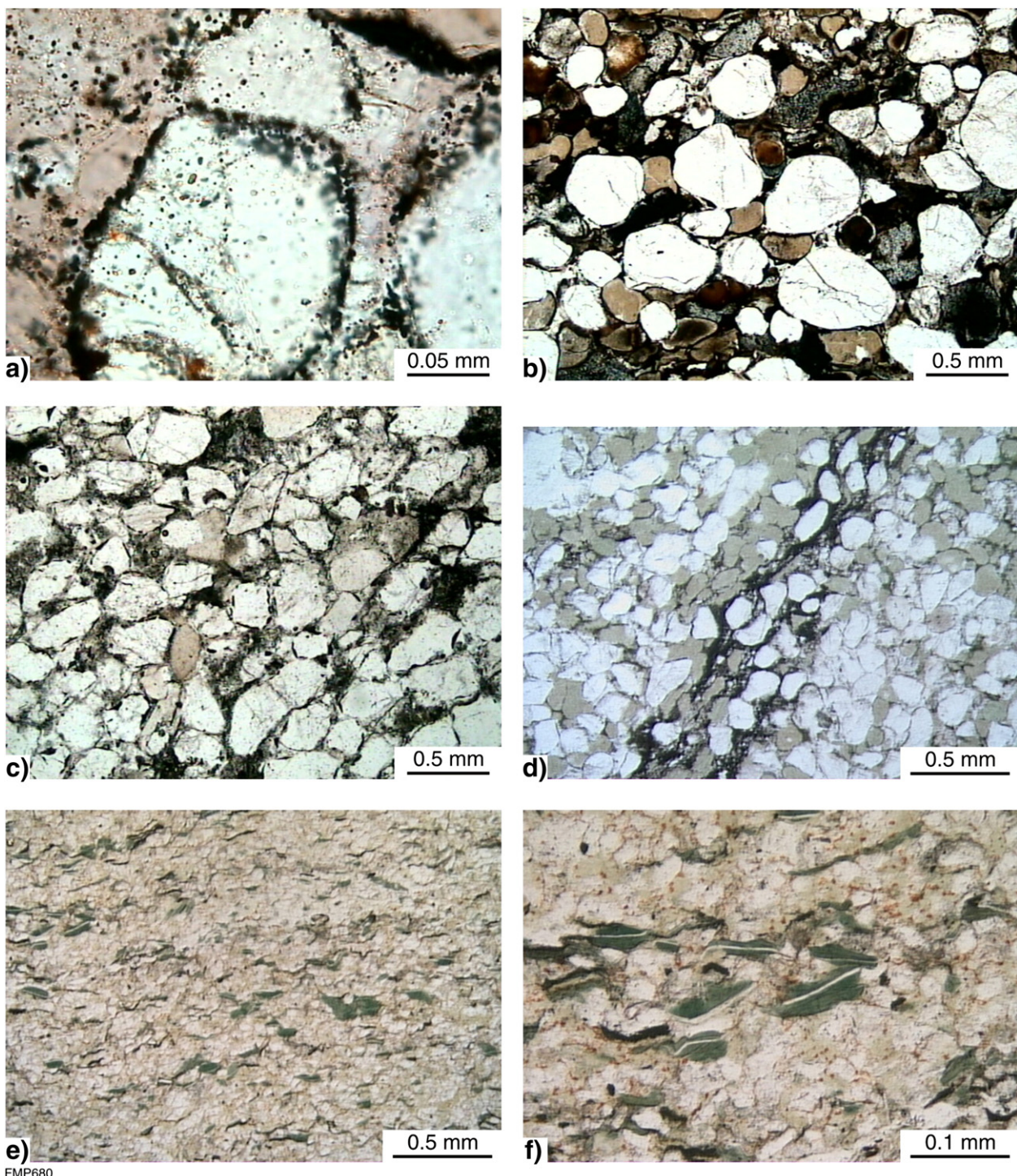


Fig. 20. Photomicrographs in plane-polarized light of rocks from the Wandiwarra and Princess Ranges Members, Chiall Formation: a) sandstone with rounded quartz grains coated by hematite granules, a feature that is typical of red beds; b) glauconitic sandstone; glauconite grains are about 0.6 mm across and are partially oxidized (brown); c) grain-supported sandstone. Quartz grains with interstitial clay, quartz, muscovite, and iron oxides; d) glauconitic sandstone of the Wandiwarra Member from the outer ring of the Shoemaker impact structure, composed of quartz grains and glauconite (pale green). Dark vein is probably pseudotachylite; e) and f) chloritic mudstone composed of quartz and iron-rich chlorite (green). The chlorite has replaced ?detrital muscovite. After [Pirajno et al. \(2004\)](#).

limestone clasts are platey to elongate, and are the same lithology as Windidda Member exposed below the breccia. Scattered quartzite clasts are also present. The breccia only extends for a few hundred metres laterally, and has not been recognized elsewhere at the base of the Chiall Formation. It may be ancient tsunami or seismic shock deposits ([Fig. 22a, b](#)), but is more likely a rip-up lag at the base of a transgression. If the latter, they provide a strong indication of a significant break between the Tooloo and Miningarra Subgroups, with

transgression over a uneven surface after a period of exposure and local weathering.

North of the Shoemaker impact structure (see [Section 6](#)), rocks of the Wandiwarra Member outcrop in a series of breakaways along the northern edge of the Lake Nabberu system ([Fig. 23](#)). Here, the rocks are gently dipping and deformed into mesoscale folds with east-trending doubly-plunging fold axes and with local reverse faults ([Figs. 23, 24](#)).



Fig. 21. Mega-ripple marks in Chiall Formation (Wandiwarra Member) sandstone, along the northeastern part of the outer collar of the Shoemaker impact structure. After Pirajno et al. (2004).

4.2.4.3. Princess Ranges Member. The Princess Ranges Member generally comprises shale, siltstone, mudstone units interbedded with very fine-grained sandstone, and siltstone-dominated units and mature quartz arenite. It is characterized by silicified quartz arenite, although quartz arenite is commonly a subordinate lithology to siltstone. On Granite Peak (Fig. 2), mature quartz–arenite-dominated horizons are mostly interpreted to be stratigraphically equivalent to the Princess Ranges Member. The sandstone is generally fine- to medium-grained and typically texturally mature, consisting of well-rounded and well-sorted quartz grains and accessory tourmaline and zircon. Mudchip intraclasts and glauconite peloids are commonly concentrated at the base of fine to medium-grained sandstone dominated units, suggesting high-energy erosional bases. Coarse-grained siltstone and very fine-grained sandstone is comprised dominantly of angular to subrounded quartz, and subordinate glauconite and detrital mica. Locally, the base of the Princess Ranges Member contains coarse-grained sandstone containing pebble-sized subangular to subrounded clasts of vein quartz and sandstone.

Sedimentary structures within the sandstone include symmetrical sharp-crested low amplitude ripples, current lineation, megaripples,

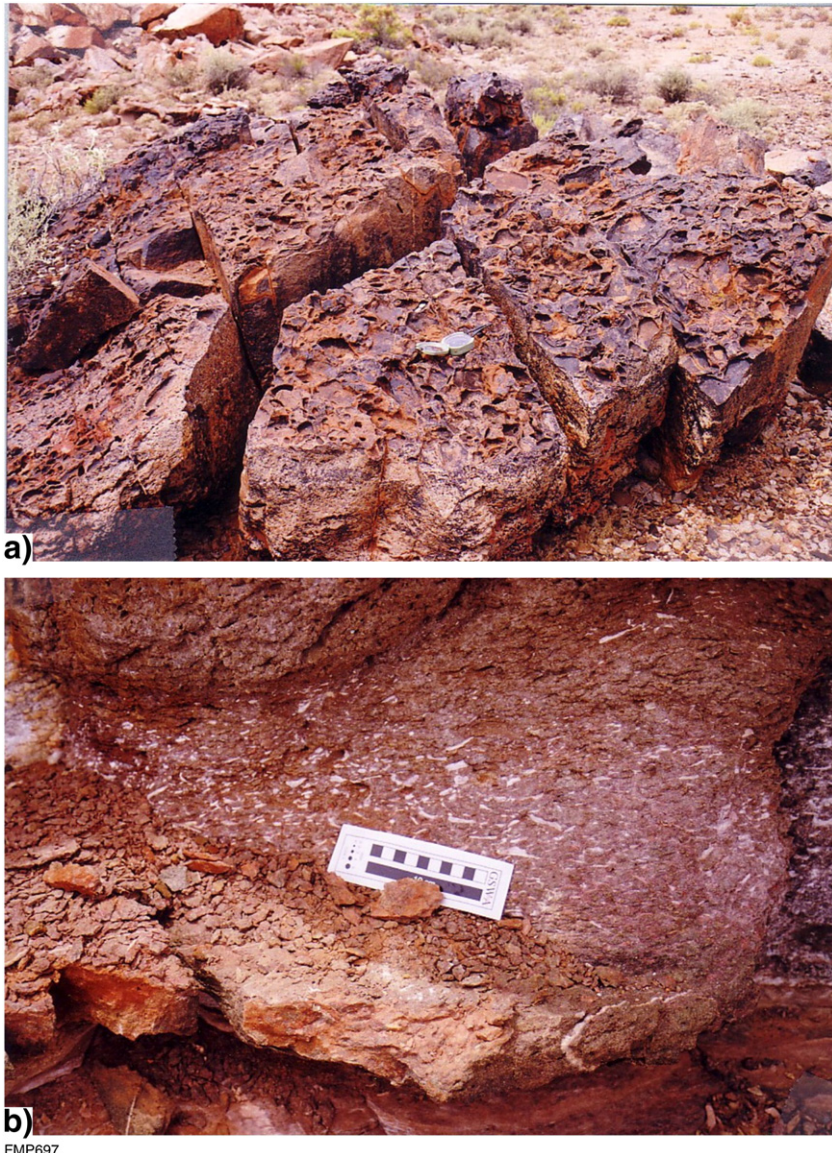


Fig. 22. Mass flow deposits at the base of the Wandiwarra Member: a) sedimentary mass-flow deposit and b) fluidized arenite, representing possible tsunamite or seismite. After Pirajno et al. (2004).

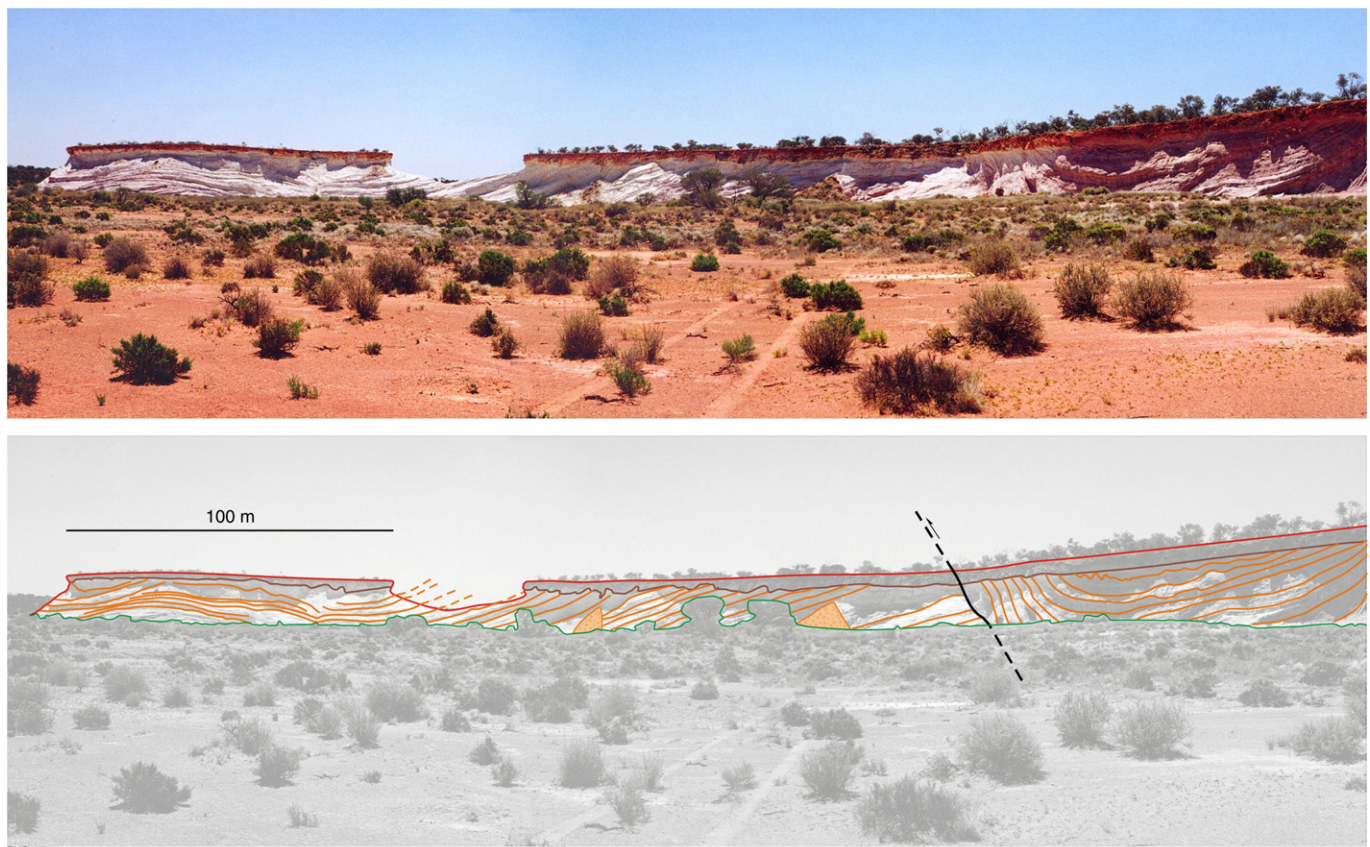


Fig. 23. Escarpments (breakaways) in Wandiarra Member quartz sandstone and siltstone at the northern margin of Nabberu, showing mesoscale folding and thrusting. The beds are capped by iron-rich weathered residual quartz sandstone and siltstone *in situ*. After Pirajno et al. (2004).

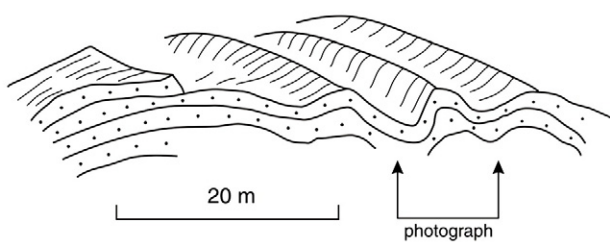


Fig. 24. Doubly plunging mesoscale fold in Wandiarra Member quartz sandstone. Sketch below shows the overall style of folding in this area. After Pirajno et al. (2004).



Fig. 25. Linguoidal ripple marks in very fine grained sandstone of the Princess Ranges Member, 3 km northeast of Wadjinyanda Pool.

shrinkage moulds, trough and planar cross-bedding and cross-lamination. Symmetrical ripples are mostly straight-crested, while asymmetric ripples vary from straight-crested to linguoid (Fig. 25). The sedimentary structures, in combination indicate that the Princess Ranges Member and the stratigraphically equivalent mature quartz arenite in the upper part of the Chiail Formation were deposited largely in an upper shoreface environment. In places ripple forms suggest shallow to tidal sandflat conditions, based on interference patterns and possible ripple washouts. Sandstone beds are probably tempestites (storm related) and/or seismites (related to earthquakes; Rodriguez-Pascua et al., 2000). Conglomeratic beds may be related to tsunamis.

Fine- to medium-grained sandstone is typically texturally mature, consisting of well-rounded and well-sorted quartz grains and accessory tourmaline and zircon. Mudchip intraclasts and glauconite peloids are commonly concentrated at the base of fine- to medium-grained sandstone dominated units, suggesting high-energy erosional bases. Coarse-grained siltstone and very fine-grained sandstone is comprised dominantly of angular to subrounded quartz, and subordinate glauconite and detrital mica. Locally, the base of the Princess Ranges Member contains coarse-grained sandstone containing pebble-sized subangular to subrounded clasts of vein quartz and sandstone.

4.2.5. Wongawol Formation

The Wongawol Formation (Hall et al., 1977; Bunting, 1986) is a monotonous succession of shale, mudstone, siltstone, very fine-grained feldspathic sandstone, and minor intraclast conglomerate. The lower contact with the Chiail Formation is placed at the top of the uppermost compositionally mature sandstone. The upper contact with the Kulele Limestone, where exposed, is transitional and placed where limestone becomes the dominant lithology (Bunting, 1986). Sandstone in the Wongawol Formation is dominantly very fine-grained, in places silicified, and locally glauconitic. In places, sandstone contains mudchip and well-rounded siltstone intraclasts, with in-situ brecciation of thin siltstone beds. Stromatolites are present at several horizons and include domal features 50 cm wide, 1 m long, and 40 to 60 cm high. Smaller parasitic domal forms encrust larger domes, and the stromatolites are associated with mudchip intraclast breccias and oolitic limestones. Compound domal forms up to about 3 m high and 4 m across are present on Lee Steere (Fig. 2).

Discontinuous conglomerate bodies are present on Wongawol and southern Lee Steere (Fig. 2). Clasts are typically well-rounded, matrix-supported, pebble-sized, and mostly composed of mudstone and carbonate fragments. Both mudstone and carbonate clasts are interpreted as intraclastic. Intraclast mud-chip conglomerates are well-exposed on Lee Steere. In this area, they are associated with small-to medium-scale pillow structures, possibly developed by sediment

loading. On Wongawol, volcaniclastic clasts with vitriclastic textures were recorded by Jones (2004). The clasts contain well-preserved relic glass shards that are uncompacted and show bubble-wall, triple point textures. The matrix consists of poorly sorted, angular to subangular clasts of quartz, feldspar, and biotite, which are dominantly silt to very fine-grained sand sized, in a micritic cement. The provenance of the clasts is unclear as there is no evidence of contemporaneous volcanism in the Earaheedy Basin. They may be from reworking of thin volcaniclastic beds, which have not been preserved, or they may be allochthonous.

Sedimentary structures in the Wongawol Formation include swash marks, ripple washouts, wrinkle marks, ball-and-pillow structures (mostly but not always at sandstone–siltstone interfaces), primary current lineation, and symmetrical and interference ripples. Symmetrical ripples typically have peaked crests and are straight-crested, with wavelengths of 8–10 cm and amplitudes around 2–3 cm. Weakly developed ladder ripples are locally present in the troughs of some symmetrical ripples. These are indicative of deposition in shallow water with intermittent emergence and reworking by swash and possibly wind. Ball-and-pillow structures formed either by loading or as a result of earthquake shock. At one locality, an extensive horizon of contorted bedding, primarily with pillow structures, with thinly bedded rippled siltstone to very fine-grained sandstone lies above an uncontorted interference-rippled siltstone. The ripple morphology indicates very shallow conditions, whereas the contortion shows no consistent orientation, suggestive of earthquake disturbance rather than slope collapse.

On Lee Steere, the Wongawol Formation is folded into multiple east-trending anticlines and synclines, and cut by a network of anastomosing east-trending faults, indicative of mild north-south compression. The intensity of the folding increases northwards, into a pattern (low in the Wongawol Formation and in the Princes Ranges Member) of sheared-out anticlinal and synclinal axes between relatively straight, moderately to steeply dipping fold limbs.

4.2.5.1. Kulele Limestone. The Kulele Limestone is a cyclic platform succession up to 300 m thick, of interbedded calcarenite, stromatolitic limestone, intraclastic carbonate breccia, oolitic and pisolithic limestone, siltstone, and sandstone. Near Thurruguddy Bore (Wongawol, Fig. 2), spectacular large individual stromatolite domes are up to 3.5 m high and 4 m wide. Domes are composed of smaller colonial columnar stromatolites. Compared to the Wongawol Formation, the Kulele Limestone records a slight deepening of the basin and decrease in terrigenous influx. Metre-scale shallowing-upward cycles are present through most of the unit, and record regular minor fluctuations in sea-level in a shallow subtidal setting.

The Kulele Limestone is preserved only in the central-eastern part of the basin, except for a small outlier, near Thurruguddy Bore on Wongawol (Fig. 2). The carbonate (mostly limestone, lesser dolomite) rocks represent the main rock type and they form cyclic sequences separated by clastic units. Cycles are typically about 10 m thick, but locally only a metre thick, and cyclic intervals are separated in places by clastic layers up to 50 m thick. The limestone units are mostly thickly bedded, and internally laminated, with the laminae on scales of 1 to 5 mm. Stromatolites range from small domes a few cm across to large domes, 2 m high and 3 m across, which coalesce to bioherms up to 30 m long (Bunting, 1986). These stromatolite domes are commonly asymmetric and elongated, presumably at right angles to the direction of wave translation—the elongation is approximately perpendicular to the shoreline. This can be seen in the Thurruguddy Bore outlier on Lee Steere and terraces on Carnegie (Fig. 2). Bunting (1986) studied the Thurruguddy Bore outlier in detail. There, the basal 25 m of Kulele Limestone is exposed and can be divided into seven cyclic pairs of limestone-shale, each from 2.5 to 7.5 m thick. Each cycle represents a transgressive (limestone)-regressive (shale) couplet. Stromatolites in the outlier form two bands. Band 1 has low domes, up to 100 mm,

circular to elongate with length:breadth ratios of about 3:1. Band 2 contains domes up to 2 m high with individual domes reaching 3 m across, forming bioherms 30 m long and 10 m wide. Stromatolite forms in the Kulele Limestone include *Haraheedia kuleliensis* (Grey 1984). The large bulbous stromatolites remain unnamed.

Oolitic and pisolithic limestone shows two types of allochems (Bunting, 1986). In one, large pisoliths are elongate with an intraclastic core, surrounded by concentric laminae up to several mm thick. The second type is smaller with both radial and concentric laminae. These features may indicate a two-stage origin, whereby ooliths initially formed in quiet water, were then transported into a more agitated environment. Locally there are breccia layers, characterised by tabular intraclasts up to 200 mm long, forming beds at the base of the limestone cycles. Calcareous shales are fine-to medium-grained rocks composed of granular calcite with minor detrital quartz. Shales are typically purple, maroon or grey-greenish in colour and contain white mica and chlorite. Sandstone interbedded with the shaly rocks, contains feldspar, quartz with a calcareous cement and with muscovite and chlorite imparting this rock a degree of fissility. In the upper part of the Formation, sandstone is coarser grained and contains glauconite at the expense of the feldspar, which becomes a minor component (Bunting, 1986).

The stromatolitic limestones and cyclic nature of the Kulele Limestone indicate deposition in shallow-marine nearshore to coastal conditions, with regular short-term sea-level change on a scale of a few metres to perhaps 20 m (based on the thickness of the cycles), possibly driven by orbital forcing. Metre-scale cyclicity has long been viewed as a fundamental component of Phanerozoic platform carbonates (Goldhammer et al., 1987; Anderson & Goodwin, 1990; Goldhammer et al., 1990; Elrick and Read, 1991; Goldhammer et al., 1993), and is commonly, but not always attributed to orbital forcing (Milankovich cyclicity) (Fischer and Bottjer, 1991; Franseen et al., 1991; House and Gale, 1995).

4.2.6. Mulgarra Sandstone

The Mulgarra Sandstone, the youngest component of the Earaheedy Group, consists of fine- to medium-grained, commonly glauconitic sandstone, shale and minor carbonate. Locally, there are intercalations of thin limestone beds, forming a mixed unit up to 40 m thick, and quartzose calcarenite horizons are widespread. Siltstone is widespread, and a significant component of the formation, but rarely outcrops. Some sand units are discrete megriples totally enclosed by siltstone, and clearly formed as isolated sand-starved megriples on mudflats or an inner shelf. The Mulgarra Sandstone is quite similar to the Wongawol Formation, but for the presence of fine- to medium-grained glauconitic sandstone.

The deposited top is not preserved, and Bunting (1986) estimated the Mulgarra Sandstone was about 100 m thick, but we consider that at least 200 m stratigraphic thickness is exposed in the syncline northwest of Mulgarra Pool (Coonaburra, Fig. 2). The youngest zircons in a sample from near the base of the Mulgarra Sandstone yielded U-Pb SHRIMP ages of ca 1.8 Ga (Halilovic et al., 2004).

The main scarp of the Timperley Range, on Carnegie (Fig. 2) exposes the basal 20 m of the Formation, where it consists of interbedded fine-grained and coarse-grained felspathic quartz arenite, locally ferruginous, and bedded on a 100–200 mm scale. Coarser grained intervals are glauconitic. Both cross bedding and parallel bedding with primary current lineation are present, together with ripples indicative of very shallow water. Flute and load casts, and ball-and-pillow structures are present near the base. The basal contact with the underlying Kulele Limestone is sharp and marked by 1–2 m of shale. Elsewhere, the contact appears to be gradational, with limestone beds gradually decreasing upwards while siltstone and fine-grained sandstone increases.

Sedimentary structures and bedforms indicate the Mulgarra Sandstone was deposited in a coastal setting, with environments

ranging from a muddy inner shelf with isolated sandy megriples, through foreshore, beach and possibly tidal sandflat environments, to a washover lagoonal setting. Adhesion surfaces, blowouts and wrinkled surfaces suggest intermittent emergence and exposure, and widespread sediment loading structures indicate continued sporadic earthquakes.

4.2.7. Depositional environment of the Miningarra Subgroup

The Earaheedy Basin deepened northwards during deposition of the Miningarra and Tooloo Subgroups. In the south symmetric and asymmetric ripples, interference ripples, megriples and trough cross-beds indicate a shallow-water, upper shoreface to foreshore, intermittently emergent, setting. To the north, fine-grained rocks, parallel bedding, and hummocky cross-bedding suggest a dominantly storm-swept sub-wave base marine shelf. Limited palaeocurrent data support this model. The Chiall Formation records a change from iron oxide and chert to iron silicate grains. The presence of iron silicate minerals, such as glauconite, berthierine and chamosite, indicate dominantly low sedimentation rates for the finer grained facies of the lower Chiall Formation. Sedimentary structures suggest that the lower Chiall Formation was deposited in a shallow marine environment with deposition from below fairweather wave-base grading up into a shallow water, possibly nearshore bathymetry. The conglomerate at the base of the Chiall Formation represents reworking of the underlying lithologies and localized channel fill, and may be a transgressive rip-up deposit formed after a significant break. Sandstone beds are probably tempestites (storm related) and/or seismites (related to earthquakes; Rodriguez-Pascua et al., 2000). Sedimentary structures in the Princess Ranges Member suggest that it was deposited in a shallow marine to locally emergent environment, which was affected by both wave and current action. These features together with the compositional and textural maturity of coarser sandstone, which indicate a higher energy depositional environment in the Princess Ranges Member, suggest deposition in a tidal sand flat environment for much of the unit.

The Wongawol Formation is similar to the shale, mudstone, siltstone, and very fine-grained sandstone facies in the Chiall Formation. However, sedimentary structures suggest deposition was in a very shallow water to locally emergent environment, similar to but lower energy than that proposed for the Princess Ranges Member. Decreased terrigenous influx and a slight deepening of the basin led to carbonate dominated deposition, forming the Kulele Limestone. This was followed by a return to shallower conditions, greater terrigenous influx, and deposition of the Mulgarra Sandstone in an environment very similar to that for the Wongawol Formation, but slightly higher energy.

5. Stanley Fold Belt

The exposed Earaheedy Basin is deformed into a regional east to east-southeasterly trending, south-verging, asymmetric syncline, which plunges gently towards the southeast. The northern limb is steeply dipping to locally overturned, and forms the Stanley Fold Belt, a 110°-trending structural domain, about 200 km long and up to 35 km wide, and which is characterized by strike-slip faulting, foliation fabrics, tight folding, and reverse faulting. Folding varies in scale, with fold limbs commonly truncated by faults. Faults trend easterly, and include both dip-slip (dipping north), and sinistral strike-slip components. Major structures within the Stanley Fold Belt generally trend east or northwest and are positively magnetized. Sedimentary rocks of the Earaheedy Group are generally weakly metamorphosed, only locally attaining lower greenschist facies. Typical metamorphic minerals in fine-grained rocks are sericite, and chlorite.

Deformed rocks of the fold belt are exposed in the northeast corner of Granite Peak (Fig. 2). The degree of deformation in the Stanley Fold Belt decreases southward resulting in open, generally gentle folds, locally with an associated axial-plane cleavage. These features are expressed on aeromagnetic images as a series of broad, low-

amplitude, east-trending ridges and swales. Doubly-plunging mesoscale folds with wavelengths of 10–20 m (Fig. 24) are well displayed along escarpments (locally referred to as breakaways). Breccias and quartz vein stockworks are commonly associated with the folded rocks. In the transition zone between the Stanley Fold Belt and folded southern margin of the Earaheedy Basin, small-scale disharmonic folding and normal faulting is common.

5.1. Folds, faults and linear (E–W, N–S and NW–SE) structures

North trending structures are probably reactivated basement structures and their orientation is similar to D₃ structures of the Yilgarn Craton, which formed during sinistral transpression (e.g. Swager, 1997; Wyche and Farrell, 2000). A north–south trending structure on Wongawol may be a continuation of a major north to north–northeast trending structure on the eastern margin of the Duketon greenstone belt. The age of initiation of east trending structures is not well constrained (Groenewald et al., 2001). They postdate D₃ structures in the Yilgarn Craton and are thought to be Palaeoproterozoic in age, because an age of 2420 Ma was obtained from some east trending dykes (Nemchin and Pidgeon, 1998). In the northeastern Yilgarn Craton, where they cut the Earaheedy Group they could be either reactivated basement structures, or later features developed during deformation after deposition of the Earaheedy Group. On aeromagnetic imagery, both north- and east-trending structures can be seen to displace northwest-trending, ?bedding-parallel structures in the lower Earaheedy Group (see below). Movement on the east-trending structures is interpreted to have been dominated by vertical displacement. Manganese oxides mineralisation is commonly associated with north-trending structures and quartz fracturing and silicification is present along east-trending structures. The relative timing relationships between the east–west and north–south structures show ambiguous overprinting relationships.

Northwest trending negatively magnetized structures are interpreted to postdate deposition of the Earaheedy Group. The aeromagnetic signature is consistent with shallow-level, low-angle structures dipping to the northeast and there are no other parallel structures in the northeast Yilgarn Craton. These structures appear to be mostly bedding parallel with the Earaheedy Group, but are not the magnetic response of layering in the Frere Formation and they do not correspond to individual Gf horizons or to any iron-rich layer. Given the intense but continuous nature of these northwest trending features it seems likely they are the product of bedding parallel fluid flow. On Granite Peak (Pirajno et al., 2003) and Merrie (Adamides, 2000) they coincide with silicification of Gf in the Frere Formation and the presence of stilpnomelane in shale and siltstone beds. Aeromagnetic images indicate that movement along east and north structures offset, and therefore postdate, northwest structures. The relative timing relationships between the east–west and north–south structures show ambiguous overprinting relationships. In addition, magnetization along north structures is discontinuous and may reflect localized movement during more than one event.

Folds generally vary from open, upright, gently plunging to localized recumbent folding with the degree and style of folding typically strongly dependant on lithology. Mesoscale folds in fine- to coarse-grained sandstone intervals, typically form doubly plunging, elongate anticlinal features. In siltstone to very fine-grained sandstone dominated intervals, mesoscale folds vary from doubly plunging folds to localized disharmonic folding. Sporadic, northeast trending anticlines, which vary in scale from tens of metres up to approximately 1 km scale, are common in fine to coarse-grained sandstone dominated intervals such as the Princess Ranges Member. Deformation associated with these features is more intense than surrounding areas suggesting they may represent localized space accommodation zones.

The structural history suggests that at least two major deformation events are recorded in the Earaheedy Group. The first major deformation event resulted in low-angle mostly bedding-parallel movement, which produced northwest trending structures at various scales. A later, predominantly north–south compression resulted in vertical displacement along east–west trending structures. The orientation of the northwest trending structures and the lack of evidence for major displacement or strike-slip movement suggest that the deformation event associated with these structures was due to southwest directed compression. The timing of both of these events is not well constrained. Pb–Pb ages on Pb–Zn mineralization in the Sweetwaters Well Member (Richards and Gee, 1985) and Rb–Sr and K–Ar ages on glauconite (Horwitz, 1975a,b; Preiss et al., 1975), which have probably been reset, suggest a thermal event about c. 1650 Ma. This age coincides with some of the granitoid ages in the Gascoyne Complex and the 1680–1620 Ma Mangaroon Orogeny (Nelson, 2002; Sheppard et al., 2007). This event could be reflected in the north-trending, the east-trending, or the northwest-trending structures that cut the Earaheedy Group.

5.2. Quartz veins

Quartz stockwork veining is developed in granular chert in the Frere Formation (Jones and Pirajno, 2003), where it is cut by major east trending structures. Intense quartz stockwork veining is developed at the intersection of east trending structures with other major structures, such as the Proterozoic northwest oriented structures and the reactivated north–south oriented structures.

Centimetre-thick veins of syntaxial fibrous quartz are common in the sandstone units of the Chiall Formation. The orientation of the veins and the syntaxial quartz fibres enables the gauging of the stress field at the time that the veins were emplaced. On Nabberu and Granite Peak, two sets of quartz veins are present, in which the fibres are oriented 355° (σ_3 , least compressive stress), in the older vein set (strike 270°) and 150° (σ_3) in the younger set (vein strike 060°). This implies that the veins may have formed as a result of northeast–southwest directed compression. This compression event is interpreted to reflect tectonic movements associated with the Yapungku Orogeny (Smithies and Bagas, 1997; Bagas and Smithies, 1998; Bagas, 2004), which may have contributed to the formation of the Stanley Fold Belt. Ar–Ar dating of micas in the Stanley Fold Belt (Section 4.1) yielded ages of ca. 1650 Ma, suggesting that further deformation may relate to the Mangaroon Orogeny (Sheppard et al., 2005).

6. Shoemaker meteorite impact structure

The Shoemaker impact structure has an outer diameter of about 30 km (Fig. 2) and consists of two well-defined concentric ring synclinal and anticlinal structures, formed in rocks of the Chiall and Frere formations, surrounding Archaean basement rocks (Teague granite and greenstone rocks; Pirajno and Glikson, 1998). The concentric rings form low hills that interrupt the continuity of the west–northwest-trending Frere Range. The structure is discussed in detail by Pirajno (2002) and Pirajno et al. (2003) and only a brief review is given here.

Evidence for an impact origin of the Shoemaker impact structure includes:

1. A well-defined circular structure with surrounding rings of synclinal and anticlinal structures, which enclose a core of Archaean basement interpreted as a central uplift (Teague Granite and greenstone rocks).
2. Shatter cones in sedimentary rocks in both inner and outer rings.
3. Planar deformation features (PDFs) in quartz crystals of Teague Granite.

The target rocks encompass undeformed and unmetamorphosed sedimentary rocks of the Earaheedy Group, dipping to the northeast

about 10–15° and the underlying Archaean granite–greenstone basement of the Yilgarn Craton (Fig. 2; Pirajno et al., 2004). The central basement uplift, with a diameter of 12 km, consists of fractured Archaean granitoids of syenitic composition (Teague Granite). The syenitic composition of the Teague Granite suggests that it could either belong to a late Archaean suite of alkaline plutons that intrude the Yilgarn Craton (Johnson, in press; Smithies and Champion, 1999), or is the product of alteration of a precursor granitoid by alkali metasomatism related to an impact-generated heat source. Locally, the Teague Granite exhibits partial to pervasive silicification, is fractured and contains hydrothermal minerals, such as fibrous amphibole, garnet, sericite and prehnite, consistent with metasomatism.

The central and the western parts of the inner structure are entirely covered by Quaternary lake sediments and sand dunes. However, aeromagnetic data indicate that granitic (possibly monzonogranite) and greenstone rocks are present beneath these surficial deposits, representing the northern continuation of the Yilgarn Craton beneath the sedimentary cover of the Earaheedy Basin (Pirajno, 2002). The presence of diagnostic impact indicators, suggest that granitic and greenstone rocks form an impact-induced central structural uplift and possibly the basement core of the original crater. The eastern side of the structural uplift is characterized by high total magnetic intensity (TMI), hydrothermal alteration (see below) and the only exposures of the granitoid rocks (Teague Granite). The TMI pattern suggests not only that the upper parts of the original impact structure were eroded away, but also that the entire structure is probably tilted towards the east (Pirajno, 2002).

The age of the Shoemaker impact is not resolved, because of thermal and tectonic resetting of the isotopic systems of the target rocks at 1670–1620 Ma (Mangaroon Orogeny; Sheppard et al., 2007), 1070 Ma (age of the Warakurna large igneous province in the region; Wingate et al., 2004) and ca 550 Ma (age of the Petermann Orogeny; Scrimgeour et al., 1999). The magmatic age of the Teague Granite is Archaean (2648 ± 8 Ma; Nelson, 1999), which is within the range of other granitic rocks in the Yilgarn Craton (e. g. Smithies and Champion, 1999). Bunting et al. (1980a,b) obtained two whole-rock Rb–Sr isochron ages of 1630 and 1260 Ma from samples of Teague Granite. Pirajno (2002) and Pirajno et al. (2003) reported K–Ar and $^{39}\text{Ar}/^{40}\text{Ar}$ determinations on K-feldspar and illite–smectite separates also from the Teague Granite. The $^{39}\text{Ar}/^{40}\text{Ar}$ system yielded unreliable results, only providing broad constraints as to a maximum age (<1300 Ma; see Pirajno 2002, p. 36 for details). The K–Ar system gave two ages: 694 ± 25 Ma and 568 ± 20 Ma for K-feldspar and illite–smectite separates, respectively. Pirajno et al. (2003) concluded that the 568 ± 20 Ma K–Ar age determined on illite could represent either resetting due to the Petermann Orogeny, or the formation of illite as a result of post-impact hydrothermal activity.

About 5 km from the eastern shore of Lake Teague, scattered, cm to m-sized round and angular boulders of sandstone are present. This could be a lag deposit of Permian age (Paterson Formation; Bunting et al., 1982; Commander et al., 1982). Alternatively, because of their position close to the outermost ring and absence of any such lithology elsewhere in the Earaheedy Group in the region, it is also possible that they are either remnants of reworked lithic breccia ejecta, or crater-fill allochthonous breccia (Pirajno, 2002).

6.1. Hydrothermal alteration

In the Shoemaker impact structure the effects of impact energy-induced hydrothermal circulation within the impact aureole are evident in the Teague Granite (Pirajno, 2002) and in rocks of the Yelma and Frere formations (Earaheedy Group) exposed in the eastern inner ring. Outcrops of Teague Granite in the east and southeast are fractured, hydrothermally altered and partially to pervasively silicified. The rocks of the Teague Granite were studied as part of a regional investigation of felsic alkaline rocks of the Yilgarn Craton by Johnson

(in press), who concluded that the granitoids that outcrop in the Shoemaker structure were modified by alkali metasomatism resulting in a granitoid of syenitic composition. Johnson's conclusion was confirmed in subsequent studies (Pirajno and Glikson, 1998; Pirajno, 2002; Pirajno et al., 2003).

Pervasive silicification affected rocks of the Yelma Formation (Sweetwaters Well Member), whereas the GIF rocks of the Frere Formation exhibit cross-cutting quartz veining and are partially silicified. In the same area, pods of chert and jasperoidal quartz are present along the eastern margin of the central uplift. The chert material consists mainly of brecciated microcrystalline quartz cemented by chalcedonic quartz. Open spaces are filled with euhedral quartz crystals. These chert pods are interpreted to have formed by precipitation from hydrothermal fluids that circulated along faults and fractures in the eastern sector of Shoemaker impact structure.

It is likely that the meteorite impact that created the Shoemaker impact structure formed a melt sheet which, together with impact-released heat in the central uplift, gave rise to a hydrothermal convection system, within and around the central uplift zone. The melt sheet would have acted as a magma-like heat source within the crater structure and would have formed several hot springs in the crater and surrounding areas. Fluid channels and degassing pipes have been reported from the Ries impact crater in Germany (Newsom et al., 1986). Hydrothermal pods are present in the annular structures associated with the Haughton impact structure in Canada that have been interpreted as hydrothermal pipe structures (Osinski et al., 2001). Similarly, the pods of quartz-jasperoidal material that are present along structural breaks in the eastern rim of the Shoemaker impact structure may be the eroded remnants of fluid channels that fed thermal springs.

7. Depositional setting and geodynamic evolution of the Earaheedy Basin

This section presents a model for the geodynamic evolution of the Earaheedy Basin (Fig. 26), based on an integration of systematic field mapping, sedimentological and petrographic studies, geophysical data (aeromagnetic and gravity) and the available geochronology. The Earaheedy Group consists of both chemical and clastic sediments indicative of a shallow marine to coastal environment, which deepened to the north and northeast (Jones et al., 2000; Pirajno et al., 2004). The exposed rocks represent only the coastal to inner or middle-shelf portion of the continental shelf that was developed on the northern margin of the Yilgarn Craton. Sedimentary deposits of the outer shelf, continental slope and rise are not exposed, suggesting that much of the original depositional system is buried or not preserved. The grain size (dominantly medium-fine sand to silt) indicates dominantly quiet, low-energy conditions, although this could be because coarser material was simply not available due to a low-gradient, weathered, basin hinterland. Deposition was strongly influenced by water chemistry, sediment supply and sea-level fluctuations. Sea-level fluctuations are envisaged to be tectonically-driven, but with short-term eustatic changes in a greenhouse climate (Read et al., 1995) producing metre-scale cyclicity in carbonates and from tens of metres to metre scale cyclicity in the iron formation (iron formation-siltstone bands), and longer term tectonism responsible for increases in sand deposition by either hinterland uplift or basin subsidence. North to northeastward deepening is consistent with the distribution of facies within the basin architecture. The Tooloo Subgroup, which is characterized by GIF, reflects initial transgression (Yelma Formation), followed by intermittent influx of iron and silica into the basin (Frere Formation), whereas the overlying Miningarra Subgroup is characterized by low-energy, sand-poor clastic settings (lower Chiall Formation and Wongawol Formation), marginally sandier clastic settings (upper Chiall Formation and Mulgarra Sandstone), and slightly deeper clastic-starved conditions (Kulele Limestone).

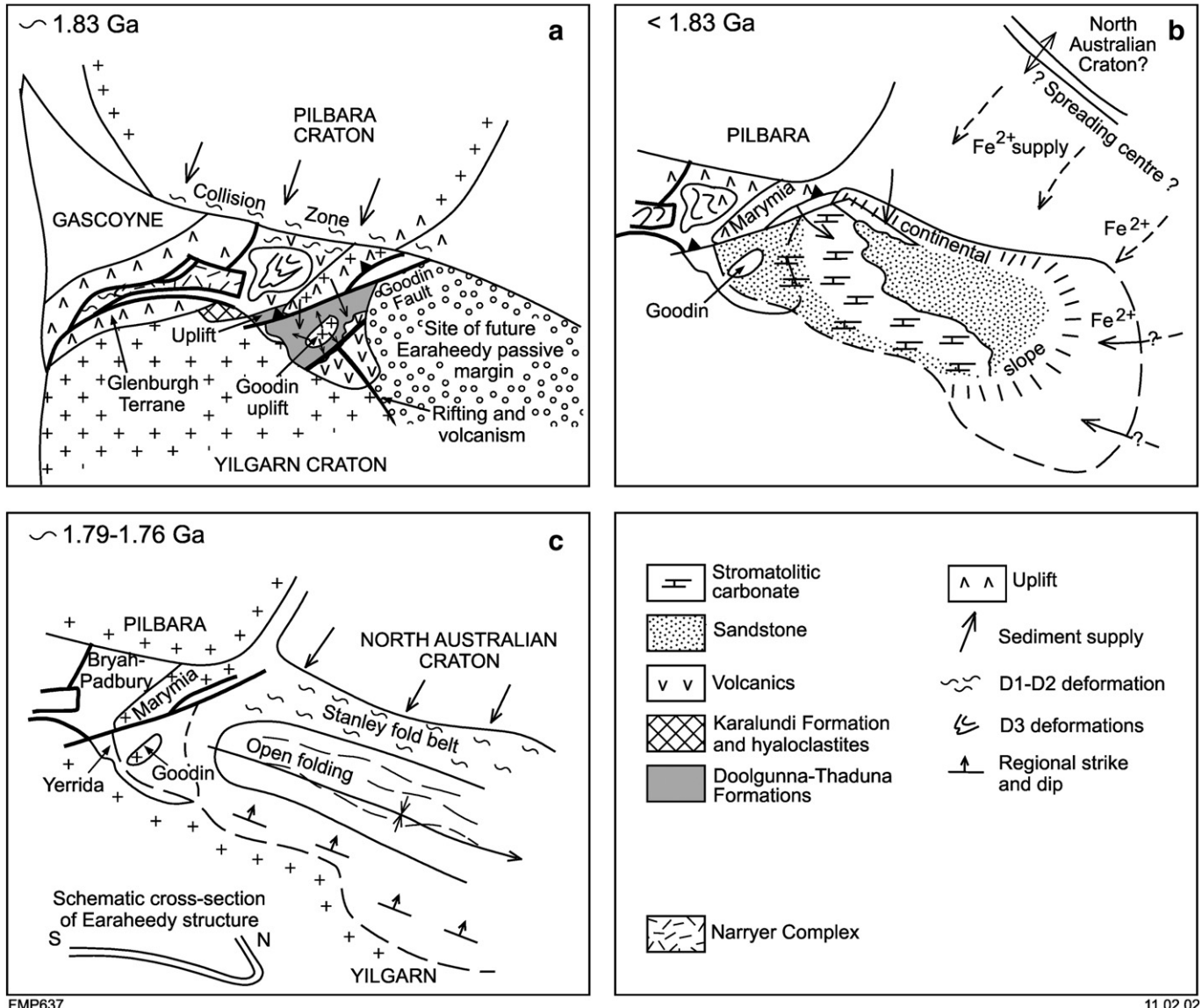


Fig. 26. Geodynamic evolution of the Earaheedy Basin. See text for details.

The lithofacies and facies trends of the Earaheedy Group suggest that it was part of a trailing passive margin (Jones et al., 2000; Pirajno et al., 2000; Pirajno et al., 2004; Pirajno, 2007), characterised by low-magnitude marine transgressions and regressions in response to fluctuating sea-level changes (Fig. 26b), due to a combination of sediment supply, subsidence and eustasy (Eriksson et al., 2001). Typically, trailing passive margins result from continental breakups (Braun and Beaumont, 1989; Bradley, 2008). Present-day exposed rocks represent only the coastal to shelfal portion of the continental shelf; sedimentary deposits of the continental slope and rise are not exposed, suggesting that much of the original depositional system is buried. The 1.99 Ga rhyodacitic subvolcanic rocks of the Imbin Inlier could be either an exotic fragment from a northern continent, or a fragment of the Dalgaringa Supersuite of the southern Gascoyne Complex that moved eastward by transcurrent movements (Occhipinti et al., 2001). Yet another possibility is that the Imbin rhyodacite is part of a bimodal (felsic–mafic) igneous suite related to continental breakup.

The GIF beds, and primary sedimentary structures preserved within them such as cross-bedding, provide a reasonable indicator of depositional setting, because in order to have large scale deposition of granular facies iron oxides, a widespread shallow-water environment

would have been required (e.g. Simonson and Hassler, 1996; Trendall, 2002). The source of iron and silica for the GIF in the Frere Formation is a key element in the understanding of the basin, together with the lack of evidence of contemporaneous volcanism and major deformation. Beukes and Klein (1992) and Isley (1995) considered GIF to be a shallow-water, higher energy equivalent of deeper water banded iron-formation. However, it should be noted that the model for the origin of the iron-formations proposed by Beukes and Klein (1992) and Isley (1995) accounts for the large volumes of iron, but it does not explain the association of iron and silica in grains of possible biogenic origin. Some of the grains classified as peloids, may have been originally oncrolites (Brown et al., 1995). If this is correct, then it is possible that biogenic activity may have played a major role in the development of the Earaheedy GIF, through a mechanism of bacterial iron oxidation (e.g. Nealson, 1982; Brown et al., 1995). Models of iron formation genesis suggest that the supply of the soluble Fe^{2+} is provided by hydrothermal effluents in oceanic settings (e.g. spreading centers or mantle-plume related oceanic plateaux; Isley, 1995). During deposition of the Tooloo Subgroup, no oceanic environment is known to have been present in the west. Lithofacies are progressively more distal to the north and northeast, oceans must have been to the north,

east and/or northeast (present-day geographic reference frame; Fig. 26b), beneath the presently exposed northwestern Officer Basin or Paterson Orogen.

The boundary between the Tooloo and Miningarra subgroups, at the base of Chiall Formation, reflects a change in depositional setting from a chemically significant, clastic-starved regime to one of greater, though still largely fine-grained, clastic supply. On Wongawol and Windidda (Fig. 2), the contact between the Chiall Formation and the underlying Windidda Formation is defined by a pebble- to cobble-sized conglomerate. Ball-and-pillow deformation is common higher in the succession in the Wandiwarra Member, Wongawol Formation, and Mulgarra Sandstone (especially the Wongawol Formation) indicating regular far-field seismicity or tectonic jiggling of the basin, but not major tectonism such as would result in high energy sandy or conglomeratic deposition. Continued high levels of dissolved iron are indicated by the widespread deposition of glauconitic sandstones. The Kulele Limestone, deposited in a subtidal stromatolitic carbonate environment, reflects a decrease in terrigenous supply, caused either by climatic or tectonic changes. The Mulgarra Sandstone shows a return to shelfal depositional setting of the Wongawol and Chiall Formations. A carbonate interval at the topmost Mulgarra Sandstone may have heralded a return to carbonate deposition, now only barely preserved because of later erosion. Bunting (1986) suggested that the Mulgarra Sandstone is disconformable on the Kulele Limestone, but this has not been confirmed by our work.

Five main sedimentary regimes, driven by sea level balanced against varying clastic influx, can be delineated (Fig. 27): An initial transgressive coarser clastic cycle (Yelma Formation) led, through continued transgression and diminished siliciclastic influx, to the deposition of platform carbonates (Sweetwaters Well Member) and culminated with the fine-grained clastic-starved succession of the Frere Formation, albeit with some rhythmicity. Comparatively strong subsidence led to another cycle of clastic sedimentation, manifested by the deposition of the Chiall Formation and then the Wongawol Formation, in a long-term shallowing-upward succession. Lessening of clastic influx, possibly at the end of the Capricorn Orogeny or possibly climate driven, resulted in deposition of the carbonate-dominated Kulele Limestone. This was followed by renewed clastic

influx, in continued shallow marine conditions, depositing the Mulgarra Sandstone.

SHRIMP U-Pb dating of detrital zircons suggests that sandstone in the Earaheedy Group was probably sourced predominantly from the Yilgarn Craton and the Gascoyne Complex to the west (Halilovic et al., 2004). Archaean ages are consistent with the Yilgarn Craton as a source. The youngest age of detrital zircons in the lower Tooloo Subgroup imply a 2.0–1.8 Ga source; the only possible source of these Palaeoproterozoic zircons in the immediate region (barring unknown continental fragments elsewhere) is to the west in the southern Gascoyne Complex. The SHRIMP data also suggest that the siliciclastic detritus was sourced from progressively younger sources during the evolution of the basin. The current age constraints for deposition of the Miningarra Subgroup are consistent with deposition beginning during the waning stages of the Capricorn Orogeny, but equally deposition could have been as late as the early stages of the Mangaroon Orogeny, immediately before deformation and development of the Stanley Fold Belt. In the former case, the subgroup may reflect rapid uplift to the west associated with granite intrusion in the western Capricorn Orogen, causing influx of siliciclastic material that overwhelmed the proportion of iron and silica in solution and consequently terminated the deposition of GIF, while favouring the deposition of glauconite peloids. Glauconite peloids, associated with clastic grains, are particularly common in shale, siltstone and very fine-grained sandstone horizons and at the base of medium to coarse-grained sandstone horizons in the Chiall Formation, and in the Mulgarra Sandstone. There is an association between glauconite and ferruginous sandstone, with alternations of glauconite-rich and ferruginous layers. In the latter case, later granite intrusions to the west may have triggered uplift and siliciclastic influx to the basin, after a hiatus of sufficient duration to allow lithification of the underlying Tooloo Subgroup.

From the above and given the age constraints, the deposition of the Tooloo Subgroup may have been synchronous with the Capricorn Orogeny, with deposition of the Miningarra Subgroup taking place in the waning stages of the Capricorn Orogeny or at a later time, prior to 1650 Ma. The present-day structure of the Earaheedy Basin along a north-south cross-section is asymmetric, with a broad shallow

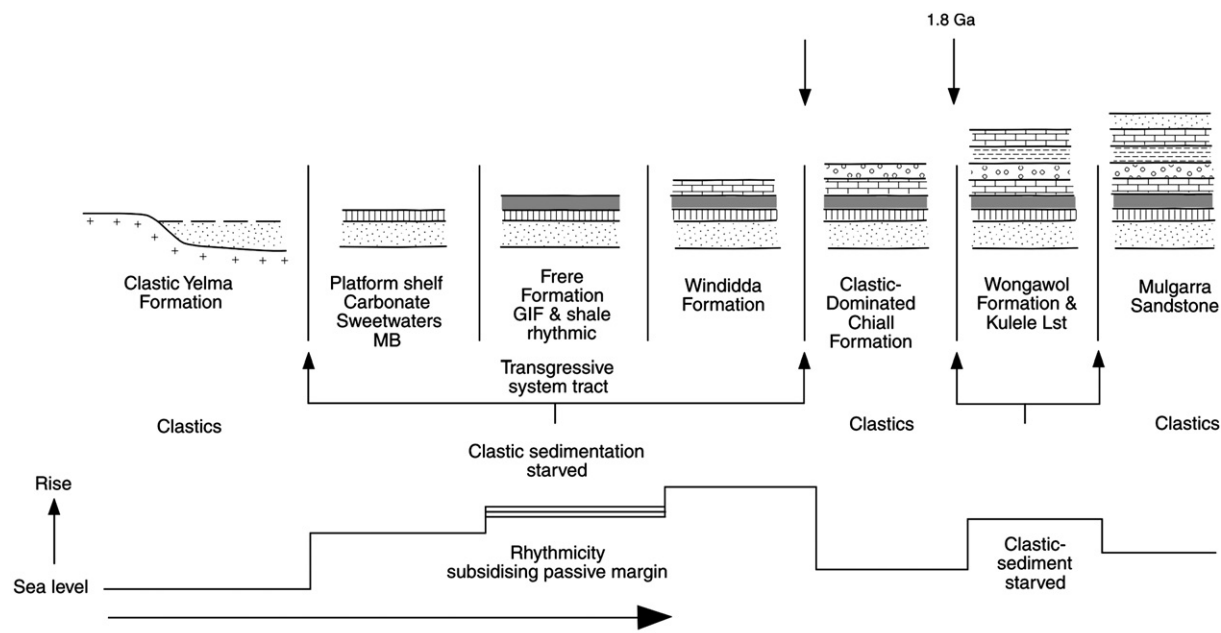


Fig. 27. Time-space diagram of deposition of Earaheedy Group lithologies, in response with sea level fluctuations. Details in text.

platform along a southern depositional margin and a strongly deformed northern tectonic margin, with reverse faulting, shearing, tight and recumbent folding, in the Stanley Fold Belt. Rare exposures and borehole intersections of undeformed, gently dipping Tooloo Subgroup, including GIF showing syndepositional pinch and swell structures, are present to the north of the fold belt. The only direct geochronological constraint on the timing of the deformation that formed the Stanley Fold Belt is the ^{39}Ar – ^{40}Ar date on metamorphic micas of ca. 1650 Ma; see Table 2 and Section 4.1). Other geochronological hints are provided by SHRIMP U–Pb dating of zircons and monazite from the Malmac Inlier (Fig. 1), which indicate a disturbance event at about 1.72 Ga (Nelson, 2002); SHRIMP U–Pb dating of zircons by McMillan and McNaughton (1995) and Vielreicher and McNaughton (2002), who also detected a disturbance, associated with hydrothermal activity, in the Marymia Inlier at about 1.72 Ga; and the age of epigenetic Mississippi Valley Type (MVT) mineralisation in the Yelma Formation, for which a Pb–Pb model age of 1.74–1.77 Ga was determined (Teen, 1996; Pirajno et al., in press).

Based on field data and the geochronological constraints above, we suggest that deposition of the Tooloo Subgroup ceased at about 1800 Ma, followed by a hiatus before deposition of the Miningarra Subgroup commenced in a major transgression at 1770 to perhaps 1750 Ma. The renewed deposition may have triggered fluid expulsion from basinal Tooloo Subgroup, largely by loading of the newly deposited Miningarra Subgroup, with fluids moving south up the basin flanks to form MVT sulphide deposits in carbonate platforms on the southern margin of the basin. Alternatively and following a more conventional model (Garven and Raffensperger, 1997), the MVT mineralisation in the Yelma Formation may reflect tectonic uplift along the Stanley Fold Belt to provide the necessary gravity gradients to drive basinal fluids updip, to form sulphide deposits in carbonate platforms on the southern margin of the basin (Pirajno, 2004). Deposition may have been terminated by the 1720 Ma event affecting the Marymia Inlier. A hiatus then followed prior to far-field deformation in the Mangaroon Orogeny forming the Stanley Fold Belt at about 1650 Ma. This model fits available geochronological data better than our previous model (Pirajno et al., 2004), which attributed formation of the fold belt to the D₂ phase of the Yapungku Orogeny (1.79–1.76 Ga; Smithies and Bagas, 1997; Bagas and Smithies, 1998; Bagas, 2004), which had a major effect in the Rudall Complex, north of the Earaheedy Basin. The deformation of the Earaheedy Group resulted in its folding into an asymmetrical syncline, conferring the apparent foreland basin-type north–south asymmetry of the Earaheedy Basin as illustrated in Figs. 2 and 5, although the depositional environments and sediment stacking pattern reflect a trailing passive margin rather than a foreland setting.

8. Discussion and conclusions

Many Archean granite–greenstone cratonic blocks are overlain by Archean or Proterozoic stable shelf sedimentary successions or platform covers, following early cratonisation, as for example in the Pilbara and Kaalpvaal Cratons, North China and the Siberian Cratons (e.g. Zhao et al., 2005). The Earaheedy Basin may be a remnant of a post-Archean platform-style sedimentary cover of the Yilgarn Craton. Cratonic basins and passive margins contain volcano-sedimentary and sedimentary successions, with banded and/or granular iron formations in the period between 2.4 and 1.8 Ga (Beukes and Gutzmer, 2008). The sedimentary rocks typically are represented by clastic sediments (arenite and shales) and shallow marine carbonates, characterised by transgression and regression sequences, reflecting the rise and fall of sea levels. The nature of the depositional systems in the post-Archean cratonic environments depends on the relative role of fluvial, aeolian, deltaic and tidal processes, wave and storm activity (Condie, 2005). Furthermore, the distribution of the sediments is controlled by regional uplifts, the extent of the shallow seas and

climate. Thus, where tectonic uplift is important, continental shelves tend to be narrow and sedimentation is dominated by wave and storm systems. In contrast, if uplift is confined to cratonic margins, fluvial and deltaic systems dominate (Condie, 2005). The reasons for the subsidence of cratonic blocks are not clear. A popular model is lithospheric stretching and thermal doming, followed by collapse. Doming of the lithosphere is a mechanism linked to upwelling asthenosphere or a mantle plume event, causing active erosion of the uplifted crust. Doming is followed by thermal contraction, resulting in the formation of cratonic platform basins and/or marginal basins around an opening ocean, which fill with sediments. A well documented example is the Neoproterozoic Centralian Superbasin, also in Australia, where crustal uplift due to a mantle plume at 825 Ma and subsequent sagging resulted in the deposition of thick successions of marine and fluvial sands (Walter et al., 1995).

Post-Archean depositional environments developed on the northern margin of the Yilgarn Craton, span some 450 million years, and were conducive to the genesis of a range of mineral systems, including seafloor hydrothermal deposits, extensive beds of granular iron formation, MVT, the world-class Magellan non-sulphide Pb deposit (Pirajno, 2008), and orogenic Au lode deposits (Pirajno et al., in press).

North of the Yilgarn Craton's present-day boundary are the Goodin, Marymia and Malmac inliers, all of which represent Archean granite–greenstone terranes and the northern extension of the Yilgarn Craton. These inliers are located within a 700-km long belt of Palaeoproterozoic volcano-sedimentary and sedimentary basins, which are considered part of the Capricorn Orogen (Fig. 1). These basins include the Bryah–Padbury, Yerrida and Earaheedy basins, developed between ca 2.2 and 1.8 Ga, recording periods of rifting, sedimentation and volcanism, along the northern passive margin of the Yilgarn Craton. The Yerrida Basin, is the oldest (ca. 2.17 Ga), and began its history as an intracontinental sag, within which low-energy siliciclastics and evaporites accumulated. To the west, the Bryah–Padbury basins formed during accretion and collision processes, related to the ca. 2.0–1.9 Ga Glenburgh and ca. 1.83–1.78 Ga Capricorn orogenies. An uplift and rifting event affected the Yerrida Basin at 1.84 Ga, resulting in coarse and immature clastic sedimentation together with the eruption of flood basalts (Mooloogool Group). To the east a passive margin developed, probably later than this uplift but the precise timing is poorly constrained. Sedimentation in this passive margin consisted of shallow-water clastic and chemical sediments (granular iron formation), which form the basal succession (Tooloo Subgroup) of the Earaheedy Basin. These events, deposition of the Mooloogool Group (uplift, rifting and volcanism) and the development of Earaheedy passive margin are difficult to explain within the framework of the Capricorn Orogeny. One possibility is that the Earaheedy passive margin formed as a result of continental breakup involving the Yilgarn Craton, perhaps as part of an Archean supercontinent. During the ca 1.74 Ga Yapungku Orogeny and the 1.65 Ga, Mangaroon Orogeny (Sheppard et al., 2005), the northern margin of the Earaheedy Basin and the western parts of the Yerrida Basin were deformed (Stanley Fold Belt).

The Yerrida and Earaheedy basins are also characterised by an asymmetry in preserved cross-section, with undeformed southern depositional margins and northern (Earaheedy), and northern–northwestern (Yerrida) tectonic margins of intensely deformed rocks, similar to foreland basin architecture (Stanley Fold Belt), but entirely post-depositional in origin; the basins were trailing margin basins and active depocentres. This may reflect the impingement of continental plates from the north and northeast.

The granular iron formation beds of the Frere Formation in the Earaheedy Basin constitute a significant Fe resource, extending along strike for at least 280 km. In the western parts of the Basin, zones of enrichment due to supergene and tectonic deformation processes, contain between 21 and 66% Fe. Locally, stratiform Fe–Mn oxides with anomalous abundances of Cu, Ba and Pb are hosted in clastic beds of

the Wongawol Formation. The origin of the vast amounts of iron and manganese required to form the observed iron and manganese formations in Proterozoic sedimentary basins is controversial, but the popular view is that submarine hydrothermal effluents are the major source of these metals as well as others, such as Cu, Co, Zn, Pb, Au and Ag. Upwelling currents transport iron and manganese in reduced form (Fe^{+2} and Mn^{+2}) from the discharge vents, with precipitation occurring just above the oxic–anoxic interface, where Fe^{2+} and Mn^{2+} are oxidised to Fe^{3+} and Mn^{4+} , with separation being constrained by the Eh–pH conditions (Trendall, 2002). Uplift of fold belts provide the topographic relief that is necessary to cause basinal brines to migrate across the basin, with rates that are measured in several m/year, but that decline over a few million years as erosion progresses. Tectonically- and/or gravity-driven flow in foreland basins is considered as one of the main causes for the origin of the second group of mineral systems, which includes Mississippi Valley type (MVT) deposits, exemplified by the carbonate-hosted Zn–Pb deposits in the Yelma Formation (Earaheedy Basin) and the Magellan non-sulphide Pb deposit (Pirajno, 2008).

The Earaheedy Basin has special importance in the tectono-stratigraphic record of Palaeoproterozoic terranes, not only because of the presence of GfF beds, but also because it provides evidence of an ancient passive margin, which developed to the northern and northeastern margins of the Archaean Yilgarn Craton, hinting at a possible breakup from a larger Archaean continent at ca. 1.8 Ga.

Acknowledgements

This paper is published with the permission of the Director of the Geological Survey of Western Australia. The authors are grateful to Prof P. G. Eriksson for his constructive comments.

Appendix A. Supplementary data

Supplementary data associated with this article can be found, in the online version, at doi:10.1016/j.earscirev.2009.03.003.

References

- Adamides, N., 2000. Geology of the Merrie 1:100000 sheet. Geological Survey of Western Australia, 1:100 000 Geological Series Explanatory Notes, 37.
- Adamides, N.G., Pirajno, F., Hocking, R.M., 2000. Geology of the Fairbairn 1:100 000 sheet. Geological Survey of Western Australia, 1:100 000 Geological Series Explanatory Notes, 26.
- Allchurch, D., Bunting, J.A., 1975. The Kaluweerie Conglomerate: a Proterozoic fluvialite sediment from the northeast Yilgarn Block, Western Australia. Geological Survey of Western Australia Annual Report 1975, 83–87.
- Altermann, W., 2004. Precambrian stromatolites: problems and definitions, classification, morphology and stratigraphy. In: Eriksson, P.G., Altermann, W., Nelson, D.R., Mueller, W.U., Catuneau, O. (Eds.), The Precambrian Earth: Tempos and Events. Precambrian Geology, vol. 12. Elsevier, Amsterdam, pp. 564–574.
- Anderson, E.J., Goodwin, P.W., 1990. The significance of metre-scale allocycles in the quest for a fundamental stratigraphic unit. Journal of the Geological Society London 147, 507–518.
- Bagas, L., 1998a. The Archaean Marymia Inlier—a review of its tectonic history and relationships to the Yilgarn Craton. Geological Survey of Western Australia, Annual Review 85–90 1997–1998.
- Bagas, L., 1998b. Geology of the Marymia 1:100000 sheet. Geological Survey of Western Australia, 1:100 000 Geological Series Explanatory Notes, 23.
- Bagas, L., 2004. Proterozoic evolution and tectonic setting of the northwest Paterson Orogen, Western Australia. Precambrian Research, 128, 475–496.
- Bagas, L., Smithies, R.H., 1998. Geology of the Connaughton 1:100 000 sheet, Western Australia. Western Australia Geological Survey, 1:100 000 Geological Series, Explanatory Notes, 38.
- Bagas, L., Williams, I.R., and Hickman, A.H., 2000. Rudall, Western Australia (2nd Edition): Western Australia Geological Survey, 1:250 000 Geological Series Explanatory Notes, 50.
- Barley, M.E., Bekker, A., Krapež, 2005. Late Archean to Early Paleoproterozoic global tectonics, environmental change and the rise of atmospheric oxygen. Earth and Planetary Science Letters 238, 156–171.
- Bau, M., Moller, P., 1993. Rare earth element systematics of the chemically precipitated component in Early Precambrian iron formations and the evolution of the terrestrial atmosphere–lithosphere system. Geochimica et Cosmochimica Acta 57, 2239–2249.
- Beukes, N.J., Klein, C., 1990. Geochemistry and sedimentology of a facies transition—from microbanded to granular iron-formation—in the early Proterozoic Transvaal Supergroup, South Africa. Precambrian Research 47, 99–139.
- Beukes, N.J., Klein, C., 1992. Models of iron-formation deposition. In: Schoppe, W., Klein, C. (Eds.), The Proterozoic Biosphere: A Multidisciplinary Study. Cambridge University Press, New York, pp. 147–151.
- Beukes, N.J., Gutzmer, J., 2008. Origin and paleoenvironmental significance of major iron formations at the Archean–Paleoproterozoic boundary. SEG Reviews 15, 5–47.
- Blatt, H., Middleton, G., Murray, R., 1980. Origin of Sedimentary Rocks, 2nd edition. Prentice Hall Inc., Englewood Cliffs, NJ. 782 pp.
- Bradley, D.C., 2008. Passive margins through earth history. Earth-Science Reviews 91, 1–26.
- Brakel, A.T., Leech, R.E.J., 1980. Trainor, W. A. Geological Survey of Western Australia, 1:250 000 Geological Series Explanatory Notes 13.
- Braun, J., Beaumont, C., 1989. A physical explanation of the relation between flank uplifts and the breakup unconformity at rifted continental margins. Geology 17, 760–764.
- Brown, D.A., Gross, G.A., Sawicki, J.A., 1995. A review of the microbial geochemistry of banded iron-formations. Canadian Mineralogist 33, 1321–1333.
- Bunting, J.A., 1980a. Kingston, W.A. Geological Survey of Western Australia, 1:250 000 Geological Series Explanatory Notes 18.
- Bunting, J.A., 1980b. Kingston, Western Australia, Sheet SG 51-10. Australia Bureau of Mineral Resources and Geological Survey of Western Australia 1:250 000 Geological Series.
- Bunting, J.A., 1986. Geology of the eastern part of the Nabberu Basin. Geological Survey of Western Australia, Bulletin 131, 130.
- Bunting, J.A., Brakel, A.T., Commander, D.P., 1982. Nabberu, Western Australia. Geological Survey of Western Australia, 1:250 000 Geological Series Explanatory Notes vol. 27.
- Butt, C.R.M., Horwitz, R.C., Mann, A.W., 1977. Uranium occurrences in calcrete and associated sediments in Western Australia. CSIRO, Div Mineralogy, Minerals Research Laboratories, Report FP16, unpublished.
- Cawood, P.A., Nemchin, A.A., 2000. Provenance record of a rift basin: U/Pb ages of detrital zircons from the Perth Basin, Western Australia. Sedimentary Geology 134, 209–234.
- Cawood, P.A., Tyler, I.M., 2004. Assembling and reactivating the Proterozoic Capricorn Orogen: lithotectonic elements, orogenies and significance. Precambrian Research 128, 201–218.
- Commander, D.P., Muhling, P.C., Bunting, J.A., 1982. Stanley, W.A. Geological Survey of Western Australia, 1:250 000 Geological Series Explanatory Notes 19.
- Condie, K.C., 2005. Earth as an Evolving Planetary System. Elsevier, Amsterdam, p. 447.
- Deer, W.A., Howie, R.A., Zussman, J., 1965. Rock forming minerals. Sheet Silicates, vol. 3. Longmans, London. 270 pp.
- Derry, L.A., Jacobsen, S.B., 1990. The chemical evolution of Precambrian seawater: evidence from REEs in banded iron formations. Geochimica et Cosmochimica Acta 54, 2965–2977.
- Donaldson, W.S., Plint, A.G., Longstaffe, F.J., 1999. Tectonic and eustatic control on deposition and preservation of Upper Cretaceous ooidal ironstone and associated facies: Peace River Arch area, NW Alberta, Canada. Sedimentology 46, 1159–1182.
- Einsele, G., 2000. Sedimentary Basins: Evolution, Facies and Sedimentary Budget, 2nd Ed. Springer-Verlag, Heidelberg. 792 pp.
- Elrick, M., Read, J.F., 1991. Cyclic ramp-to-basin carbonate deposits, Lower Mississippian, Wyoming and Montana, a combined field and computer modelling study. Journal of Sedimentary Petrology 61, 1194–1224.
- Eriksson, P.G., Martins-Neto, M.A., Nelson, D.R., Aspöler, L.B., Chiarenzelli, J.R., Catuneau, O., Sarkar, S., Altermann, W., Rautenberg, C.J.D.E.W., 2001. An introduction to Precambrian basins: their characteristics and genesis. Sedimentary Geology 141–142, 1–35.
- Fischer, A.G., Bottjer, D.J., 1991. Orbital forcing and sedimentary sequences. Journal of Sedimentary Petrology 61, 1063–1069.
- Franseen, E.K., Watney, W.L., Kendall, C.G.St.C., Ross, W. (Eds.), 1991. Sedimentary modelling: computer simulations and methods for improved parameter definition, 233. Kansas Geological Survey Bulletin. 524 p.
- Garven, G., Raffensperger, J.P., 1997. Hydrogeology and geochemistry of ore genesis in sedimentary basins, In: Barnes, H.L. (Ed.), Geochemistry of Ore Deposits, 3rd Ed. John Wiley & Sons, pp. 125–189.
- Giles, E., 1889. Australia twice traversed; the romance of exploration, being a narrative compiled from the journals of five exploring expeditions into and through central South Australia and Western Australia, from 1872 to 1876. London, Low, Marston, Searle and Rivington.
- Goode, A.D.T., Hall, W.D.M., Bunting, J.A., 1983. The Nabberu Basin of Western Australia. In: Trendall, A.F., Morris, R.C. (Eds.), Iron formation: Facts and Problems. Developments in Precambrian Geology, vol. 6. Elsevier, pp. 295–323. Monograph.
- Goldhammer, R.K., Dunn, P.A., Hardie, L.A., 1987. High-frequency, glacioeustatic sealevel oscillations with Milankovich characteristics recorded in Middle Triassic platform carbonates in northern Italy. American Journal of Science 287, 853–892.
- Goldhammer, R.K., Dunn, P.A., Hardie, L.A., 1990. Depositional cycles, composite sealevel changes, cycle stacking patterns, and the hierarchy of stratigraphic forcing—examples from platform carbonates of the Alpine Triassic. Geological Society of America Bulletin 102, 535–562.
- Goldhammer, R.K., Lehmann, P.J., Dunn, P.A., 1993. The origin of high-frequency platform carbonate cycles and third order sequences (Lower Ordovician El Paso Group, West Texas): constraints from outcrop data and stratigraphic modelling. Journal Sedimentary Petrology 63, 318–359.
- Grey, K., 1984. Biostratigraphic studies of stromatolites from the Proterozoic Earaheedy Group, Nabberu Basin, Western Australia. Geological Survey of Western Australia Bulletin 130, 123.
- Grey, K., 1994. Stromatolites from the Palaeoproterozoic Earaheedy Group, Earaheedy Basin, Western Australia. Alcheringa 18, 187–218.

- Grey, K., Thorne, A.M., 1985. Biostratigraphic significance of stromatolites in upward shallowing sequences of the early Proterozoic Duck Creek Dolomite, Western Australia. *Precambrian Research* 29, 183–206.
- Groenewald, P.B., Painter, M.G.M., McCabe, M., 2001. East Yilgarn geoscience database: north Eastern Goldfields, Cunyu to Cosmo Newbery 1:100 000 digital geological data package. Western Australia Geological Survey, Report 83, 39.
- Gromet, L.P., Dynek, R.F., Haskin, L.A., Korotev, R.L., 1984. The "North American Shale Composite": its compilation, major and trace element characteristics. *Geochimica et Cosmochimica Acta* 48, 2469–2482.
- Hall, W.D.M., Goode, A.D.T., 1975. The Nabberu Basin; a newly discovered Lower Proterozoic basin in Western Australia. First Australian Geological Convention, Abs. Geological Society of Australia, pp. 88–89.
- Hall, W.D.M., Goode, A.D.T., 1978. The early Proterozoic Nabberu Basin and associated iron formations of Western Australia. *Precambrian Research* 7, 129–184.
- Hall, W.D.M., Goode, A.D.T., Bunting, J.A., Commander, D.P., 1977. Stratigraphic terminology of the Earaheedy Group, Nabberu Basin. Geological Survey of Western Australia, Annual Report 1976, 40–43.
- Halilovic, J., Cawood, P.A., Jonaes, J.A., Pirajno, F., Nemchin, A.A., 2004. Provenance of the Earaheedy Basin, Western Australia: palaeogeographic and tectonic implications. *Precambrian Research* 128, 343–366.
- Hamilton, R., 1992. Geology and structural setting of ultramafic lamprophyres from Bulljiah Pool, central Western Australia. *Journal of the Royal Society of Western Australia* 75, 51–56.
- Hamilton, R., Rock, N.M.S., 1990. Geochemistry, mineralogy and petrology of a new find of ultramafic lamprophyres from Bulljiah Pool, Nabberu Basin, Yilgarn Craton, Western Australia. *Lithos* 24, 275–290.
- Heikoop, J.M., Tsujita, C.J., Risk, M.J., Tomascil, T., Mah, A.J., 1996. Modern iron ooids from a shallow-marine volcanic setting: Mahegetang, Indonesia. *Geology* 24, 759–762.
- Hocking, R.M., Jones, J.A., 1999. Methwin, W.A. Sheet 3047. Geological Survey of Western Australia, 1:100 000 Geological Series.
- Hocking, R.M., Jones, J.A., Pirajno, F., Grey, K., 2000a. Revised Lithostratigraphy for Proterozoic Rocks in the Earaheedy Basin and Nearby Areas. Geological Survey of Western Australia. Record 2000/16, 22.
- Hocking, R.M., Grey, K., Bagas, L., Stevens, M.K., 2000b. Mesoproterozoic stratigraphy in the Oldham Inlier, Little Sandy Desert, central Western Australia. Geological Survey of Western Australia, Annual Review 49–56 (1999–2000).
- Horwitz, R.C., 1975a. The southern boundaries of the Hamersley and Bangemall Basins of sedimentation. First Australian Geological Convention, Abs. Geological Society of Australia, pp. 88–89.
- Horwitz, R.C., 1975b. Provisional geological map at 1:2500000 of the north-east margin of the Yilgarn Block, Western Australia. Australia Commonwealth Scientific Industrial Research Organization, Mineral Research Lab. Report F10.
- Horwitz, R.C., 1976. Two unrecorded basal sections in older Proterozoic rocks of Western Australia. Australia CSIRO Mineral Research Lab. Report FP 10.
- House, M.R., Gale, A.S. (Eds.), 1995. Orbital Forcing Timescales and Cyclostratigraphy. Geological Society Special Publication, p. 85.
- Isley, A.E., 1995. Hydrothermal plumes and the delivery of iron to banded iron formation. *The Journal of Geology* 103, 169–185.
- Jacobsen, S.B., Pimentel-Klose, M.R., 1988. Nd isotopic variations in Precambrian banded iron formations. *Geophysical Research Letters* 15, 393–396.
- Johnson, G.I., in press. The petrology, geochemistry and geochronology of the felsic alkaline suite of the eastern Yilgarn block, Western Australia. South Australia, University of Adelaide, PhD thesis.
- Jones, J.A., 2004. Geology of the Wongawol 1:100 000 sheet. Geological Survey of Western Australia Explanatory Notes 1:100 000 Geological Series, 28 p.
- Jones, J.A., Pirajno, F., 2003. Cracke breccias in the Earaheedy Basin: implications for a newly recognised epithermal mineralization event. Geological Survey of Western Australia Record 2003/5, 20–24.
- Jones, J.A., Pirajno, F., Hocking, R.M., Grey, K., 2000. Revised stratigraphy for the Earaheedy Group: implications for the tectonic evolution and mineral potential of the Earaheedy Basin. Geological Survey of Western Australia, Annual Review 57–63 (1999–2000).
- Johnston, D.A., Hall, W.D.M., 1980. Final Report temporary Reserves 6639H, 7000H, 7001H, 7002H, and mineral claims 69/966 to 69/999, Sweetwaters Well, Nabberu Mining District, Western Australia. Dampier Mining Co. (unpublished).
- Kappeler, A., Pasquero, C., Konhauser, K.O., Newman, D.K., 2005. Deposition of banded iron formations by anoxygenic phototrophic Fe(II)-oxidizing bacteria. *Geology* 33, 865–868.
- Kimberley, M.M., 1989. Nomenclature for iron formations. *Ore Geology Reviews* 5, 1–12.
- Kinny, P.D., Nutman, A.P., Occhipinti, S.A., 2004. Reconnaissance dating of events recorded in the southern part of the Capricorn Orogen. *Precambrian Research* 128, 279–294.
- Klein, C., Ladeira, E.A., 2000. Geochemistry and petrology of some Proterozoic banded iron formations of the Quadrilatero Ferrifero, Minas Gerais, Brazil. *Economic Geology* 95, 405–428.
- Konhauser, K.O., Hamade, T., Morris, R.C., Ferris, F.G., Southam, G., Raiswell, R., Canfield, D., 2002. Could bacteria have formed the Precambrian banded iron formations? *Geology* 30, 1079–1082.
- LaBerge, G.L., 1966. Altered pyroclastic rocks in iron formations in the Hamersley Range, Western Australia. *Economic Geology* 61, 147–161.
- Langford, R.L., Wyche, S., Liu, S.F., 2000. Geology of the Wiluna 1: 100 000 sheet. Geological Survey of Western Australia, 1:100 000 Geological Series Explanatory Notes 26.
- Le Blanc Smith, G., Pirajno, F., Nelson, D.R., Grey, K., 1995. Base-metal deposits in the Early Proterozoic Glengarry terrane, Western Australia. Geological Survey of Western Australia Annual Review 1993–94, 59–62.
- Leech, R.E.J., Brakel, A.T., 1980. Bullen, Western Australia. Geological Survey of Western Australia, 1:250 000 Geological Series Explanatory Notes 11.
- Lindsay, J., Brasier, M., 2002. Did global tectonics drive early biosphere evolution? Carbon isotope record from 2.6 to 1.9 Ga carbonates of Western Australia. *Precambrian Research* 114, 1–34.
- Martin, D.McB., Thorne, A.M., 2004. Tectonic and basin evolution of the Bangemall Supergroup in the northwestern Capricorn Orogen. *Precambrian Research* 128, 385–410.
- Martin, D.McB., Thorne, A.M., 2001. New insights into the Bangemall Supergroup, in GSWA 2001 extended abstracts: new geological data for WA explorers. Geological Survey of Western Australia, Record 2001/5, 1–2.
- McMillan, N.M., McNaughton, N.J., 1995. The post-magmatic history of felsic rocks from the Archaean Marymia Dome—a SHRIMP study of the relationship between zircon morphology, Th/U and geological history. Third Australian Conference on Geochronology and Isotope Geoscience, Abstracts, p. 18.
- McNaughton, N.J., Rasmussen, B., Fletcher, I.R., 1999. SHRIMP uranium-lead dating of diagenetic xenotime in siliciclastic sedimentary rocks. *Science* 285, 78–80.
- Morris, P.A., Pirajno, F., 2005. Mesoproterozoic sill complexes in the Bangemall Supergroup, Western Australia. *Geology, geochemistry and mineralization potential*. Geological Survey of Western Australia. Report 99, 75 p.
- Morris, P.A., Pirajno, F., Shevchenko, S., 2003. Proterozoic mineralization identified by integrated regional regolith geochemistry, geophysics and bedrock mapping in Western Australia. *Geochemistry: Exploration, Environment, Analysis* 3 (2003), 13–28.
- Myers, J.S., Shaw, R., Tyler, I.M., 1996. Tectonic evolution of Proterozoic Australia. *Tectonics* 15–6, 1431–1446.
- Nealson, K.H., 1982. Microbiological oxidation and reduction of iron. In: Holland, H.D., Schidlowski, M. (Eds.), *Mineral Deposits and the Evolution of the Biosphere*. Springer-Verlag, pp. 51–66.
- Nelson, D.R., 1997. Compilation of SHRIMP U-Pb zircon geochronology data, 1996. Geological Survey of Western Australia, p. 189. Record 1997/2.
- Nelson, D.R., 1999. Compilation of SHRIMP U-Pb zircon geochronology data, 1998. Geological Survey of Western Australia, p. 222. Record 1999/2.
- Nelson, D.R., 2001a. An assessment of the determination of depositional ages for Precambrian clastic sedimentary rocks by U-Pb dating of detrital zircons. *Sedimentary Geology* 141–142, 37–60.
- Nelson, D.R., 2001b. Compilation of geochronology data, 2000. Geological Survey of Western Australia, p. 205. Record, 2001/2.
- Nelson, D.R., 2002. Compilation of geochronology data, 2001. Geological Survey of Western Australia, p. 282. Record, 2002/2.
- Nemchin, A.A., Pidgeon, R.T., 1998. Precise conventional and SHRIMP baddelyite U-Pb age for the Binneringie Dyke, near Narrogin, Western Australia. *Australian Journal of Earth Sciences* 45, 673–675.
- Newsom, H.E., Graup, G., Seward, T., Keil, K., 1986. Fluidization and hydrothermal alteration of the suevite deposit at the Ries Crater, West Germany, and implications for Mars. *Journal of Geophysical Research* 91, E239–E251.
- Occhipinti, S.A., Sheppard, S., 2001. Stuck between two cratons—latest Archaean crust in the Gascoyne Complex, Western Australia. The Fourth International Archaean Symposium, Extended Abstracts, pp. 72–74.
- Occhipinti, S.A., Sheppard, S., Nelson, D.R., Myers, J.S., Tyler, I.M., 1998. Syntectonic granite in the southern margin of the Palaeoproterozoic Capricorn Orogen, Western Australia. *Australian Journal of Earth Sciences* 45, 509–512.
- Occhipinti, S.A., Sheppard, S., Myers, J.S., Tyler, I.M., Nelson, D.R., 2001. Archaean and Palaeoproterozoic geology of the Narryer terrane (Yilgarn Craton) and the southern Gascoyne Complex (Capricorn Orogen), Western Australia—a field guide. *Geological Survey of Western Australia Record* 70 2001/8.
- Occhipinti, S.A., Sheppard, S., Passchier, C., Tyler, I.M., 2004. Paleoproterozoic crustal accretion and collision in the southern Capricorn Orogen: the Glenburgh Orogeny. *Precambrian Research* 198, 237–256.
- Osinski, G.R., Spray, G., Lee, P., 2001. Impact-induced hydrothermal activity within the Haughton impact structure, arctic Canada: generation of a transient, warm, wet oasis. *Meteoritic and Planetary Science* 36, 731–745.
- Pirajno, F., 2002. Geology of the Shoemaker Impact Structure, Western Australia. Geological Survey of Western Australia, Report 82, 52.
- Pirajno, F., 2004. Metallogeny in the Capricorn Orogen, Western Australia, the result of multiple ore-forming processes. *Precambrian Research* 128, 411–440.
- Pirajno, F., 2007. Metallogeny of Palaeoproterozoic depositional environments on the northern margin of the Yilgarn Craton. In: Bierlein, F., Knob-Robinson, C.M. (Eds.), *Proceedings of Kalgoorlie '07 Conference*, Kalgoorlie, pp. 77–79.
- Pirajno, F., 2008. *Hydrothermal Processes and Mineral Systems*. Springer, Berlin. 1250 pp.
- Pirajno, F., Adamides, N.G., 1998. Geology of the Thaduna 1:100 000 sheet. Geological Survey of Western Australia, 1:100 000 Geological Series Explanatory Notes 24.
- Pirajno, F., Glikson, A., 1998. Shoemaker impact structure, Western Australia. *Celestial Mechanics and Dynamical Astronomy* 69, 25–30.
- Pirajno, F., Occhipinti, S.A., 1998. Geology of the Bryah 1:100 000 sheet. Geological Survey of Western Australia, 1:100 000 Series Explanatory Notes, 41 p.
- Pirajno, F., Adamides, N.G., 2000. Iron–manganese oxides and glauconite-bearing rocks of the Earaheedy Group: implications for the base metal potential of the Earaheedy Basin. Geological Survey of Western Australia, Annual Review 65–71 (1999–2000).
- Pirajno, F., Hocking, R.M., 2001a. Rhodes, W.A. Sheet 3147: Geological Survey of Western Australia, 1:100 000 Geological Series.
- Pirajno, F., Hocking, R.M., 2001b. Mudan, W.A. Sheet 3247: Geological Survey of Western Australia, 1:100 000 Geological Series.
- Pirajno, F., Hocking, R.M., 2002. Glenayle, W.A. Sheet 3347: Geological Survey of Western Australia, 1:100 000 Geological Series.
- Pirajno, F., Hocking, R.M., Jones, J.A., 2000. Rhodes, W.A. Sheet 3147. Geological Survey of Western Australia, 1:100 000 Geological Series.

- Pirajno, F., Hawke, P., Glikson, A.Y., Haines, P.W., Uysal, T., 2003. Shoemaker impact structure, Western Australia. *Australian Journal of Earth Sciences* 34 (No. 5), 775–796.
- Pirajno, F., Jones, J.A., Hocking, R.M., Halilovic, J., 2004. Geology and tectonic evolution of Palaeoproterozoic basins of the eastern Capricorn Orogen, Western Australia. *Precambrian Research* 128, 315–342.
- Pirajno, F., Hocking, R.M., Jones, J.A., Reddy, S.J., in press. Geology and mineral systems of the Palaeoproterozoic Earaheedy Basin, Western Australia. *Geological Survey of Western Australia Report*.
- Pratt, B.R., 2002. Storms versus tsunamis: dynamic interplay of sedimentary, diagenetic and tectonic processes in the Cambrian of Montana. *Geology* 30, 423–426.
- Preiss, W.V., Jackson, M.J., Page, R.W., Compston, W., 1975. Regional geology, stromatolite biostratigraphy and isotopic data bearing on the age of a Precambrian sequence near Lake Carnegie, Western Australia. 1st Australian Geological Convention, Abstracts. *Geological Society of Australia*, pp. 92–93.
- Price, J., 2003. Depositional setting of granular iron formation in the Palaeoproterozoic Frere Formation, Earaheedy Basin, Western Australia. BSc (Hon) thesis, unpublished, The University of Western Australia, 80 pp.
- Rasmussen, B., Fletcher, I.R., 2002. Indirect dating of mafic intrusions by SHRIMP U–Pb analysis of monazite in contact metamorphosed shale: an example from the Palaeoproterozoic Capricorn Orogen, Western Australia. *Earth and Planetary Science Letters* 197, 287–299.
- Read, J.F., Kerans, C., Webber, L.J., Sarg, J.F., Wright, F.M. (Eds.), 1995. Milankovich sea-level changes, cycles, and reservoirs on carbonate platforms in greenhouse and icehouse worlds. *SEPM Short Course Notes*, vol. 35, p. 212.
- Reddy, S.M., Collins, A.S., Buchan, A.C., Mruma, A., 2004. Heterogeneous excess argon and Neoproterozoic heating in the Usagaran Orogen, Tanzania, revealed by single grain $^{40}\text{Ar}/^{39}\text{Ar}$ thermochronology. *Journal of African Earth Sciences* 39, 165–176.
- Richards, J.R., Gee, R.D., 1985. Galena lead isotopes from the eastern part of the Nabberu Basin, Western Australia. *Australian Journal of Earth Sciences* 32, 47–54.
- Rock, N.M.S., 1990. Lamprophyres: the Global Occurrence, Petrology, Origin and Economic Significance of Some Rocks of Deep Origin. Blackie, Glasgow. 250 pp.
- Rodriguez-Pascua, M.A., Clavo, J.P., De Vicente, G., Gomez-Gras, D., 2000. Soft-sediment deformation structures interpreted as seismites in lacustrine sediments of the Prebetic Zone, SE Spain, and their potential use as indicators of earthquake magnitudes during the Late Miocene. *Sedimentary Geology* 135, 117–135.
- Russell, J., Grey, K., Whitehouse, M., Moorbatn, S., 1994. Direct Pb/Pb age determination of Proterozoic stromatolites from the Ashburton Nabberu basins, Western Australia, in 8th International Conference on Geochronology, Cosmochemistry and Isotope Geology, Berkeley, California, U.S.A., Abstracts. U.S. Geological Survey Circular 1107, 275.
- Scrimgeour, I.R., Close, D.F., Edgecumbe, C.J., 1999. Petermann Ranges SG-52-7. 1:2500000 Geological map series, Explanatory Notes. Northern Territory Geological Survey.
- Shee, S.R., Vercoe, S.C., Wyatt, B.A., Hwang, P.H., Campbell, A.N., Colgan, E.A., 1999. Discovery and geology of the Nabberu Kimberlite Province, Western Australia. In: Gurney, J.J. (Ed.), Proceedings of the VIIth International kimberlite conference, Cape Town, pp. 764–772.
- Sheppard, S., Occhipinti, S., Nelson, D.R., Tyler, I.M., 1999. Granites of the southern Capricorn Orogen, Western Australia, two billion years of Tectonics and Mineralisation. *Tectonics Special Research Centre Conference Proceedings*, pp. 44–46.
- Sheppard, S., Occhipinti, S., Nelson, D.R., 2005. Intracontinental reworking in the Capricorn Orogen, Western Australia: the 1680–1620 Mangaaro Orogeny. *Australian Journal of Earth Sciences* 52, 443–460.
- Sheppard, S., Occhipinti, S., Tyler, I.M., 2004. A 2005–1970 Ma Andean-type batholith in the southern Gascoyne Complex, Western Australia. *Precambrian Research* 128, 257–277.
- Sheppard, S., Rasmussen, B., Muhling, J.R., Farrell, T.R., Fletcher, I.R., 2007. Grenvillian-aged orogenesis in the Palaeoproterozoic Gascoyne Complex, Western Australia: 1030–950 Ma reworking of the Proterozoic Capricorn Orogen. *Journal of Metamorphic Geology* 25, 477–494.
- Simonson, B.M., Hassler, S.W., 1996. Was the deposition of large Precambrian iron formations linked to major marine transgressions? *Journal of Geology* 104, 665–676.
- Smithies, R.H., Bagas, L., 1997. High pressure amphibolite–granulite facies metamorphism in the Palaeoproterozoic Rudall Complex, central Western Australia. *Precambrian Research*, 83, 243–265.
- Smithies, R.H., Champion, D.C., 1999. Late Archaean felsic alkaline igneous rocks in the Eastern Goldfields, Yilgarn Craton, Western Australia: a result of lower crustal delamination? *London Geological Society, Journal* 156, 561–576.
- Steiger, R.H., Jager, E., 1977. Subcommission on geochronology: convention on the use of decay constants in geo- and cosmochronology. *Earth and Planetary Science Letters* 36, 359–362.
- Swager, C.P., 1997. Tectono-stratigraphy of the late Archaean greenstone terranes in the southern Eastern Goldfields, Western Australia. *Precambrian Research*, 83, 11–42.
- Talbot, H.W.B., 1910. Geological observations in the country between Wiluna, Hall's Creek, and Tanami. *Geological Survey of Western Australia, Bulletin* 39, 88.
- Talbot, H.W.B., 1914. The country between lat. 23° and 26°S, and long. 119° and 121°E. *Geological Survey of Western Australia, Annual Report* 1913, 24–25.
- Talbot, H.W.B., 1919. Notes on the geology and mineral resources of parts of the North-West, Central and Eastern Divisions. *Geological Survey of Western Australia, Annual Report* 1918, 83–93.
- Talbot, H.W.B., 1920. Geology and mineral resources of the North-west, Central, and Eastern Divisions between Long. 119° and 122° E., and Lat. 22° and 28° S. *Geological Survey of Western Australia, Bulletin* 83, 226.
- Talbot, H.W.B., 1926. A geological reconnaissance in the Central and Eastern Divisions between 122° 30'E and 123° 30'E Longitude, and Lat. 25° 30'S and 28° 15'S Latitude. *Geological Survey of Western Australia, Bulletin* 87, 30.
- Teen, M.T., 1996. Silicification and base metal mineralization within the Earaheedy Basin, Western Australia. BSc (Hon) thesis, Centre for Ore Deposit and Exploration Studies, University of Tasmania, 128 p.
- Tobin, K.J., 1990. The paleoecology and significance of the Gunflint-type microbial assemblages from the Frere Formation (Early Proterozoic), Nabberu Basin, Western Australia. *Precambrian Research*, 47, 71–81.
- Trendall, A.F., 2002. The significance of iron-formation in the Precambrian stratigraphic record. In: Altermann, W., Corcoran, L. (Eds.), *Precambrian Sedimentary Environments: A Modern Approach to Ancient Depositional Systems*. Blackwell Science, Oxford, pp. 33–66.
- Tyler, I.M., Pirajno, F., Bagas, L., Myers, J.S., 1998. Geology and mineral deposits of the Proterozoic of Western Australia. *AGSO Journal of Geology and Geophysics* 17, 223–244.
- Vielreicher, N.M., McNaughton, N.J., 2002. SHRIMP U–Pb geochronology of magmatism and thermal event in the Archaean Marymia Inlier, central Western Australia. *International Journal of Earth Sciences (Geol Rundsch)* 91, 406–432.
- Walraven, F., Armstrong, R.A., Kruger, F.J., 1990. A chronostratigraphic framework for the north-central Kaapvaal Craton, the Bushveld Complex and the Vredefort structure. *Tectonophysics* 171, 23–48.
- Walter, M.R., Goode, A.D.T., Hall, J.A., 1976. Microfossils from the newly discovered Precambrian stromatolitic iron formation in Western Australia. *Nature* 261, 221–223.
- Walter, M.R., Veevers, J.J., Calver, C.R., Grey, K., 1995. Late Proterozoic stratigraphy of the Centralian Superbasin, Australia. *Precambrian Research*, 73, 173–175.
- Wingate, M.T.D., Pirajno, F., Morris, P.A., 2004. The Warakurna large igneous province: a new Mesoproterozoic large igneous province in west-central Australia. *Geology* 32, 105–108.
- Wyche, S., Farrell, T.R., 2000. Regional geological setting of the Yandal greenstone belt, northeast Yilgarn Craton. Yandal Greenstone Belt, Australian Institute of Geoscientists, Bulletin 32, 41–50.
- Zhao, G.C., Min, S., Wilde, S.A., Li, S.Z., 2005. Late Archean to Paleoproterozoic evolution of the North China Craton: key issues revisited. *Precambrian Research* 136, 177–202.